

12

Geomagnetic Attitude Control of Satellites Using Generalized Multiple Scales

by

Tiauw Hiong Go

Sarjana Teknik Mesin, Institut Teknologi Bandung, Indonesia (1990)

Submitted to the Department of Aeronautics and Astronautics
in partial fulfillment of the requirements for the degree of

Master of Science in Aeronautics and Astronautics

at the

MASSACHUSETTS INSTITUTE OF TECHNOLOGY

June 1994

© Tiauw Hiong Go, MCMXCIV. All rights reserved.

The author hereby grants to MIT and Vimanic Systems
permission to reproduce and distribute publicly paper and electronic
copies of this thesis document in whole or in part.

Author

Department of Aeronautics and Astronautics

May 6, 1994

Certified by

Rudrapatna V. Ramnath

Adjunct Professor of Aeronautics and Astronautics

Thesis Supervisor

Accepted by

Professor Harold Y. Wachman

Chairman, Departmental Graduate Committee

MASSACHUSETTS INSTITUTE
OF TECHNOLOGY

JUN 09 1994

LIBRARIES

Aero

Geomagnetic Attitude Control of Satellites Using Generalized Multiple Scales

by

Tiauw Hiong Go

Submitted to the Department of Aeronautics and Astronautics
on May 6, 1994, in partial fulfillment of the
requirements for the degree of
Master of Science in Aeronautics and Astronautics

Abstract

The dynamics of satellites utilizing geomagnetic attitude control with a specific control law are analyzed. Two types of satellites are considered, namely single spin asymmetric satellites and dual spin satellites. Stability criteria and approximate description of the motion of the satellites are obtained in a parametric form (analytical) using the Generalized Multiple Scales (GMS) method. By means of this method, the rapid and slow parts of the dynamics are systematically separated, leading to insight into the nature of the system. Finally, a good agreement between the approximate analytical and numerical solutions is demonstrated.

Thesis Supervisor: Rudrapatna V. Ramnath

Title: Adjunct Professor of Aeronautics and Astronautics

Acknowledgments

I would like to express my sincerest thanks and my deepest gratitude to my thesis supervisor, Prof. R. Ramnath, for his guidance and encouragement. His inspiring comments throughout the course of the preparation of the thesis have certainly broadened my horizon of thinking. His deep insight on the multiple scales concept is especially enlightening.

I would like also to thank my parents, who always give me their invaluable supports even in the time when they need them most. Their love and understanding are always strengthening.

Special thanks goes to my fiancée, Mey Lyen. Her love and patience have played an important role in the successful completion of this thesis.

Finally, I would express my appreciation to PT Industri Pesawat Terbang Nusantara (IPTN) for giving me financial support in the last two years.

Contents

1	Introduction	6
1.1	Background	6
1.2	Contribution of the Dissertation	8
1.3	Outline of the Dissertation	8
2	The Generalized Multiple Scales Method	10
2.1	Basic Idea of the Multiple Scales Approach	10
2.2	Mathematical Concept of the GMS Approach	12
2.3	Principle of Minimal and Subminimal Simplification	14
2.4	An Illustrative Example of the Application of the GMS Method . . .	17
3	Magnetic Attitude Control System	20
3.1	The Coordinate Systems	20
3.2	The Geomagnetic Field	21
3.3	The Control Law and The Control Torque	24
4	Magnetic Attitude Control of an Asymmetric Spinning Satellite	27
4.1	The Equations of Motion	27
4.1.1	Euler Angles and Euler's Equation	27
4.1.2	The Magnetic Control Torque	31
4.1.3	The Controlled Dynamic Equations	32
4.2	Stability Analysis and Performance Prediction Using the GMS Method	36
4.2.1	Roll Motion	36
4.2.2	Yaw Motion	50

4.2.3	Summary and Performance Evaluation	57
4.2.4	Comparison with Numerical Results	60
5	Magnetic Attitude Control of a Dual Spin Satellite	67
5.1	The Equations of Motion	67
5.1.1	The Modified Euler's Equations	67
5.1.2	The Magnetic Control Torque	71
5.1.3	The Controlled Dynamic Equations	72
5.2	Stability Analysis and Performance Prediction Using the GMS Method	75
5.2.1	Roll Motion	75
5.2.2	Yaw Motion	92
5.2.3	Summary and Performance Evaluation	101
5.2.4	Comparison with Numerical Results	103
6	Conclusion	110
A	Gravity Gradient Torque on a Satellite Orbiting the Earth	112
B	Extended First to Fourth Order Derivative Operators	117
C	Natural Frequencies of Torque-Free Dual Spin Satellite	119
D	Detail of the Functions $G_2(\tau_0)$ and $G_4(\tau_0)$ in Chapter 5	121

Chapter 1

Introduction

1.1 Background

The techniques of controlling the attitude of a satellite by using an interaction between the satellite and an environmental field has received considerable attention since the beginning of the space era. The primary advantage of these techniques is that they eliminate the need for the control propellant which usually limits the lifetime of a satellite. Another advantage is that the generation of the control torques can usually be done in a simple manner, and thus, the increase of the reliability of the system is attained. In this regard, the attitude control by utilizing the geomagnetic field is particularly attractive since the control torque can be generated by passing electric currents through a coil which then produces a magnetic dipole. The interaction of this magnetic dipole with the geomagnetic field will then produce the desired control torque. Although this method can be applied to a nonspinning or spinning satellite, in this dissertation the discussion will be restricted to the spinning satellite case.

The major challenges in the magnetic attitude control for satellites are the development of the control law and the prediction of the performance of the system under the specific control law. The resulting dynamic equations of the satellite system utilizing magnetic attitude control are quite complicated, even though the concept of the magnetic attitude control itself is relatively simple. The complexity mainly comes from the varying magnitude of the geomagnetic field experienced by the satellite from

time to time on its orbit. In general, this necessitates the analysis of the equations of motion of the system with time varying coefficients.

Magnetic control techniques have been the subject of a number of prior investigations ([1, 2, 3, 4, 5]). Wheeler [1] developed a feedback control law for active nutation damping of a spinning axisymmetric satellite. He then analyzed the performance of the system using the method of averaging. Shigehara [2] proposed a control law in the form of a switching function for attitude stabilization of an axisymmetric spinning satellite. Some works on this subject for dual spin satellites have also been done. Goel and Rajaram [3] investigated a magnetic control system for a dual spin satellite in near equatorial orbit, where the geomagnetic field variations can be neglected. In this fashion, the linearized governing equations will be a set of linear time invariant differential equations and hence, the control theory for the linear time invariant system, which is relatively mature, can readily be applied. Alfriend [4] studied the geomagnetic control system for a dual spin satellite on an orbit at any inclination. He applied the Multiple Time Scales (MTS) method for his analysis and was able to obtain a stability criterion for the specific control law he selected. His analysis, however, was based on the assumption that the earth is non-rotating, and so some of the results are valid only for satellites at low altitude orbits. Another more general work is by Stickler and Alfriend [5], in which the use of magnetic attitude control for initial acquisition and for on-orbit control of a dual spin satellite are discussed.

In general, the difficulties in analyzing the properties of the magnetic attitude control system arise from the fact that no relatively easy methods are available for analyzing a time varying system. The Multiple Time Scales (MTS) method used by Alfriend [4] is promising since it provides not only the approximate solutions of a problem but it also provides physical insight. However, only linear scales are used in the MTS approach. The MTS method has been generalized by Ramnath and Sandri [6] in the Generalized Multiple Scales (GMS) Method to include nonlinear and complex scales. This GMS approach will be used in the magnetic attitude control analysis in this dissertation.

1.2 Contribution of the Dissertation

This dissertation will be a further development on what have been done so far on the subject of magnetic attitude control. In general, there are two main cases that are discussed in this dissertation. One case is the magnetic attitude control of a single spin satellite, and the other is the magnetic attitude control of a dual spin satellite. Both cases are of academic and practical interest. A particular control law will be developed in both cases. The goal is to obtain stability criteria for the cases of interest and to predict the performance of the resulting systems.

The works on the magnetic attitude control for a single spin satellite mentioned in the previous section deal with axisymmetric satellite only. A considerable amount of complexities will arise if the satellite is asymmetric. In this dissertation, an asymmetric satellite which is spun on its maximum principal axis is considered. Thus, the results obtained are more general and include the results for the axisymmetric satellite as the limiting case. The GMS method will be used throughout the course of analysis.

For the dual spin case, the work by Alfriend [4] will be generalized to take into account the rotation of the earth. Thus the results obtained are not limited to low orbit satellites only, but can also be applied to medium or high altitude satellites. The satellite considered consists of a general asymmetric non-spinning body but has an axisymmetric spinning part (called the rotor). Also, the GMS approach will be used in the analysis instead of the MTS approach. As we shall see later, for the dual spin case, it is necessary to use nested-multiple scaling in the analysis.

1.3 Outline of the Dissertation

This dissertation is divided into six chapters and four appendices, which can be summarized as follows.

Chapter 1 provides the background of the problem investigated and also the contributions of the dissertation.

Chapter 2 describes the concept of the GMS method, which will be used in the problem analysis, along with an example of its application. The concept of minimal and subminimal simplifications is also briefly explained.

Chapter 3 specifies the geomagnetic field model to be used in the analysis. It also discusses the principle of the magnetic control system used and the control law selected.

Chapter 4 presents the detailed analysis of the dynamics of a magnetically controlled asymmetric spin stabilized satellite using the GMS method. Comparison of the results with numerical simulations are also presented.

Chapter 5 presents the detailed analysis of the dynamics of a magnetically controlled dual spin satellite using the GMS approach. The results obtained are also compared with numerical simulations.

Chapter 6 presents some conclusions drawn from the analysis.

Appendix A gives the derivation of the gravity gradient torque on a satellite and justifies the order of magnitude of the torque.

Appendix B provides the extended first to fourth order derivative operators that will be used in Chapters 4 and 5.

Appendix C presents the derivation of the natural frequencies of a torque-free dual spin satellite.

Appendix D gives the detail expressions of some functions defined in Chapter 5.

Chapter 2

The Generalized Multiple Scales Method

2.1 Basic Idea of the Multiple Scales Approach

This chapter will describe briefly the Generalized Multiple Scales (GMS) Method. The interested reader may refer to [6] and [7] for a more complete treatment of the matter.

The motion of many dynamic systems consists of a mixture of fast and slow behaviors. Some parameters of a system may have dominant effect on the fast behaviour, while some others may have dominant effect on the slow behavior of the system. In most dynamic systems, this is not easy to detect. It would be nice to have knowledge on what the effect of a certain parameter on the system behavior, since this would give us a clue on what to do if we are to alter the system behavior. For this reason, it would be advantageous to separate the fast and the slow behaviors of a system. A technique that is based on this idea is the Multiple Time Scales (MTS) approach.

The MTS method belongs to a larger body of knowledge called *Perturbation Methods*. As other perturbation methods, the MTS method obtains approximate solutions to a problem in *limiting cases*. This kind of problem is usually recognized by the existence of a very small or very large parameter in a system. In dynamic systems the existence of such parameters generally implies to the existence of fast or slow

behaviors in the systems. Since many physical systems of interest contain such parameters, the MTS method can find a wide range of applications. One example of such a system is a rigid body in orbit around the earth (see [8]). For this system, the small parameter is the ratio of the orbital frequency to the nutational frequency.

The main idea of the MTS approach is choosing the appropriate *scales* to observe the behavior of a system. For a dynamic system, in most cases time is the independent variable, hence the words *time scales* or *clocks* is often used instead of *scales*. In general, we can employ as many scales as we wish to represent the dynamics of a system, depending on the level of accuracy to be achieved. In many applications, however, the use of two scales only is adequate to capture the important dynamics of the system. It is worth noting here that the choice of scales determines the quality of the solution.

Some authors differentiate between the ordinary MTS approach and the GMS approach by virtue of the type of scales used for analyzing a certain problem. If the scales used are linear, it belongs to the ordinary MTS approach, and if the scales used are nonlinear, then it belongs to the GMS approach (see for example Nayfeh [12]). Usually in ordinary MTS approach, the scales are determined before the analysis. In essence, this is like guessing for the right scales for the problem at hand. For the reason of simplicity, normally linear scales are employed. The inappropriateness of the scales used will show up as an incompatibility with the assumptions previously made or as a nonuniformity in the solution. In GMS approach, the problem analyzed will determine the appropriate scales. So, more degrees of freedom are available and are determined by the problem itself. This is the generalization developed by Ramnath [6]. The degree of freedom associated with the selection of scales, in principle, is still in our control. However, the nature of the problem will give us necessary information for the selection of the appropriate scales. The type of scales we get by doing so can be very general. The scales may be linear, nonlinear, real, or complex. The result of this approach is in general better than the ordinary MTS approach. This can be understood since the scales employed are the "right" ones or in other words, the *natural scales* of the problem.

2.2 Mathematical Concept of the GMS Approach

The following presentation is based on Ramnath's [6, 7] development of the GMS technique.

The GMS approach relies on the concept of extension. The fundamental idea of the concept of extension is to enlarge the domain of the independent variable to a space of higher dimension. Since our main interest is on dynamic systems, we will think of *time* as our independent variable. *Time* as the independent variable is extended to a set of new independent timelike-variables which we will call *stroboscopic clocks* or *time scales*. The term *stroboscopic clocks* is used here, since each of these variables acts like a stroboscope, which means that each clock captures only a specific behavior of the system. For example, the fast clock captures the fast behavior of the system. We symbolize the extension of time t as follows :

$$t \longrightarrow \{t_0, t_1, \dots, t_n\} \quad (2.1)$$

where t_0, t_1, \dots, t_n are the stroboscopic clocks or the time scales, which are normally functions of t and the small or large parameter in the system ϵ , that is

$$t_i = t_i(t, \epsilon) \quad (2.2)$$

How t_i relates to t determine the nature of the time scale. In GMS approach, this relation is determined in the course of analysis and not determined a priori. The relation of t_i to ϵ in this case determine whether the clock is fast or slow. The locus defined by Equation 2.2 is called the *trajectory* in the extended domain.

We suppose now that $y(t, \epsilon)$ is the dependent variable in a dynamic equation. We restrict our discussion to a dynamic equation in the form of an ordinary differential equation. Then, since t is extended, $y(t, \epsilon)$ is also extended to $Y(t_0, t_1, \dots, t_n)$. From the definition of extension given in [6] and [7], when Equation 2.2 is inserted into

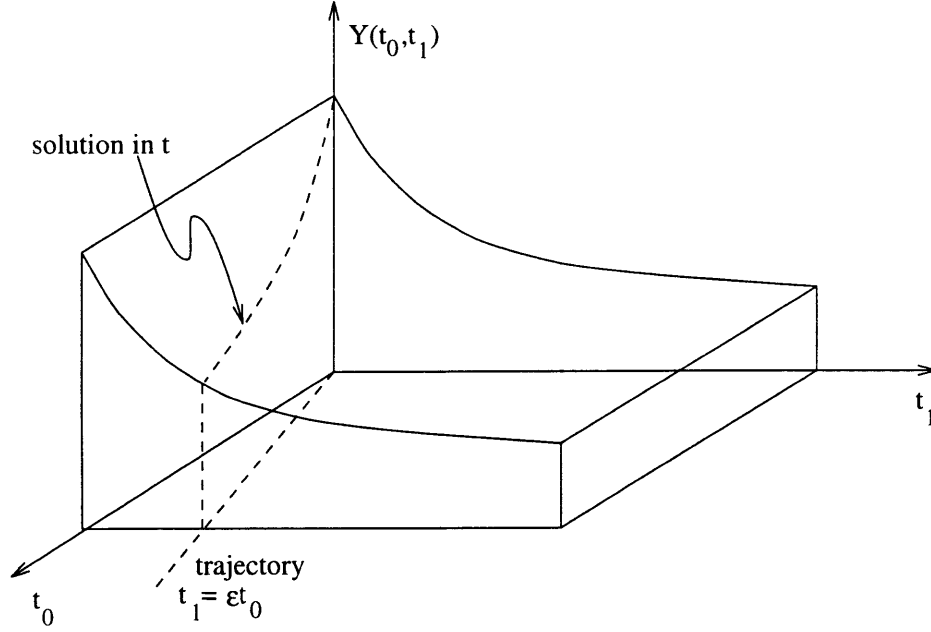


Figure 2-1: Function surface in the extended time scales (from [6])

extended function Y we must have

$$Y(t_0(t, \epsilon), t_1(t, \epsilon), \dots, t_n(t, \epsilon)) = y(t, \epsilon) \quad (2.3)$$

The result of substituting the trajectory in the extended function Y is called the *restriction* of Y .

A geometric interpretation of the concept will be given by the following simple example. Suppose we extend the variables as follows.

$$\begin{aligned} t &\longrightarrow \{t_0, t_1\} \\ y(t, \epsilon) &\longrightarrow Y(t_0, t_1) \end{aligned}$$

where

- ϵ is a small parameter.
- $t_0 = t$ and $t_1 = \epsilon t$, which means that t_0 is a fast time scale and t_1 is a slow time scale.

We will suppose also that Y is given by

$$Y(t_0, t_1) = e^{-t_1}$$

The geometric illustration of this example is presented in Figure 2-1. In that figure, t_0 , t_1 , and Y form an orthogonal axes system. Graphically, $Y(t_0, t_1)$ is represented by the surface in the figure. The intersection of the surface with the $t_0 - Y$ -plane represents the observation on the fast clock, which is constant for this example, and the intersection of the surface with the $t_1 - Y$ -plane represents the observation on the slow clock, which is an exponential decay for this example. The trajectory of t_1 is a straight line with a slope of ϵ with respect to t_0 axis. A vertical plane containing this trajectory will intersect the $Y(t_0, t_1)$ surface. This intersection, which is also illustrated in Figure 2-1, is the restriction of $Y(t_0, t_1)$.

It is clear from the discussion above that due to the extension of the independent variable, an ordinary differential equation will become a partial differential equation. This is not a limitation, however, since the resulting partial differential equation is usually simpler than the initial ordinary differential equation.

2.3 Principle of Minimal and Subminimal Simplification

The purpose of all approximation methods, including the GMS method, is to make a difficult problem become more tractable. In essence, by employing these methods, we wish to have a simpler problem. One subtle question is how far we can simplify a problem. Of course, what we want is to capture all the important behaviors of the system. In other words, the simplification should be as minimal as possible so as to retain all the important information of the system. This is what is called by the *principle of minimal simplification*. The following treatment is based on the development by Ramnath [9].

In the context of the GMS approach, this principle will be applied to determine

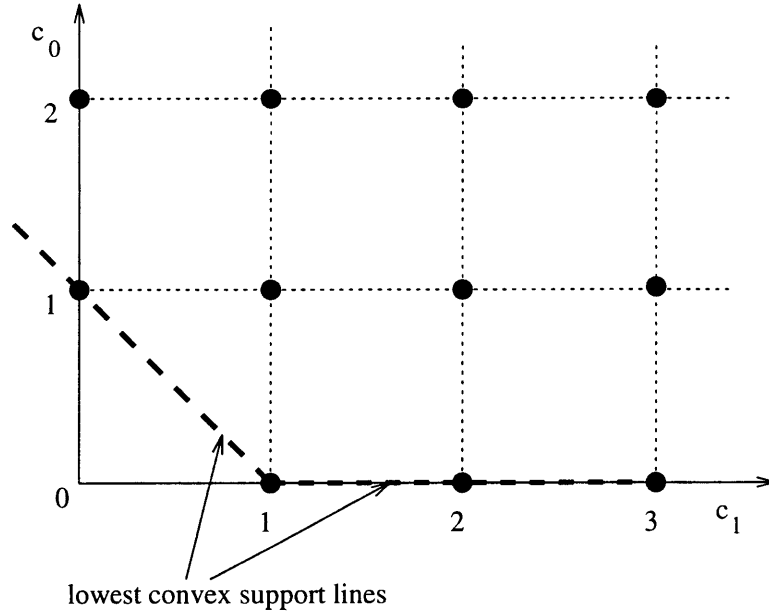


Figure 2-2: Graphical method for minimal simplification : PMS diagram

how fast should the clock be to get as much information as possible from the system. In other words, it will be used to determine the appropriate relationship between t_i and ϵ . In many of the GMS applications, we will deal with the following form of t_i .

$$t_i = \epsilon^\nu k(t) ; \quad 0 < \epsilon \ll 1 \quad (2.4)$$

$k(t)$ is a general clock function, which is to be determined in the course of analysis. $k(t)$ is essentially the extra degree of freedom offered by the GMS method, as we have already mentioned in the first section of this chapter. Applying this form of t_i to a differential equation will yield a partial differential equation with terms of the form

$$\epsilon^{c_0 + c_1 \nu}(\cdot)$$

where the quantity in the parenthesis is assumed to be of $O(1)$. To get a meaningful approximation of the system, the value of ν should be such that the dominant terms in the equation balance to each other. Physically this means that the dominant behaviors of the system can be captured by the approximation.

The idea presented in the previous paragraph can easily be implemented graph-

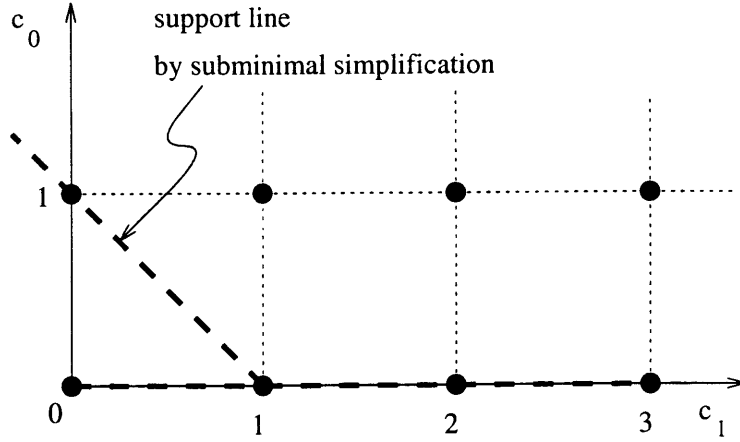


Figure 2-3: Example of principle of subminimal simplification

ically. c_1 will serve as the abscissa and c_0 as the ordinate. See Figure 2-2. We will call such a diagram as *PMS diagram*, where *PMS* stands for *Principle of Minimal Simplification*, developed by Kruskal (see Reference [9]). Each point in the diagram will be assumed to represent each term in the partial differential equation resulted after extending the independent variable. In essence, each point represents the order of a particular term. It can be understood that the dominant terms are represented by the lowest points in the diagram. Hence, based on our previous discussion, the value of ν is determined by the *lowest convex support lines* of that set of graphed points. We then balance the points connected by these lines to get the proper value of ν . For this specific example, the values of ν we get after balancing are 0 and 1. However, $\nu = 0$ is not meaningful and may be discarded, since it only says that no time scaling is needed and we are led to straight perturbation theory. Thus, only $\nu = 1$ is meaningful. The reason described here is true for most cases, that is the meaningful ν is obtained by balancing the points connected by lowest convex support lines which are not horizontal.

There are some cases where the principle of minimal simplification fails. It is possible to get an arrangement of points in a PMS diagram where the only lowest convex support line is a horizontal line, and so, the result we get is not meaningful. In such cases, we have to seek an ordering of terms that are not minimally simplified, but it is minimal in the next rank of terms. Graphically, this corresponds to

finding the lowest convex support lines that do not include the smallest number of dominant points. This is illustrated in Figure 2-3. This refinement, i.e. the *principle of subminimal simplification* was developed by Ramnath [6, 9] and has been applied successfully by Ramnath [10]. It will find its application in our analysis later on.

2.4 An Illustrative Example of the Application of the GMS Method

As has been mentioned earlier, the GMS method can find a wide range of applications. An important example is the analysis of the dynamics of a space vehicle during entry into the Earth's atmosphere, developed by Ramnath [11]. Analytical asymptotic solutions of the angle-of-attack variations during entry were derived, and because they are analytical, they can be used for a variety of stability and control investigations. The development of the asymptotic solutions will now be described and follows [11].

Subject to certain conditions, the equation for the angle-of-attack α during the entry leads to the following (see Reference [11]).

$$\alpha'' + \omega_1(\xi)\alpha' + \omega_0(\xi)\alpha = f(\xi) \quad (2.5)$$

In the above equation the independent variable has been changed from t to ξ according to

$$L\dot{\xi} = V(t) \quad (2.6)$$

where L is a characteristic length and $V(t)$ is the flight speed.

The primes in Equation 2.5 denote differentiation with respect to ξ . The terms ω_1 , ω_0 , and f are solely functions of ξ and can be determined explicitly if the trajectory flown by the center of mass is known. For the details of these functions, see [11]. Since Equation 2.5 is a second order nonautonomous differential equation, then in general it is impossible to obtain its exact solution.

Next, since the variations of the coefficients in Equation 2.5 are slow compared to

the time constant of the motion of the vehicle, such variations can be expressed in a new slow variable

$$\bar{\xi} = \epsilon \xi \quad (2.7)$$

where ϵ is a small positive parameter, which is a measure of the ratio of the time constants of the dynamic motion and the coefficient variation. In terms of this new variable $\bar{\xi}$, Equation 2.5 becomes

$$\epsilon^2 \alpha'' + \epsilon \omega_1(\bar{\xi}) \alpha' + \omega_0(\bar{\xi}) \alpha = f(\bar{\xi}) ; \quad \bar{\xi} \in (\xi_0, \xi_f) \quad (2.8)$$

where the primes now denote differentiation with respect to $\bar{\xi}$. The solution to the inhomogeneous differential equation above can be constructed if the solution to the homogeneous equation is known. So, the solution to the forced system, Equation 2.8, will be developed by first finding the solution to the homogeneous problem by the GMS method.

By means of this method, the resulting approximate homogeneous solution for α can be written as

$$\alpha_h(\bar{\xi}) = \alpha_s(\bar{\xi}) \alpha_f(\bar{\xi}) \quad (2.9)$$

where α_s denotes the slow part of the solution, describing the decrease in the amplitude of the motion, and α_f denotes the fast part of the solution and is given by

$$\alpha_f(\bar{\xi}) = C_1 \hat{\alpha}_1(\bar{\xi}) + C_2 \hat{\alpha}_2(\bar{\xi}) \quad (2.10)$$

with

$$\begin{aligned} \hat{\alpha}_1(\bar{\xi}) &= e^{\int^{\bar{\xi}} k_r(\tau_0) d\tau_0} \sin \left(\int^{\bar{\xi}} k_i(\tau_0) d\tau_0 \right) \\ \hat{\alpha}_2(\bar{\xi}) &= e^{\int^{\bar{\xi}} k_r(\tau_0) d\tau_0} \cos \left(\int^{\bar{\xi}} k_i(\tau_0) d\tau_0 \right) \end{aligned} \quad (2.11)$$

C_1 and C_2 are arbitrary constants. k_r and k_i denote the real and imaginary parts of the clock function k . Then, the particular solution α_p of Equation 2.8 can be found by the method of variation of parameters. The approximate general solution can be

expressed as

$$\alpha(\bar{\xi}) = \alpha_h(\bar{\xi}) + \alpha_p(\bar{\xi}) \quad (2.12)$$

The comparison of the approximate analytical solutions with the numerical solutions were given in Reference [11]. Excellent agreement was shown to be achieved. Besides of this, we get another advantage, that is the separation of the fast and slow dynamics is displayed explicitly, leading to insight into the nature of the shuttle entry dynamics.

Chapter 3

Magnetic Attitude Control System

3.1 The Coordinate Systems

There are several coordinate systems that will be employed in analyzing the magnetic torque on a satellite. The choice of these coordinate systems is actually arbitrary, however we will use the coordinate systems which are also convenient for satellite attitude dynamic analysis. Note also that the term *magnetic torque* in this dissertation will be used loosely to describe the torque which is resulted from the interaction of the geomagnetic field with the magnet onboard of a satellite. For the purpose of analysis here, the earth is assumed fixed in space.

The coordinate systems employed in the analysis along with the description of them are as follows.

- *The inertial coordinate system $(X_I Y_I Z_I)$.*

The origin of this coordinate system is on the center of the Earth. The Z_I axis is aligned with the Earth's polar axis and its positive direction is toward the North Pole. The X_I and Y_I axes lie in the equator plane.

- *The orbiting coordinate system $(X_o Y_o Z_o)$.*

This coordinate system has its origin on the center of mass of the satellite. The

X_o axis lies on the satellite's orbital plane and points radially outward. The Y_o axis also lies on the satellite's orbital plane and it is in the direction of the satellite's center of mass motion, perpendicular to the X_o axis. The Z_o axis completes the right-handed Cartesian coordinate system and thus, it is normal to the orbital plane. Note that only the origin of this coordinate system is fixed in the satellite, while the orientation of this coordinate system is free of the satellite orientation.

- *The body-fixed coordinate system $(X_b Y_b Z_b)$.*

As the name implies, this coordinate system is fixed on the satellite's body and its origin is on the center of mass of the satellite. In case there is relative motion among parts of the satellite, as in the dual spin case, we will mention clearly to which part of the satellite that this coordinate system is fixed. Since the choice of this coordinate system varies for different cases, we will define the orientation of this coordinate system later. As a usual convention, the rotational motion about the X_b , Y_b and Z_b axis will be called yaw, roll, and pitch, respectively.

Figure 3-1 illustrate these coordinate systems.

3.2 The Geomagnetic Field

The geomagnetic model employed here is the tilted magnetic dipole model. The assumption used in this model is that the geomagnetic field can be represented by a magnetic dipole passing through the center of the Earth and having an inclination γ with respect to the Earth's polar axis. This magnetic dipole is fixed to the Earth, and hence, it rotates about the Earth's polar axis with the period of approximately 24 hours. Because of this rotation, the variations in the geomagnetic field that a satellite experiences depends not only on the satellite's orbital geometry but also on the rotation of the Earth. There are of course some exceptions where the magnetic field experienced by the satellite does not vary, for example if the satellite is in geostationary orbit.

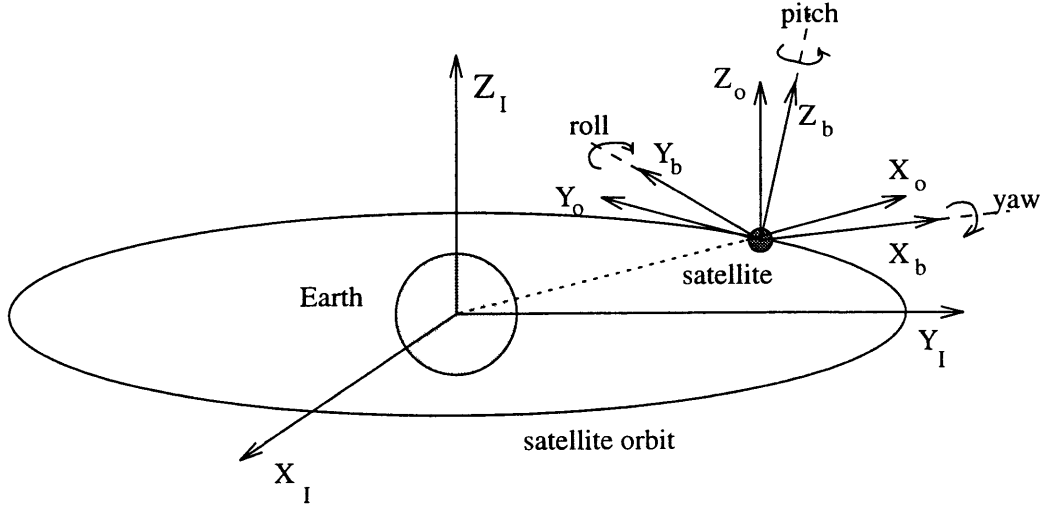


Figure 3-1: The coordinate systems

For the tilted magnetic dipole model, the geomagnetic field vector is given by [13]

$$\mathbf{B} = \frac{\mu_b}{R^5} \left[R^2 \mathbf{i}_m - 3(\mathbf{i}_m \cdot \mathbf{R})\mathbf{R} \right] \quad (3.1)$$

where

- $\mu_b = 7.943 \times 10^{15} \text{ Wb m}$ is the geomagnetic dipole moment.
- \mathbf{R} is the radius vector.
- R is the magnitude of the radius vector.
- \mathbf{i}_m is the unit vector in the opposite direction to the dipole moment vector. This definition is just for convenience.

For later uses, we will derive the components of the geomagnetic field vector on a satellite expressed in the orbiting coordinate system. We will restrict our discussion for a satellite in a circular orbit. To get a better picture on the geometry involved see Figure 3-2. Without loss of generality we will assume that at $t = 0$ the satellite is at the ascending node. Then by using a series of coordinate transformations, we can

By substituting Equations 3.2 and 3.3 to Equation 3.1, and by defining

$$\begin{aligned}
B_0 &= \frac{\mu_b}{R^3} \\
B_1 &= \sin \gamma \cos u \\
B_2 &= \cos \gamma \sin i + \sin \gamma \sin u \cos i \\
B_3 &= \cos \gamma \cos i - \sin \gamma \sin u \sin i
\end{aligned} \tag{3.4}$$

we obtain the components of the geomagnetic field expressed in the orbiting coordinate system as follows

$$\begin{aligned}
B_{x_o} &= -2B_0 (B_1 \cos \Omega t + B_2 \sin \Omega t) \\
B_{y_o} &= B_0 (-B_1 \sin \Omega t + B_2 \cos \Omega t) \\
B_{z_o} &= B_0 B_3
\end{aligned} \tag{3.5}$$

We note here that for a satellite on a specific orbit, γ and i are constants, while u varies periodically in time with the period equal to the period of the Earth rotation, T_e . Thus, B_1 , B_2 , and B_3 are periodic functions with period T_e .

3.3 The Control Law and The Control Torque

The purpose of the magnetic attitude control considered in this dissertation is to maintain the pitch axis of the satellite on its nominal direction. The nominal direction in this case is normal to the satellite's orbital plane. Maintaining the pitch axis on its nominal position is equivalent to keeping the roll and yaw angle zero. The magnetic control should provide the torque which will attenuate any angular deviations on the roll and yaw axes.

As has been mentioned before, the magnetic torque is produced by the interaction between the geomagnetic field and the magnet onboard of the satellite. For our purposes, we assume that the magnet used for attitude control is a magnetic dipole \mathbf{M}_c which is placed aligned with the pitch axis of the satellite. The strength of

the magnetic dipole is determined by the amount of the control torque necessary to counteract the deviations and can be varied from time to time. This can be done for example by passing a variable electric current through a coil. The control law in this case governs the strength of the magnetic dipole from the information on the current deviations.

We will consider the following control law

$$\mathbf{M}_c = [K_1 B_\phi \phi - K_2 (B_\psi \dot{\phi} - B_\phi \dot{\psi})] \mathbf{i}_\theta \equiv M_c \mathbf{i}_\theta \quad (3.6)$$

where

- K_1 and K_2 are the control gains.
- ϕ is the roll angle deviation.
- $\dot{\phi}$ and $\dot{\psi}$ are roll rate and yaw rate deviations, respectively.
- B_ϕ and B_ψ are the components of the geomagnetic field vector in the roll and yaw axes of the satellite, respectively.
- \mathbf{i}_θ is unit vector in the direction of the pitch axis of the satellite.

Clearly this control law leads to a closed loop control system. As we see the manifestation of this control law requires some angular and angular rate sensors and also some magneto-sensors to measure the magnitude of some components of the geomagnetic field. This control law has some similarities to the control law used by Alfrend [4]. The difference is that the control law (3.6) uses the angular rate deviations information instead of the rate of change of the geomagnetic field along the pitch axis as used by Alfrend.

We note here that the control gains K_1 and K_2 are related to the amount of power needed by the control system. The larger K_1 and K_2 , the larger the power needed to drive the system. Thus, power availability should be taken into account in selecting the control gains.

The magnetic control torque exerted on the satellite is then

$$\mathbf{L}_c = \mathbf{M}_c \times \mathbf{B}_b \quad (3.7)$$

with $\mathbf{B}_b \equiv [B_\phi \ B_\psi \ B_\theta]^T$ the geomagnetic field vector expressed in the body fixed axes. Using the property of vector cross product, Equation 3.7 can be expanded as follows

$$\begin{aligned} \mathbf{L}_c &= M_c B_\psi \mathbf{i}_\phi - M_c B_\phi \mathbf{i}_\psi \\ &\equiv L_{c_\phi} \mathbf{i}_\phi - L_{c_\psi} \mathbf{i}_\psi \end{aligned}$$

\mathbf{i}_ϕ and \mathbf{i}_ψ are unit vectors in the direction of the roll axis and yaw axis, respectively. We may expand the above equation further and write

$$L_{c_\phi} = K_1 B_\phi B_\psi \phi - K_2 (B_\psi^2 \dot{\phi} - B_\phi B_\psi \dot{\psi}) \quad (3.8)$$

$$L_{c_\psi} = -K_1 B_\phi^2 \phi + K_2 (B_\phi B_\psi \dot{\phi} - B_\phi^2 \dot{\psi}) \quad (3.9)$$

Since different sets of body fixed axes are employed in analyzing the single and dual spin satellite case, the detail expression of Equation 3.9 will be different for the two cases. Further discussion is given later.

Chapter 4

Magnetic Attitude Control of an Asymmetric Spinning Satellite

4.1 The Equations of Motion

4.1.1 Euler Angles and Euler's Equation

In deriving the equations of motion of the satellite, we assume the following :

- The orbit of the satellite is circular and thus, the orbital angular speed Ω is constant.
- The satellite is rigid and may have no axis of symmetry.
- The body-fixed axes ($X_b Y_b Z_b$) coincide with the satellite's principal axes. We will denote the principal moments of inertia of the satellite about X_b , Y_b and Z_b as I_x , I_y , and I_z , respectively. This assumption will discard the terms containing the product of inertia from the equations of motion.
- The spin axis of the satellite is the Z_b -axis and in nominal condition this spin axis is normal to the satellite's orbital plane. We will assume that the spin axis is the axis of maximum moment of inertia.
- The spin rate of the satellite is constant.

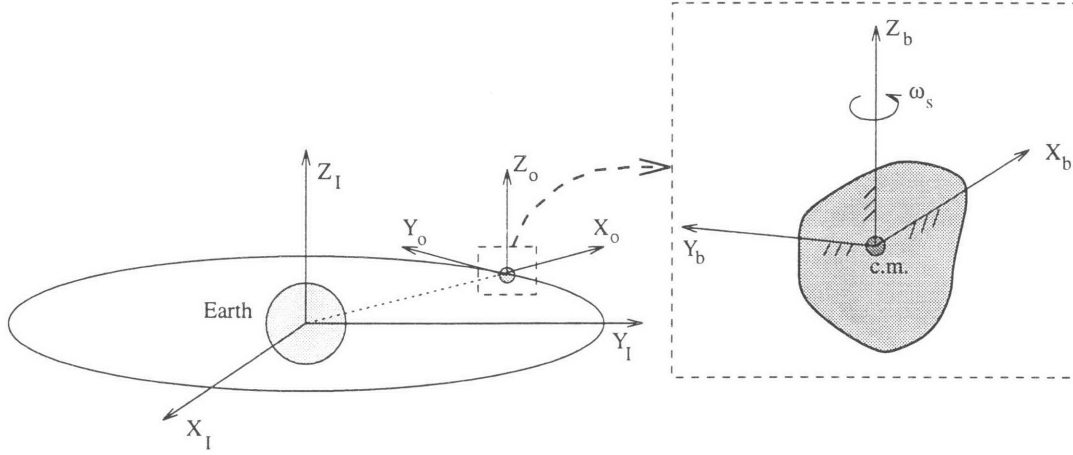


Figure 4-1: The axes system for single spin asymmetric satellite

The above assumptions are the main ones. We will mention the additional assumptions used as we proceed with our discussion.

The nominal position of the spin axis of the satellite coincides with the Z_o -axis (see Figure 4-1). Hence, it is a natural choice to express all the deviations from the nominal condition with respect to the orbiting coordinate system $(X_oY_oZ_o)$. We will use the following sequence of rotations and the associated Euler angles for the transformation between the orbiting coordinate system and the body-fixed coordinate system.

First : The rotation about the Z_o -axis through an angle θ , which will bring the $X_oY_oZ_o$ -axes to the $X_1Y_1Z_1$ -axes.

Second : The rotation about the X_1 -axis through an angle ψ , which will bring the $X_1Y_1Z_1$ -axes to the $X_2Y_2Z_2$ -axes.

Third : The rotation about the Y_2 -axis ($\equiv Y_b$) through an angle ϕ , which will bring the $X_2Y_2Z_2$ -axes to the $X_bY_bZ_b$ -axes.

Now, the angular velocity vector of the satellite is

$$\begin{aligned}\omega &= \omega_x \mathbf{i}_{x_b} + \omega_y \mathbf{i}_{y_b} + \omega_z \mathbf{i}_{z_b} \\ &= (\dot{\theta} + \Omega) \mathbf{i}_{z_o} + \dot{\psi} \mathbf{i}_{x_1} + \dot{\phi} \mathbf{i}_{y_b}\end{aligned}\tag{4.1}$$

where again \mathbf{i}_{x_k} , \mathbf{i}_{y_k} , and \mathbf{i}_{z_k} represent unit vectors in the direction of X_k , Y_k , and Z_k , respectively. Since the spin rate is assumed constant, then $\dot{\theta} = \omega_s = \text{constant}$, where ω_s is the spin rate of the satellite observed in the orbiting coordinate system. By the above mentioned transformation, we can write

$$\begin{aligned}\mathbf{i}_{x_1} &= \cos \phi \mathbf{i}_{x_b} + \sin \phi \mathbf{i}_{z_b} \\ \mathbf{i}_{z_0} &= -\cos \psi \sin \phi \mathbf{i}_{x_b} + \sin \psi \mathbf{i}_{y_b} + \cos \psi \cos \phi \mathbf{i}_{z_b}\end{aligned}$$

Then, by substituting these expressions into Equation 4.1 we will get the expressions for ω_x , ω_y , and ω_z in terms of ϕ , θ , and ψ . We will next assume that the magnitude and the rate of change of the deviation of the Z_b -axis with respect to the Z_o -axis are small. This implies ϕ , ψ , $\dot{\phi}$ and $\dot{\psi}$ be small. By this assumption, the expressions we get are as follows.

$$\begin{aligned}\omega_x &= \dot{\psi} - (\omega_s + \Omega)\phi \\ \omega_y &= \dot{\phi} + (\omega_s + \Omega)\psi \\ \omega_z &= \omega_s + \Omega\end{aligned}\tag{4.2}$$

and

$$\begin{aligned}\dot{\omega}_x &= \ddot{\psi} - \Omega\dot{\phi} \\ \dot{\omega}_y &= \ddot{\phi} + \Omega\dot{\psi} \\ \dot{\omega}_z &= 0\end{aligned}\tag{4.3}$$

The components of the angular momentum of the satellite are

$$\begin{aligned}H_x &= I_x [\dot{\psi} - (\omega_s + \Omega)\phi] \\ H_y &= I_y [\dot{\phi} + (\omega_s + \Omega)\psi] \\ H_z &= I_z(\omega_s + \Omega)\end{aligned}\tag{4.4}$$

Substitution of Equations 4.4 into Euler's equation

$$\dot{\mathbf{H}} + \boldsymbol{\omega} \times \mathbf{H} = \mathbf{L} \quad (4.5)$$

with \mathbf{L} is the external torque acting on the satellite,

will yield the general equations of motion of a spinning rigid satellite as follows.

$$\begin{aligned} I_x \ddot{\phi} + (I_z - I_x)(\omega_s + \Omega)^2 \phi + (I_x + I_y - I_z)(\omega_s + \Omega) \dot{\psi} &= L_y \\ I_y \ddot{\psi} + (I_z - I_y)(\omega_s + \Omega)^2 \psi - (I_x + I_y - I_z)(\omega_s + \Omega) \dot{\phi} &= L_x \end{aligned} \quad (4.6)$$

In the above equations, L_x and L_y are the components of the external torque along the yaw and roll axes, respectively.

To simplify Equation 4.6, we will define the following inertia ratios.

$$\begin{aligned} r_1 &\equiv \frac{I_z - I_x}{I_y} \\ r_2 &\equiv \frac{I_z - I_y}{I_x} \end{aligned} \quad (4.7)$$

Clearly by the assumption that the spin axis is the axis of maximum moment of inertia, r_1 and r_2 are positive. Also since the inertia properties of a body obey the triangle inequality, then the possible values of r_1 and r_2 are only between 0 and 1. By using the inertia ratio definition given in Equation 4.7, Equation 4.6 becomes

$$\begin{aligned} \ddot{\phi} + r_1(\omega_s + \Omega)^2 \phi + (1 - r_1)(\omega_s + \Omega) \dot{\psi} &= L_y^* \\ \ddot{\psi} + r_2(\omega_s + \Omega)^2 \psi - (1 - r_2)(\omega_s + \Omega) \dot{\phi} &= L_x^* \end{aligned} \quad (4.8)$$

where

$$L_y^* = \frac{L_y}{I_y} \quad L_x^* = \frac{L_x}{I_x}$$

In Equation 4.8, L_y^* and L_x^* come from the contributions of any external torque that acts on the satellite, including the control torque. For a satellite orbiting the earth, the major contributions on external torques come from the gravity gradient

and the geomagnetic field. As shown in Appendix A, if we utilize the geomagnetic field to control the satellite's attitude, the gravity gradient effect is of second order in magnitude. For this reason, we will neglect the gravity gradient effect and all other external effects in our analysis. So, only the magnetic control torque will appear on the righthand side of Equation 4.8.

4.1.2 The Magnetic Control Torque

Chapter 3 has discussed the control law to be used in the magnetic control system. We also see from Equation 3.9 that to obtain the detail of the components of the control torque on the roll and yaw axes of the satellite, we need the details of the components of the geomagnetic field on these axes.

The expressions for the components of the geomagnetic field in the orbiting coordinate system have been derived in Chapter 3 (see Equation 3.5). By using the Euler angles convention given in the previous section, the transformation matrix from the orbiting coordinate system to the body-fixed coordinate system for small ϕ and ψ is the following.

$$C_o^b = \begin{pmatrix} \cos \theta & -\sin \theta & \phi \cos \theta + \psi \sin \theta \\ \sin \theta & \cos \theta & \phi \sin \theta - \psi \cos \theta \\ -\phi & \psi & 1 \end{pmatrix}$$

Therefore,

$$\begin{aligned} B_\phi &\approx B_{x_o} \cos \theta + B_{y_o} \sin \theta \\ B_\psi &\approx -B_{x_o} \sin \theta + B_{y_o} \cos \theta \end{aligned} \tag{4.9}$$

Substitution of Equation 4.9 into Equation 3.9 will yield the details of the components of magnetic torque about the roll and yaw axes. To shorten the notations, we define the following.

$$\begin{aligned}
S_1(t) &= \frac{1}{4} (B_1^2 + B_2^2) \\
S_2(t) &= \frac{1}{4} (B_1^2 - B_2^2) \\
S_3(t) &= \frac{1}{2} B_1 B_2
\end{aligned} \tag{4.10}$$

and

$$\begin{aligned}
f_1(t) &= 5S_1(t) + 3S_2(t) \cos 2\Omega t + 3S_3(t) \sin 2\Omega t \\
f_2(t) &= 3S_1(t) + 5S_2(t) \cos 2\Omega t + 5S_3(t) \sin 2\Omega t \\
f_3(t) &= 4[S_3(t) \cos 2\Omega t - S_2(t) \sin 2\Omega t]
\end{aligned} \tag{4.11}$$

where B_1 , B_2 , and B_3 are given by Equation 3.4. Thus, the components of the magnetic control torque on the roll and yaw axes are as follows.

$$L_{c_\phi} = K_1 B_\phi B_\psi \phi - K_2 (B_\psi^2 \dot{\phi} - B_\phi B_\psi \dot{\psi}) \tag{4.12}$$

$$L_{c_\psi} = -K_1 B_\phi^2 \phi + K_2 (B_\phi B_\psi \dot{\phi} - B_\phi^2 \dot{\psi}) \tag{4.13}$$

where

$$\begin{aligned}
B_\phi^2 &= B_o^2 [f_1(t) - f_2(t) \cos 2\theta + f_3(t) \sin 2\theta] \\
B_\psi^2 &= B_o^2 [f_1(t) + f_2(t) \cos 2\theta - f_3(t) \sin 2\theta] \\
B_\phi B_\psi &= -B_o^2 [f_3(t) \cos 2\theta + f_2(t) \sin 2\theta]
\end{aligned} \tag{4.14}$$

Note that S_i 's and f_i 's vary periodically with time. Hence, B_ϕ^2 , B_ψ^2 , and $B_\phi B_\psi$ are periodic functions.

4.1.3 The Controlled Dynamic Equations

By including the magnetic control torque, Equation 4.13, into the equations of motion of the satellite, Equation 4.8, we get

$$\begin{aligned}
\ddot{\phi} + \frac{K_2}{I_y} B_\psi^2 \dot{\phi} + \left[r_1(\omega_s + \Omega)^2 - \frac{K_1}{I_y} B_\phi B_\psi \right] \phi + \left[(1 - r_1)(\omega_s + \Omega) - \frac{K_2}{I_y} B_\phi B_\psi \right] \dot{\psi} &= 0 \\
\ddot{\psi} + \frac{K_2}{I_x} B_\phi^2 \dot{\phi} + r_2(\omega_s + \Omega)^2 \psi - \left[(1 - r_2)(\omega_s + \Omega) + \frac{K_2}{I_x} B_\phi B_\psi \right] \dot{\phi} + \frac{K_1}{I_x} B_\phi^2 \phi &= 0 \quad (4.15)
\end{aligned}$$

For spin-stabilized satellite in practice, the satellite's spin rate is normally much larger than the orbital angular speed. Mathematically we can express this as

$$\frac{\Omega}{\omega_s} = \epsilon \quad ; \quad 0 < |\epsilon| \ll 1 \quad (4.16)$$

Without loss of generality we will assume that at $t = 0$, the satellite is at the ascending node and $u = 0$, so that we can write

$$\begin{aligned}
\Omega t &= \epsilon \bar{t} \\
u &= \omega_e t = n \epsilon \bar{t}
\end{aligned}$$

where

- $\bar{t} \equiv \omega_s t$ is a nondimensional time
- $n \equiv \frac{\omega_e}{\Omega}$ is the ratio of the earth's spin rate and the orbital angular speed of the satellite. This ratio is a small number for low orbit satellite and 1 for geosynchronous satellite.

Expressed in terms of the nondimensional time \bar{t} ,

$$\theta = \omega_s t = \bar{t}$$

and

$$\frac{d^i}{dt^i} = \omega_s^i \frac{d^i}{d\bar{t}^i}$$

Then Equation 4.15 can be written in terms of \bar{t} as follows.

$$\begin{aligned}
\phi'' + \frac{K_2 B_o^2}{I_y \omega_s} [f_1(\epsilon \bar{t}) + f_2(\epsilon \bar{t}) \cos 2\bar{t} - f_3(\epsilon \bar{t}) \sin 2\bar{t}] \phi' + \\
\left[r_1(1 + 2\epsilon + \epsilon^2) + \frac{K_1 B_o^2}{I_y \omega_s^2} (f_3(\epsilon \bar{t}) \cos 2\bar{t} + f_2(\epsilon \bar{t}) \sin 2\bar{t}) \right] \phi + \\
\left[(1 - r_1)(1 + \epsilon) + \frac{K_2 B_o^2}{I_y \omega_s} (f_3(\epsilon \bar{t}) \cos 2\bar{t} + f_2(\epsilon \bar{t}) \sin 2\bar{t}) \right] \psi' = 0 \\
\psi'' + \frac{K_2 B_o^2}{I_x \omega_s} [f_1(\epsilon \bar{t}) - f_2(\epsilon \bar{t}) \cos 2\bar{t} + f_3(\epsilon \bar{t}) \sin 2\bar{t}] \psi' + \\
r_2(1 + 2\epsilon + \epsilon^2) \psi - \\
\left[(1 - r_2)(1 + \epsilon) - \frac{K_2 B_o^2}{I_x \omega_s} (f_3(\epsilon \bar{t}) \cos 2\bar{t} + f_2(\epsilon \bar{t}) \sin 2\bar{t}) \right] \phi' + \\
\frac{K_1 B_o^2}{I_x \omega_s^2} [f_1(\epsilon \bar{t}) - f_2(\epsilon \bar{t}) \cos 2\bar{t} + f_3(\epsilon \bar{t}) \sin 2\bar{t}] \phi = 0
\end{aligned} \tag{4.17}$$

where $(\cdot)'$ denotes differentiation with respect to \bar{t} . We put $\epsilon \bar{t}$ in the arguments of f_i 's to indicate that f_i 's are slowly varying functions.

The magnitude of the geomagnetic field is relatively small. For example at a 500 km-altitude orbit, B_o is of the order of 10^{-5} in SI units. Therefore, it is reasonable to assume that

$$\begin{aligned}
\frac{K_1 B_o^2}{\sqrt{I_x I_y} \omega_s^2} &= \epsilon K_1^* \\
\frac{K_2 B_o^2}{\sqrt{I_x I_y} \omega_s} &= \epsilon K_2^*
\end{aligned} \tag{4.18}$$

If we also define

$$\begin{aligned}
a &\equiv \sqrt{\frac{I_y}{I_x}} \\
b &\equiv \sqrt{\frac{I_x}{I_y}}
\end{aligned} \tag{4.19}$$

then we can write Equation 4.17 as

$$\begin{aligned}
\phi'' &+ \epsilon b K_2^* [f_1(\epsilon \bar{t}) + f_2(\epsilon \bar{t}) \cos 2\bar{t} - f_3(\epsilon \bar{t}) \sin 2\bar{t}] \phi' + \\
&\left[r_1(1 + 2\epsilon + \epsilon^2) + \epsilon b K_1^* (f_3(\epsilon \bar{t}) \cos 2\bar{t} + f_2(\epsilon \bar{t}) \sin 2\bar{t}) \right] \phi + \\
&[(1 - r_1)(1 + \epsilon) + \epsilon b K_2^* (f_3(\epsilon \bar{t}) \cos 2\bar{t} + f_2(\epsilon \bar{t}) \sin 2\bar{t})] \psi' = 0 \quad (4.20)
\end{aligned}$$

$$\begin{aligned}
\psi'' &+ \epsilon a K_2^* [f_1(\epsilon \bar{t}) - f_2(\epsilon \bar{t}) \cos 2\bar{t} + f_3(\epsilon \bar{t}) \sin 2\bar{t}] \psi' + \\
&r_2(1 + 2\epsilon + \epsilon^2) \psi - \\
&[(1 - r_2)(1 + \epsilon) - \epsilon a K_2^* (f_3(\epsilon \bar{t}) \cos 2\bar{t} + f_2(\epsilon \bar{t}) \sin 2\bar{t})] \phi' + \\
&\epsilon a K_1^* [f_1(\epsilon \bar{t}) - f_2(\epsilon \bar{t}) \cos 2\bar{t} + f_3(\epsilon \bar{t}) \sin 2\bar{t}] \phi = 0 \quad (4.21)
\end{aligned}$$

These dynamic equations form a system of coupled linear differential equations. Also they are nonautonomous, as the coefficients are time varying. To be more specific, the coefficients vary periodically in time and their frequencies are a mixture of relatively high (due to the existence of $\cos 2\bar{t}$ and $\sin 2\bar{t}$ in the terms that build up the coefficients) and low frequencies (due to the f_i 's in the coefficients). We also observe that some of the coefficients are of $O(1)$ and some are small (of $O(\epsilon)$). The exact solutions of Equation 4.21 in general cannot be obtained. If we take a simplistic approach by merely neglecting the terms with small coefficients, we will arrive at the equations of free rigid body motion, hence the result we get is not realistic. We can of course integrate Equations 4.20 and 4.21 numerically and get an answer. However, the answer we get will only be valid for a certain values of parameters. Since our purpose is to get the whole picture of the dynamics of the system, it is clear that numerical approach is not useful. For this reason, asymptotic approach using the GMS method will be used for the dynamic analysis. From the discussion in Chapter 2, we can see that in fact Equations 4.20 and 4.21 are in the form suitable for the application of this method.

4.2 Stability Analysis and Performance Prediction Using the GMS Method

4.2.1 Roll Motion

The motion about each axis will be examined separately. We will first decouple Equations 4.20 and 4.21 before applying the GMS method. The roll equation we get after decoupling is as follows

$$\phi^{iv} + \epsilon P_1(\bar{t}) \phi''' + P_2(\bar{t}) \phi'' + \epsilon P_3(\bar{t}) \phi' + P_4(\bar{t}) \phi = 0 \quad (4.22)$$

where

$$\begin{aligned} P_1(\bar{t}) &= K_2^* \left[(a+b)f_1(\epsilon\bar{t}) - (a-b + \frac{4b}{1-r_1})(f_2(\epsilon\bar{t})\cos 2\bar{t} - f_3(\epsilon\bar{t})\sin 2\bar{t}) \right] + O(\epsilon) \\ &\equiv p_{11}(\bar{t}) + O(\epsilon) \\ P_2(\bar{t}) &= 1 + r_1 r_2 + \epsilon[2 + r_2 + 2r_1 r_2 + (K_1^* b + K_2^*[a(1-r_1) - b(3+r_2) + \frac{b(4+r_2)}{1-r_1}]) (f_2(\epsilon\bar{t})\sin 2\bar{t} + f_3(\epsilon\bar{t})\cos 2\bar{t})] + O(\epsilon^2) \\ &\equiv p_{21}(\bar{t}) + \epsilon p_{22}(\bar{t}) + O(\epsilon^2) \\ P_3(\bar{t}) &= [K_2^*(ar_1 + br_2) - K_1^*a(1-r_1)]f_1(\epsilon\bar{t}) + (K_1^*[a(1-r_1) + 4b] - K_2^*[a(2-r_1) + b(2+r_2) + \frac{2b(1+r_1-r_2+r_1 r_2)}{1-r_1}]) \\ &\quad (f_2(\epsilon\bar{t})\cos 2\bar{t} - f_3(\epsilon\bar{t})\sin 2\bar{t}) + O(\epsilon) \\ &\equiv p_{31}(\bar{t}) + O(\epsilon) \\ P_4(\bar{t}) &= r_1 r_2 + \epsilon[5r_1 r_2 + (K_2^*[2ar_1 + \frac{br_1(4+r_2)}{1-r_1}] - K_1^*[2a(1-r_1) + b(4-r_2)]) (f_2(\epsilon\bar{t})\sin 2\bar{t} + f_3(\epsilon\bar{t})\cos 2\bar{t})] + O(\epsilon^2) \\ &\equiv p_{41}(\bar{t}) + \epsilon p_{42}(\bar{t}) + O(\epsilon^2) \end{aligned} \quad (4.23)$$

The GMS method is now invoked. We will use two time scales in our approach. So, we extend the independent and dependent variables as follows.

$$\begin{aligned}
\bar{t} &\longrightarrow \{\tau_0, \tau_1\} \\
\phi(\bar{t}, \epsilon) &\longrightarrow \phi(\tau_0, \tau_1)
\end{aligned} \tag{4.24}$$

where

$$\begin{aligned}
\tau_0 &= \bar{t} \\
\tau_1 &= \epsilon^\nu \int k(\bar{t}) d\bar{t}
\end{aligned} \tag{4.25}$$

In the above, $k(\bar{t})$ is a clock function which will be determined in the course of analysis. Note that τ_1 still contains variable ν . The right value of ν will be determined later by utilizing the principle of minimal simplification [9] as described in Chapter 2. The extended first to fourth order derivative operators are given in Appendix B. Written in terms of the extended variables, Equation 4.22 leads to the following partial differential equation:

$$\begin{aligned}
&\frac{\partial^4 \phi}{\partial \tau_0^4} + P_2(\tau_0) \frac{\partial^2 \phi}{\partial \tau_0^2} + P_4(\tau_0) \phi + \epsilon \left[P_1(\tau_0) \frac{\partial^3 \phi}{\partial \tau_0^3} + P_3(\tau_0) \frac{\partial \phi}{\partial \tau_0} \right] + \\
&\epsilon^\nu \left[k''' \frac{\partial \phi}{\partial \tau_1} + 3k'' \frac{\partial^2 \phi}{\partial \tau_0 \partial \tau_1} + 5k' \frac{\partial^3 \phi}{\partial \tau_0^2 \partial \tau_1} + k' P_2(\tau_0) \frac{\partial \phi}{\partial \tau_1} + \right. \\
&\quad \left. 4k \frac{\partial^4 \phi}{\partial \tau_0^3 \partial \tau_1} + 2k P_2(\tau_0) \frac{\partial^2 \phi}{\partial \tau_0 \partial \tau_1} \right] + \\
&\epsilon^{2\nu} \left[4kk'' \frac{\partial^2 \phi}{\partial \tau_1^2} + 3k'^2 \frac{\partial^2 \phi}{\partial \tau_1^2} + 11kk' \frac{\partial^3 \phi}{\partial \tau_0 \partial \tau_1^2} + 6k^2 \frac{\partial^4 \phi}{\partial \tau_0^2 \partial \tau_1^2} + k^2 P_2(\tau_0) \frac{\partial^2 \phi}{\partial \tau_1^2} \right] + \\
&\epsilon^{3\nu} \left[6k^2 k' \frac{\partial^3 \phi}{\partial \tau_1^3} \right] + \epsilon^{4\nu} k^4 \frac{\partial^4 \phi}{\partial \tau_1^4} + \\
&\epsilon^{1+\nu} \left[k'' P_1(\tau_0) \frac{\partial \phi}{\partial \tau_1} + 2k' P_1(\tau_0) \frac{\partial^2 \phi}{\partial \tau_0 \partial \tau_1} + 3k P_1(\tau_0) \frac{\partial^3 \phi}{\partial \tau_0^2 \partial \tau_1} + k P_3(\tau_0) \frac{\partial \phi}{\partial \tau_1} \right] + \\
&\epsilon^{1+2\nu} \left[3kk' P_1(\tau_0) \frac{\partial^2 \phi}{\partial \tau_1^2} + 3k^2 P_1(\tau_0) \frac{\partial^3 \phi}{\partial \tau_0 \partial \tau_1^2} \right] + \\
&\epsilon^{1+3\nu} k^3 P_1(\tau_0) \frac{\partial^3 \phi}{\partial \tau_1^3} = 0
\end{aligned} \tag{4.26}$$

The terms in Equation 4.26 are of the form $\epsilon^{\lambda_0 + \lambda_1 \nu}(\cdot)$ where the quantities in the

differential equation with constant coefficient as follows.

$$\frac{\partial^4 \phi}{\partial \tau_0^4} + (1 + r_1 r_2) \frac{\partial^2 \phi}{\partial \tau_0^2} + r_1 r_2 \phi = 0 \quad (4.29)$$

We suppose the solution to be of the form

$$\phi = A(\tau_1) e^{\eta \tau_0} \quad (4.30)$$

Then the substitution of Equation 4.30 into Equation 4.29 yields

$$\begin{aligned} \eta^4 + (1 + r_1 r_2) \eta^2 + r_1 r_2 &= 0 \\ \iff (\eta^2 + 1)(\eta^2 + r_1 r_2) &= 0 \\ \iff \eta = \pm j \quad \eta = \pm j \sqrt{r_1 r_2} & \end{aligned} \quad (4.31)$$

Therefore,

$$\phi(\tau_0, \tau_1) = A_1(\tau_1) e^{j\tau_0} + A_2(\tau_1) e^{j\sqrt{r_1 r_2} \tau_0} + c.c. \quad (4.32)$$

where *c.c.* denotes the complex conjugates of the preceding terms.

So, in this case the dominant roll motion consists of two oscillatory modes with the dominant frequencies of 1 and $\sqrt{r_1 r_2}$. These frequencies correspond to the natural frequencies of the torque-free rigid body motion. In fact, if A_1 and A_2 are constant, Equation 4.32 becomes exactly the solution of the torque-free rigid body motion. Obviously, the magnetic attitude control system will mainly influence the amplitude and only slightly alter the frequency of the motion. The amplitude and frequency corrections due to the magnetic control will come from the subdominant order analysis. For convenience, the two modes in Equation 4.32 will be referred to as *first mode* and *second mode*, respectively. Note that the maximum limiting value of $r_1 r_2$ is 1, so that in general the second mode is slower than the first mode. In the following, the first and second modes are studied separately.

First Mode

The effect of the magnetic control system on the first mode, which is

$$\phi_1(\tau_0, \tau_1) = A_1(\tau_1)e^{j\tau_0} + c.c. \quad (4.33)$$

will now be studied. The subdominant order of Equation 4.26 is

$$\begin{aligned} O(\epsilon) : \quad & k''' \frac{\partial \phi}{\partial \tau_1} + 3k'' \frac{\partial^2 \phi}{\partial \tau_0 \partial \tau_1} + p_{21}k' \frac{\partial \phi}{\partial \tau_1} + 5k' \frac{\partial^3 \phi}{\partial \tau_0^2 \partial \tau_1} + 2p_{21}k \frac{\partial^2 \phi}{\partial \tau_0 \partial \tau_1} + 4k \frac{\partial^4 \phi}{\partial \tau_0^3 \partial \tau_1} + \\ & p_{11}(\tau_0) \frac{\partial^3 \phi}{\partial \tau_0^3} + p_{31}(\tau_0) \frac{\partial \phi}{\partial \tau_0} + p_{22}(\tau_0) \frac{\partial^2 \phi}{\partial \tau_0^2} + p_{42}(\tau_0)\phi = 0 \end{aligned} \quad (4.34)$$

For the first mode, this equation becomes

$$\begin{aligned} & [k_1''' + (p_{21} - 5)k_1' + j[3k_1'' + (2p_{21} - 4)k_1]] \frac{dA_1}{d\tau_1} \\ & + [p_{42}(\tau_0) - p_{22}(\tau_0) + j(p_{31}(\tau_0) - p_{11}(\tau_0))] A_1 = 0 \end{aligned} \quad (4.35)$$

In the above equation, subscript 1 has been added on the clock function k to indicate that it is the clock function of the first mode. In the last equation, A_1 is a function of τ_1 , while the coefficients are functions of τ_0 , therefore we can separate the variables as follows.

$$\frac{\frac{dA_1}{d\tau_1}}{A_1} = - \frac{p_{42}(\tau_0) - p_{22}(\tau_0) + j(p_{31}(\tau_0) - p_{11}(\tau_0))}{k_1''' + (p_{21} - 5)k_1' + j[3k_1'' + (2p_{21} - 4)k_1]} = \text{constant} \quad (4.36)$$

For simplicity, we will choose the constant in the above equation to be -1. This choice of constant leads to the following amplitude and clock equations.

$$A_1(\tau_1) = \bar{A}_{1_0} e^{-\tau_1} ; \quad \bar{A}_{1_0} = \text{arbitrary constant} \quad (4.37)$$

$$\begin{aligned} k_1''' - (4 - r_1 r_2)k_1' + j[3k_1'' - 2(1 - r_1 r_2)k_1] &= M_1 + M_2(\epsilon \tau_0) \cos 2\tau_0 + M_3(\epsilon \tau_0) \sin 2\tau_0 \\ &+ j[N_1 + N_2(\epsilon \tau_0) \cos 2\tau_0 - N_3(\epsilon \tau_0) \sin 2\tau_0 + N_4(\epsilon \tau_0)] \end{aligned} \quad (4.38)$$

where

$$\begin{aligned}
M_1 &= 3r_1 r_2 - r_2 - 2 \\
M_2(\epsilon\tau_0) &= -[[2a(1-r_1) + b(5-r_2)]K_1^* + [a(1-r_1) + b]K_2^*] f_3(\epsilon\tau_0) \\
M_3(\epsilon\tau_0) &= -[[2a(1-r_1) + b(5-r_2)]K_1^* + [a(1-r_1) + b]K_2^*] f_2(\epsilon\tau_0) \\
N_1 &= -\frac{5}{2} [a(1-r_1)K_1^* - [a(1-r_1) + b(1-r_2)]K_2^*] U \\
N_2(\epsilon\tau_0) &= [[4b + a(1-r_1)]K_1^* - [a(1-r_1) + b(1-r_2)]K_2^*] f_2(\epsilon\tau_0) \\
N_3(\epsilon\tau_0) &= [[4b + a(1-r_1)]K_1^* - [a(1-r_1) + b(1-r_2)]K_2^*] f_3(\epsilon\tau_0) \\
N_4(\epsilon\tau_0) &= -[a(1-r_1)K_1^* - [a(1-r_1) + b(1-r_2)]K_2^*] \left[f_1(\epsilon\tau_0) - \frac{5}{2}U \right]
\end{aligned} \tag{4.39}$$

with

$$U = \frac{1}{4} \sin^2 \gamma (1 + \cos^2 i) + \frac{1}{2} \cos^2 \gamma \sin^2 i \tag{4.40}$$

U is always positive and it is constant for a particular orbit.

Note that M_1 and N_1 are constant, while M_2, M_3, N_2, N_3 , and N_4 are slowly periodic functions.

Equation 4.38 is an inhomogeneous linear ordinary differential equation with constant coefficients, hence in principle, its solution can be found exactly. However, the existence of a combination of slow and fast periodic functions in the righthand side of Equation 4.38 makes the task of obtaining the exact solution very complicated. Therefore, as a first attempt we will try to obtain the approximate solution for $k(\tau_0)$ by taking advantage of the specific form of the righthand side of Equation 4.38.

In most applications, only the particular solution of $k(\tau_0)$ is important, since we always have the freedom to take the coefficients of the homogeneous solution to be zero. However, from the theory of the differential equations, we know that the homogeneous solution has an influence on the form of the particular solution. Thus, eventhough it is not needed, the homogeneous part of the solution must be considered. The possibility of resonance has to be examined. By *resonance* we mean that the homogeneous solution contains the same type of function with one or more

inhomogeneous terms (terms in the righthand side of the differential equation) so that secular terms are produced in the particular solution. If such terms exist, further examination is needed. The homogeneous solution of Equation 4.38 is

$$k_{h1}(\tau_0) = \sum_{i=1}^3 C_i e^{s_i \tau_0} \quad (4.41)$$

where

- C_i ; $i = 1, 2, 3$, are arbitrary constants, which will be taken to be zero later on.
- s_i ; $i = 1, 2, 3$, are the roots of the characteristic equation of the differential equation :

$$s^3 + 3js^2 - (4 - r_1 r_2)s - 2j(1 - r_1 r_2) = 0 \quad (4.42)$$

The locus of s_i in complex plane for all possible values of $r_1 r_2$ considered is presented in Figure 4-3. This figure shows that in general the homogeneous solution is of the form

$$e^{\Re(s_i)\tau_0} (\cos \Im(s_i)\tau_0 + j \sin \Im(s_i)\tau_0)$$

with $\Re(s_i)$ and $\Im(s_i)$ denote the real part and the imaginary part of s_i , respectively. It is only for the limiting case $r_1 r_2 = 1$ that a constant term will appear in the homogeneous solution, and this constant term will give rise to resonance condition. This case however is not physically possible, and therefore will be omitted.

The inhomogeneous terms of Equation 4.38 consist of constant and periodic terms. None of the inhomogeneous terms has the same type of function as the homogeneous solution. Hence, the possibility of resonance to occur can be ruled out. It is then clear that the particular solution for $k(\tau_0)$ will consist of constant and periodic terms only.

By the previous argument, it is possible to construct the stability criterion of the first mode without actually solving the differential equation 4.38. From the amplitude expression 4.37, it is obvious that the stability of the first mode is determined by the constant real part of $k(\tau_0)$. By observing Equation 4.38, we see that this constant real part appears due to the contribution of N_1 . The constant real part of $k(\tau_0)$ is as

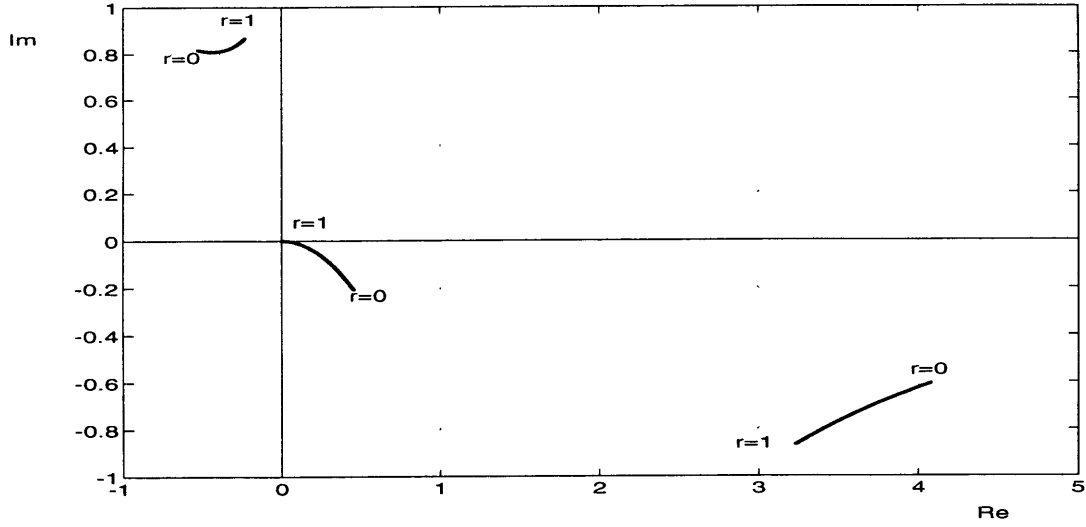


Figure 4-3: Root locus of the first mode clock equation ($r = r_1 r_2$)

follows.

$$k_{r_1} = \frac{5}{2} \frac{a(1-r_1)K_1^* + [a(1-r_1) + b(1-r_2)]K_2^*}{2(1-r_1 r_2)} U \quad (4.43)$$

For asymptotic stability,

$$k_{r_1} > 0 \quad (4.44)$$

Since U is a positive constant and $0 < r_1 r_2 < 1$, then the above criterion for asymptotic stability can be written as

$$a(1-r_1)K_1^* + [a(1-r_1) + b(1-r_2)]K_2^* > 0 \quad (4.45)$$

To predict the response of the first mode, the approximate solution for $k(\tau_0)$ will now be constructed. The slowly periodic factor ($M_i(\epsilon\tau_0)$ and $N_i(\epsilon\tau_0)$) in the inhomogeneous terms, which is similar to $M_i(\epsilon\tau_0) \sin 2\tau_0$, will be treated as a constant in the integration step, since for each cycle of the fast periodic factor, the variation of the slowly periodic factor is very small. By doing so, we obtain

$$\begin{aligned}
k_1(\tau_0) = & k_{r_1} + jk_{i_1} + k_{fs_1} \sin 2\tau_0 + k_{fc_1} \cos 2\tau_0 + \\
& \sum_{i=1}^m [k_{ss_{1i}} \sin \alpha_i \tau_0 + jk_{sc_{1i}} \cos \alpha_i \tau_0] + \\
& \sum_{i=1}^n [jk_{cs_{1i}} \sin \beta_i \tau_0 + k_{cc_{1i}} \cos \beta_i \tau_0]
\end{aligned} \tag{4.46}$$

where

$$\begin{aligned}
k_{i_1} &= \frac{M_1}{2(1 - r_1 r_2)} \\
k_{fs_1} &= \frac{1}{2} \left[\frac{-(8 - r_1 r_2)M_2(\epsilon\tau_0) - (7 - r_1 r_2)N_3(\epsilon\tau_0)}{15 - 2r_1 r_2} + \right. \\
& \quad \left. j \frac{-(7 - r_1 r_2)M_3(\epsilon\tau_0) - (8 - r_1 r_2)N_2(\epsilon\tau_0)}{15 - 2r_1 r_2} \right] \\
k_{fc_1} &= \frac{1}{2} \left[\frac{(8 - r_1 r_2)M_3(\epsilon\tau_0) + (7 - r_1 r_2)N_2(\epsilon\tau_0)}{15 - 2r_1 r_2} + \right. \\
& \quad \left. j \frac{-(7 - r_1 r_2)M_2(\epsilon\tau_0) - (8 - r_1 r_2)N_3(\epsilon\tau_0)}{15 - 2r_1 r_2} \right] \\
k_{ss_{1i}} &= \frac{a_i(2 - 2r_1 r_2 + 3\alpha_i^2)}{D_1(\alpha_i)} \\
k_{sc_{1i}} &= \frac{a_i \alpha_i(4 - r_1 r_2 + \alpha_i^2)}{D_1(\alpha_i)} \\
k_{cs_{1i}} &= -\frac{b_i \beta_i(4 - r_1 r_2 + \beta_i^2)}{D_1(\beta_i)} \\
k_{cc_{1i}} &= \frac{b_i(2 - 2r_1 r_2 + 3\beta_i^2)}{D_1(\beta_i)} \\
D_1(\theta) &= -4 + 8r_1 r_2 - 4r_1^2 r_2^2 + (4 + 4r_1 r_2 + r_1^2 r_2^2)\theta^2 - (1 + 2r_1 r_2)\theta^4 + \theta^6
\end{aligned} \tag{4.47}$$

m is the number of terms in $N_4(\epsilon\tau_0)$ of the form:

$$a_i \sin \alpha_i \tau_0$$

and n is the number of terms in $N_4(\epsilon\tau_0)$ of the form:

$$b_i \cos \beta_i \tau_0$$

So, the time scale τ_1 in this case is nonlinear.

By combining all the previous results and restricting, we can express the first mode as follows.

$$\phi_1(\bar{t}) = \bar{A}_{1_0} e^{\epsilon k_{r_1} \bar{t}} e^{\epsilon \int k_1^*(\bar{t}) d\bar{t}} e^{j\bar{t}} + c.c. \quad (4.48)$$

with $k_1^*(\bar{t}) = k_1(\bar{t}) - k_{r_1}(\bar{t})$. Expressed in real function form, Equation 4.48 becomes

$$\phi_1(\bar{t}) = A_{1_0} e^{[\epsilon k_{r_1} \bar{t} + \epsilon \Re(\int k_1^*(\bar{t}) d\bar{t})]} \sin(\bar{t} + \epsilon \Im(\int k_1^*(\bar{t}) d\bar{t}) + \theta_{1_0}) \quad (4.49)$$

where A_{1_0} and θ_{1_0} are constants to be determined from the initial conditions.

Second Mode

We concentrate now on the second mode of the roll motion of the satellite, that is

$$\phi_2(\tau_0 \tau_1) = A_2(\tau_1) e^{j\sqrt{r_1 r_2} \tau_0} + c.c. \quad (4.50)$$

Substitution of this mode into Equation 4.34 yields

$$\begin{aligned} & [k_2''' + (p_{21} - 5r_1 r_2)k_2' + j[3\sqrt{r_1 r_2}k_2'' + 2\sqrt{r_1 r_2}(p_{21} - 2)k_2]] \frac{dA_2}{d\tau_1} \\ & + [p_{42}(\tau_0) - r_1 r_2 p_{22}(\tau_0) + j\sqrt{r_1 r_2}(p_{31}(\tau_0) - r_1 r_2 p_{11}(\tau_0))] A_2 = 0 \end{aligned} \quad (4.51)$$

Again, we see that A_2 is a function of τ_1 , while the coefficients are the function of τ_0 , so we can separate the variables as follows.

$$\frac{\frac{dA_2}{d\tau_1}}{A_2} = -\frac{p_{42}(\tau_0) - r_1 r_2 p_{22}(\tau_0) + j\sqrt{r_1 r_2}(p_{31}(\tau_0) - r_1 r_2 p_{11}(\tau_0))}{k_2''' + (p_{21} - 5r_1 r_2)k_2' + j[3\sqrt{r_1 r_2}k_2'' + 2\sqrt{r_1 r_2}(p_{21} - 2)k_2]} = \text{constant} = -1 \quad (4.52)$$

In the above, the constant has been chosen to be -1 for simplicity. Therefore, we get

$$A_2 = \bar{A}_{2_0} e^{-\tau_1} ; \quad \bar{A}_{2_0} = \text{arbitrary constant} \quad (4.53)$$

and the following clock equation.

$$k_2''' + (1 - 4r_1r_2)k_2' + j[3\sqrt{r_1r_2}k_2'' - 2\sqrt{r_1r_2}(1 - r_1r_2)k_2] = V_1 + V_2(\epsilon\tau_0)\cos 2\tau_0 + V_3(\epsilon\tau_0)\sin 2\tau_0 + j[W_1 + W_2(\epsilon\tau_0)\cos 2\tau_0 - W_3(\epsilon\tau_0)\sin 2\tau_0 + W_4(\epsilon\tau_0)] \quad (4.54)$$

where

$$\begin{aligned} V_1 &= 3r_1r_2 - r_1r_2^2 - 2r_1^2r_2^2 \\ V_2(\epsilon\tau_0) &= [[-2a(1 - r_1) - b(4 - r_2 - r_1r_2)]K_1^* - \\ &\quad \left[-ar_1(r_1r_2 + r_2 - 2) + br_1r_2(3 + r_2) + \frac{br_1(4 - 3r_2 - r_2^2)}{1 - r_1} \right] K_2^*] f_3(\epsilon\tau_0) \\ V_3(\epsilon\tau_0) &= [[-2a(1 - r_1) - b(4 - r_2 - r_1r_2)]K_1^* - \\ &\quad \left[-ar_1(r_1r_2 + r_2 - 2) + br_1r_2(3 + r_2) + \frac{br_1(4 - 3r_2 - r_2^2)}{1 - r_1} \right] K_2^*] f_2(\epsilon\tau_0) \\ W_1 &= \frac{5}{2}[-a(1 - r_1)K_1^* + [ar_1(1 - r_2) + br_2(1 - r_1)]K_2^*]U \\ W_2(\epsilon\tau_0) &= [[4b + a(1 - r_1)]K_1^* + \\ &\quad \left[a(r_1r_2 + r_1 - 2) - b(r_1r_2 + r_2 + 2) + \frac{2b(r_1r_2 - r_1 + r_2 - 1)}{1 - r_1} \right] K_2^*] f_2(\epsilon\tau_0) \\ W_3(\epsilon\tau_0) &= [[4b + a(1 - r_1)]K_1^* + \\ &\quad \left[a(r_1r_2 + r_1 - 2) - b(r_1r_2 + r_2 + 2) + \frac{2b(r_1r_2 - r_1 + r_2 - 1)}{1 - r_1} \right] K_2^*] f_3(\epsilon\tau_0) \\ W_4(\epsilon\tau_0) &= [-a(1 - r_1)K_1^* + [ar_1(1 - r_2) + br_2(1 - r_1)]K_2^*] \left[f_1(\epsilon\tau_0) - \frac{5}{2}U \right] \quad (4.55) \end{aligned}$$

with U as defined previously.

Note that V_1 and W_1 are constant, while V_2 , V_3 , W_2 , W_3 , and W_4 are periodic functions.

The possibility of resonance (in the sense as we have already discussed) will now

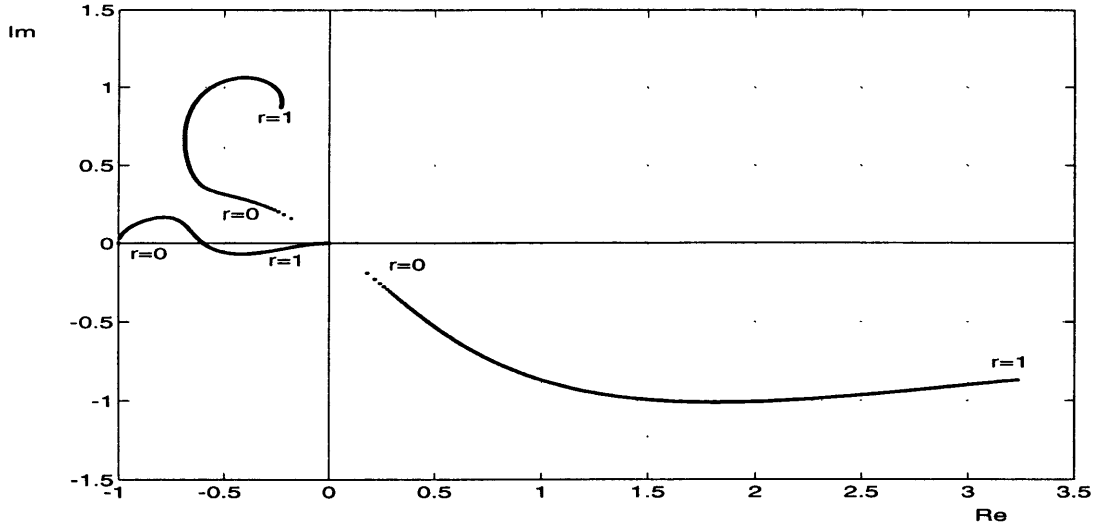


Figure 4-4: Root locus of the second mode clock equation ($r = r_1 r_2$)

be examined. The homogeneous solution of Equation 4.54 is as follows.

$$k_{h_2}(\tau_0) = \sum_{i=1}^3 D_i e^{s_i \tau_0} \quad (4.56)$$

where D_i 's are arbitrary constant, which will be chosen to be zero in the later analysis, and s_i 's are the roots of the characteristic equation:

$$s^3 + j3\sqrt{r_1 r_2} s^2 + (1 - 4r_1 r_2)s + 2j\sqrt{r_1 r_2}(1 - r_1 r_2) = 0 \quad (4.57)$$

Figure 4-4 shows the locus of the characteristic roots for all possible values of $r_1 r_2$. The limiting case where one of the s_i 's becomes zero is again ruled out, since this is not a physically meaningful case. So, in general the homogeneous solution will be of the form

$$D_i e^{\Re(s_i) \tau_0} [\cos \Im(s_i) \tau_0 + j \sin \Im(s_i) \tau_0]$$

Since none of the terms in the righthand side of Equation 4.54 is of this form, then resonance does not occur for the whole range of $r_1 r_2$ of interest.

The righthand side of Equation 4.54 consists of constant and periodic terms, hence in the nonresonance condition, the particular solution of $k(\tau_0)$ will also consist of

constant and periodic terms. Then, from the expression for the amplitude of the second mode 4.53, we can deduce that the stability of this mode is determined by the constant real part of the particular solution of $k(\tau_0)$, which is

$$k_{r_2} = \frac{5}{2} \frac{[ar_1(1-r_2) + br_2(1-r_1)]K_2^* - a(1-r_1)K_1^*}{2(1-r_1r_2)} U \quad (4.58)$$

For the second mode to be asymptotically stable, k_{r_2} must be positive. Since U is a positive constant, then the criterion for asymptotic stability of the second mode is as follows.

$$a(1-r_1)K_1^* < [ar_1(1-r_2) + br_2(1-r_1)] K_2^* \quad (4.59)$$

This stability criterion together with the stability criterion for the first mode 4.45 must be satisfied to get an asymptotically stable roll motion.

Both K_1^* and K_2^* dissipate energy of the first mode. Hence the larger the values of K_1^* and K_2^* , the faster the first mode damped. However, this is not the case for the second mode. K_2^* dissipates energy, but K_1^* pumps energy into the second mode.

Simplifying assumptions as in the case of the first mode are also used to obtain the approximate expression for $k(\tau_0)$. The result is as follows.

$$\begin{aligned} k_2(\tau_0) = & k_{r_2} + jk_{i_2} + k_{fs_2} \sin 2\tau_0 + k_{fc_2} \cos 2\tau_0 + \\ & \sum_{i=1}^m [k_{ss_{2i}} \sin \alpha_i \tau_0 + jk_{sc_{2i}} \cos \alpha_i \tau_0] + \\ & \sum_{i=1}^n [jk_{cs_{2i}} \sin \beta_i \tau_0 + k_{cc_{2i}} \cos \beta_i \tau_0] \end{aligned} \quad (4.60)$$

where

$$\begin{aligned} k_{i_2} &= \frac{V_1}{2\sqrt{r_1r_2}(1-r_1r_2)} \\ k_{fs_2} &= \frac{1}{2} \left[\frac{(3+4r_1r_2)V_2(\epsilon\tau_0) + \sqrt{r_1r_2}(5+r_1r_2)W_3(\epsilon\tau_0)}{-9+r_1r_2-6r_1^2r_2^2+r_1^3r_2^3} + \right. \\ & \quad \left. j \frac{\sqrt{r_1r_2}(5+r_1r_2)V_3(\epsilon\tau_0) + (3+4r_1r_2)W_2(\epsilon\tau_0)}{-9+r_1r_2-6r_1^2r_2^2+r_1^3r_2^3} \right] \\ k_{fc_2} &= -\frac{1}{2} \left[\frac{(3+4r_1r_2)V_3(\epsilon\tau_0) + \sqrt{r_1r_2}(5+r_1r_2)W_2(\epsilon\tau_0)}{-9+r_1r_2-6r_1^2r_2^2+r_1^3r_2^3} - \right. \end{aligned}$$

$$\begin{aligned}
& j \frac{\sqrt{r_1 r_2} (5 + r_1 r_2) V_2(\epsilon \tau_0) + (3 + 4 r_1 r_2) W_3(\epsilon \tau_0)}{-9 + r_1 r_2 - 6 r_1^2 r_2^2 + r_1^3 r_2^3} \Big] \\
k_{ss_{2i}} &= \frac{a_i \sqrt{r_1 r_2} (2 - 2 r_1 r_2 - 3 \alpha_i^2)}{D_2(\alpha_i)} \\
k_{sc_{2i}} &= \frac{a_i \alpha_i (1 - 4 r_1 r_2 - \alpha_i^2)}{D_2(\alpha_i)} \\
k_{cs_{2i}} &= -\frac{b_i \beta_i (1 - 4 r_1 r_2 - \beta_i^2)}{D_2(\beta_i)} \\
k_{cc_{2i}} &= \frac{b_i (2 - 2 r_1 r_2 + 3 \beta_i^2)}{D_2(\beta_i)} \\
D_2(\theta) &= 4 r_1 r_2 - 8 r_1^2 r_2^2 + 4 r_1^3 r_2^3 - (1 + 4 r_1 r_2 + 4 r_1^2 r_2^2) \theta^2 + \\
& (2 + 2 r_1 r_2) \theta^4 - \theta^6
\end{aligned} \tag{4.61}$$

with m the number of terms in $W_4(\epsilon \tau_0)$ of the form:

$$a_i \sin \alpha_i \tau_0$$

and n the number of terms in $W_4(\epsilon \tau_0)$ of the form:

$$b_i \cos \beta_i \tau_0$$

Again, the clock function $k_2(\tau_0)$ is complex and nonlinear. Therefore, the time scale τ_1 is also nonlinear.

Next, by restricting, we can express the second mode as follows

$$\phi_2(\bar{t}) = \bar{A}_{2_0} e^{\epsilon k_{r_2} \bar{t}} e^{\epsilon \int k_2^*(\bar{t}) d\bar{t}} e^{j\bar{t}} + c.c. \tag{4.62}$$

with $k_2^*(\bar{t}) = k_2(\bar{t}) - k_{r_2}(\bar{t})$. Expressed in real function form, Equation 4.62 becomes

$$\phi_2(\bar{t}) = A_{2_0} e^{[\epsilon k_{r_2} \bar{t} + \epsilon \Re(\int k_2^*(\bar{t}) d\bar{t})]} \sin(\bar{t} + \epsilon \Im(\int k_2^*(\bar{t}) d\bar{t}) + \theta_{2_0}) \tag{4.63}$$

where A_{2_0} and θ_{2_0} are constants to be determined from the initial conditions.

The resulting roll motion is then

$$\phi(\bar{t}) = \phi_1(\bar{t}) + \phi_2(\bar{t}) \quad (4.64)$$

with $\phi_1(\bar{t})$ and $\phi_2(\bar{t})$ given by Equations 4.49 and 4.63, respectively.

Hence, the roll motion consists of two oscillatory modes and the amplitude of both modes vary exponentially.

4.2.2 Yaw Motion

The yaw motion is very similar to the roll motion in many respects. For the sake of completeness, the yaw motion analysis is presented here. However many details of the derivation of the results, which are similar to the roll motion case, will be omitted.

The uncoupled equation of yaw motion is as follows.

$$\psi^{IV} + \epsilon Q_1(\bar{t}) \psi''' + Q_2(\bar{t}) \psi'' + \epsilon Q_3(\bar{t}) \psi' + Q_4(\bar{t}) \psi = 0 \quad (4.65)$$

where

$$\begin{aligned} Q_1(\bar{t}) &= K_2^*(a+b)f_1(\epsilon\bar{t}) - \left[\left(\frac{b}{r_1} + \frac{2a}{r_1(1-r_2)} \right) K_1^* + \left(a-b - \frac{4a}{1-r_2} \right) K_2^* \right] \\ &\quad (f_2(\epsilon\bar{t}) \cos 2\bar{t} - f_3(\epsilon\bar{t}) \sin 2\bar{t}) + O(\epsilon) \\ &\equiv q_{11}(\bar{t}) + O(\epsilon) \\ Q_2(\bar{t}) &= 1 + r_1 r_2 + \epsilon[2 + 2r_1 + 2r_1 r_2 + \left[K_1^*(b + \frac{4a}{1-r_2}) + K_2^*[a(3+r_1) - b(1+r_2) - \frac{5a}{1-r_2}] \right] (f_2(\epsilon\bar{t}) \sin 2\bar{t} + f_3(\epsilon\bar{t}) \cos 2\bar{t})] + O(\epsilon^2) \\ &\equiv q_{21}(\bar{t}) + \epsilon q_{22}(\bar{t}) + O(\epsilon^2) \\ Q_3(\bar{t}) &= [K_2^*(ar_1 + br_2) - K_1^*a(1-r_1)]f_1(\epsilon\bar{t}) + \left[K_1^*(3a + 2b + \frac{a(3+r_2)}{r_1(1-r_2)}) + \right. \\ &\quad \left. K_2^*[a(2-r_1) + b(2-r_2) + \frac{a(2+r_2)}{1-r_2}] \right] \\ &\quad (f_2(\epsilon\bar{t}) \cos 2\bar{t} - f_3(\epsilon\bar{t}) \sin 2\bar{t}) + O(\epsilon) \\ &\equiv q_{31}(\bar{t}) + O(\epsilon) \end{aligned}$$

$$\begin{aligned}
Q_4(\bar{t}) &= r_1 r_2 + \epsilon \left[5r_1 r_2 + \left(K_2^* [2br_2 + \frac{a(r_1 + 2r_2)}{1 - r_2}] + K_1^* [b + \frac{2a(1 + r_2)}{1 - r_2}] \right) (f_2(\epsilon \bar{t}) \sin 2\bar{t} + f_3(\epsilon \bar{t}) \cos 2\bar{t}) \right] + O(\epsilon^2) \\
&\equiv q_{41}(\bar{t}) + \epsilon q_{42}(\bar{t}) + O(\epsilon^2)
\end{aligned} \tag{4.66}$$

We then extend the variables as follows.

$$\begin{aligned}
\bar{t} &\longrightarrow \{\tau_0, \tau_1\} \\
\psi(\bar{t}, \epsilon) &\longrightarrow \psi(\tau_0, \tau_1)
\end{aligned} \tag{4.67}$$

where

$$\begin{aligned}
\tau_0 &= \bar{t} \\
\tau_1 &= \epsilon^\nu \int k(\bar{t}) d\bar{t}
\end{aligned} \tag{4.68}$$

The order of the coefficients of the yaw equation 4.65 is similar to the order of the coefficient of the roll equation 4.22. Hence the extended version of Equation 4.65 will also be the same as Equation 4.26 with ϕ replaced by ψ and P_i 's replaced by Q_i 's, and so will not be repeated here. It is also obvious that the application of the principle of subminimal simplification will obtain the same result as in the roll motion case, that is

$$\nu = 1 \tag{4.69}$$

The dominant order analysis then gives us

$$\frac{\partial^4 \psi}{\partial \tau_0^4} + (1 + r_1 r_2) \frac{\partial^2 \psi}{\partial \tau_0^2} + r_1 r_2 \psi = 0 \tag{4.70}$$

the solution of which is

$$\psi = B_1(\tau_1) e^{j\tau_0} + B_2(\tau_1) e^{j\sqrt{r_1 r_2} \tau_0} + c.c. \tag{4.71}$$

As can be expected, two modes are revealed, which will be studied separately.

First Mode

As before, the following will be referred as the first mode.

$$\psi_1(\tau_0\tau_1) = B_1(\tau_1) e^{j\tau_0} \quad (4.72)$$

Subdominant order analysis of the first mode then yields

$$B_1(\tau_1) = \bar{B}_{1_0} e^{-\tau_1} \ ; \ \bar{B}_{1_0} = \text{arbitrary constant} \quad (4.73)$$

and

$$\begin{aligned} k_3''' - (4 - r_1 r_2)k_3' + j[3k_3'' - 2(1 - r_1 r_2)k_3] &= \hat{M}_1 + \hat{M}_2(\epsilon\tau_0) \cos 2\tau_0 + \hat{M}_3(\epsilon\tau_0) \sin 2\tau_0 \\ &+ j[\hat{N}_1 + \hat{N}_2(\epsilon\tau_0) \cos 2\tau_0 - \hat{N}_3(\epsilon\tau_0) \sin 2\tau_0 + \hat{N}_4(\epsilon\tau_0)] \end{aligned} \quad (4.74)$$

where

$$\begin{aligned} \hat{M}_1 &= 3r_1 r_2 - 2r_1 - 2 \\ \hat{M}_2(\epsilon\tau_0) &= -[2aK_1^* + [a(3 + r_1) - b(1 + r_2) - \frac{a(5 + r_1 + 2r_2)}{1 - r_2}]K_2^*]f_3(\epsilon\tau_0) \\ \hat{M}_3(\epsilon\tau_0) &= -[2aK_1^* + [a(3 + r_1) - b(1 + r_2) - \frac{a(5 + r_1 + 2r_2)}{1 - r_2}]K_2^*]f_2(\epsilon\tau_0) \\ \hat{N}_1 &= -\frac{5}{2}[a(1 - r_1)K_1^* - [a(1 - r_1) + b(1 - r_2)]K_2^*]U \\ \hat{N}_2(\epsilon\tau_0) &= \left[-[3a + 2b - \frac{a + 2b}{r_1}]K_1^* + [a(3 - r_1) + b(1 - r_2) - \frac{a(2 - r_2)}{1 - r_2}]K_2^* \right] f_2(\epsilon\tau_0) \\ \hat{N}_3(\epsilon\tau_0) &= \left[-[3a + 2b - \frac{a + 2b}{r_1}]K_1^* + [a(3 - r_1) + b(1 - r_2) - \frac{a(2 - r_2)}{1 - r_2}]K_2^* \right] f_3(\epsilon\tau_0) \\ \hat{N}_4(\epsilon\tau_0) &= -[a(1 - r_1)K_1^* - [a(1 - r_1) + b(1 - r_2)]K_2^*] \left[f_1(\epsilon\tau_0) - \frac{5}{2}U \right] \end{aligned} \quad (4.75)$$

with U as defined in the previous section.

The coefficients of the clock differential equation 4.74 are exactly the same as the ones of the roll's first mode. Moreover the righthand side of Equation 4.74 consists of the same type of functions as the righthand side of the similar equation in the roll

case. Hence, we can deduce that resonance will not occur for all possible values of $r_1 r_2$.

The term that determines the stability of the first mode (that contributes to the constant real part of the particular solution of $k_3(\tau_0)$) is \hat{N}_1 . This term is the same with N_1 , in the previous section. Thus, the stability criterion of the first mode of the yaw motion is the same with that of the roll motion, that is

$$a(1 - r_1)K_1^* + [a(1 - r_1) + b(1 - r_2)] K_2^* > 0 \quad (4.76)$$

The approximate solution of $k(\tau_0)$ using the simplifying assumptions as in the roll case is as follows.

$$\begin{aligned} k_3(\tau_0) = & k_{r_3} + j k_{i_3} + k_{fs_3} \sin 2\tau_0 + k_{fc_3} \cos 2\tau_0 + \\ & \sum_{i=1}^m [k_{ss_{3i}} \sin \alpha_i \tau_0 + j k_{sc_{3i}} \cos \alpha_i \tau_0] + \\ & \sum_{i=1}^n [j k_{cs_{3i}} \sin \beta_i \tau_0 + k_{cc_{3i}} \cos \beta_i \tau_0] \end{aligned} \quad (4.77)$$

where

$$\begin{aligned} k_{r_3} &= k_{r_1} \\ k_{i_3} &= \frac{\hat{M}_3}{2(1 - r_1 r_2)} \\ k_{fs_3} &= \frac{1}{2} \left[\frac{-(8 - r_1 r_2) \hat{M}_2(\epsilon \tau_0) - (7 - r_1 r_2) \hat{N}_3(\epsilon \tau_0)}{15 - 2r_1 r_2} + \right. \\ & \quad \left. j \frac{-(7 - r_1 r_2) \hat{M}_3(\epsilon \tau_0) - (8 - r_1 r_2) \hat{N}_2(\epsilon \tau_0)}{15 - 2r_1 r_2} \right] \\ k_{fc_3} &= \frac{1}{2} \left[\frac{(8 - r_1 r_2) \hat{M}_3(\epsilon \tau_0) + (7 - r_1 r_2) \hat{N}_2(\epsilon \tau_0)}{15 - 2r_1 r_2} + \right. \\ & \quad \left. j \frac{-(7 - r_1 r_2) \hat{M}_2(\epsilon \tau_0) - (8 - r_1 r_2) \hat{N}_3(\epsilon \tau_0)}{15 - 2r_1 r_2} \right] \\ k_{ss_{3i}} &= \frac{a_i(2 - 2r_1 r_2 + 3\alpha_i^2)}{D_3(\alpha_i)} \\ k_{sc_{3i}} &= \frac{a_i \alpha_i(4 - r_1 r_2 + \alpha_i^2)}{D_3(\alpha_i)} \end{aligned}$$

$$\begin{aligned}
k_{cs_{3i}} &= -\frac{b_i \beta_i (4 - r_1 r_2 + \beta_i^2)}{D_3(\beta_i)} \\
k_{cc_{3i}} &= \frac{b_i (2 - 2r_1 r_2 + 3\beta_i^2)}{D_3(\beta_i)} \\
D_3(\theta) &= -4 + 8r_1 r_2 - 4r_1^2 r_2^2 + (4 + 4r_1 r_2 + r_1^2 r_2^2) \theta^2 - (1 + 2r_1 r_2) \theta^4 + \theta^6
\end{aligned} \tag{4.78}$$

with m the number of terms in $N_4(\epsilon \tau_0)$ of the form:

$$a_i \sin \alpha_i \tau_0$$

and n the number of terms in $N_4(\epsilon \tau_0)$ of the form:

$$b_i \cos \beta_i \tau_0$$

By restriction, we get the following expression for the first mode of the yaw motion.

$$\psi_1(\bar{t}) = B_{1_0} e^{[\epsilon k_{r_3} \bar{t} + \epsilon \Re(\int k_3^*(\bar{t}) d\bar{t})]} \sin(\bar{t} + \epsilon \Im(\int k_3^*(\bar{t}) d\bar{t}) + \theta_{3_0}) \tag{4.79}$$

where B_{1_0} and θ_{3_0} are constants to be determined from the initial conditions. In the above equation, $k_3^*(\bar{t}) = k_3(\bar{t}) - k_{r_3}(\bar{t})$.

Second Mode

Subdominant order analysis of the second mode

$$\psi_2(\tau_0 \tau_1) = B_1(\tau_1) e^{j\sqrt{\tau_1 \tau_2} \tau_0} \tag{4.80}$$

leads to the following.

$$B_2 = \bar{B}_{2_0} e^{-\tau_1} ; \quad \bar{B}_{2_0} = \text{arbitrary constant} \tag{4.81}$$

$$k_4''' + (1 - 4r_1r_2)k_4' + j[3\sqrt{r_1r_2}k_4'' - 2\sqrt{r_1r_2}(1 - r_1r_2)k_4] = \hat{V}_1 + \hat{V}_2(\epsilon\tau_0) \cos 2\tau_0 + \hat{V}_3(\epsilon\tau_0) \sin 2\tau_0 + j[\hat{W}_1 + \hat{W}_2(\epsilon\tau_0) \cos 2\tau_0 - \hat{W}_3(\epsilon\tau_0) \sin 2\tau_0 + \hat{W}_4(\epsilon\tau_0)] \quad (4.82)$$

where

$$\begin{aligned} \hat{V}_1 &= 3r_1r_2 - 2r_1^2r_2 - 2r_1^2r_2^2 \\ \hat{V}_2(\epsilon\tau_0) &= \left[\left[b(1 - r_1r_2) + \frac{2a(1 + r_2 - 2r_1r_2)}{1 - r_2} \right] K_1^* + \left[-ar_1r_2(3 + r_1) + br_2(r_1r_2) + r_1 - 2 + \frac{a(5r_1r_2 - r_1 - 2r_2)}{1 - r_2} \right] K_2^* \right] f_3(\epsilon\tau_0) \\ \hat{V}_3(\epsilon\tau_0) &= \left[\left[b(1 - r_1r_2) + \frac{2a(1 + r_2 - 2r_1r_2)}{1 - r_2} \right] K_1^* + \left[-ar_1r_2(3 + r_1) + br_2(r_1r_2) + r_1 - 2 + \frac{a(5r_1r_2 - r_1 - 2r_2)}{1 - r_2} \right] K_2^* \right] f_2(\epsilon\tau_0) \\ \hat{W}_1 &= \frac{5}{2} [-a(1 - r_1)K_1^* + [ar_1(1 - r_2) + br_2(1 - r_1)]K_2^*] U \\ \hat{W}_2(\epsilon\tau_0) &= \left[\left[3a + 2b(1 + r_2) + \frac{a(4r_1r_2 + r_2 + 3)}{r_1(1 - r_2)} \right] K_1^* + \left[a(r_1r_2 - r_1 + 2) - b(r_1r_2 + r_2 - 2) - \frac{a(4r_1r_2 - r_2 - 2)}{1 - r_2} \right] K_2^* \right] f_2(\epsilon\tau_0) \\ \hat{W}_3(\epsilon\tau_0) &= \left[\left[3a + 2b(1 + r_2) + \frac{a(4r_1r_2 + r_2 + 3)}{r_1(1 - r_2)} \right] K_1^* + \left[a(r_1r_2 - r_1 + 2) - b(r_1r_2 + r_2 - 2) - \frac{a(4r_1r_2 - r_2 - 2)}{1 - r_2} \right] K_2^* \right] f_3(\epsilon\tau_0) \\ \hat{W}_4(\epsilon\tau_0) &= [-a(1 - r_1)K_1^* + [ar_1(1 - r_2) + br_2(1 - r_1)]K_2^*] \left[f_1(\epsilon\tau_0) - \frac{5}{2}U \right] \quad (4.83) \end{aligned}$$

Again, we observe that the term that contributes to the constant real part of $k_4(\tau_0)$, namely \hat{W}_1 , is the same as W_1 in the previous section. Therefore, we will arrive at the same stability criterion as the second mode of the roll motion. That is, to get an asymptotically stable second mode, we must have

$$a(1 - r_1)K_1^* < [ar_1(1 - r_2) + br_2(1 - r_1)]K_2^* \quad (4.84)$$

Thus, the roll and yaw motion of the magnetically controlled spinning asymmetric satellite are governed by the same stability criteria.

The approximate solution of $k(\tau_0)$ can be shown to be as follows.

$$\begin{aligned}
k_4(\tau_0) = & k_{r_4} + jk_{i_4} + k_{fs_4} \sin 2\tau_0 + k_{fc_4} \cos 2\tau_0 + \\
& \sum_{i=1}^m [k_{ss_{4i}} \sin \alpha_i \tau_0 + jk_{sc_{4i}} \cos \alpha_i \tau_0] + \\
& \sum_{i=1}^n [jk_{cs_{4i}} \sin \beta_i \tau_0 + k_{cc_{4i}} \cos \beta_i \tau_0]
\end{aligned} \tag{4.85}$$

where

$$\begin{aligned}
k_{r_4} &= k_{r_2} \\
k_{i_4} &= \frac{\hat{V}_1}{2\sqrt{r_1 r_2}(1 - r_1 r_2)} \\
k_{fs_4} &= \frac{1}{2} \left[\frac{(3 + 4r_1 r_2)\hat{V}_2(\epsilon\tau_0) + \sqrt{r_1 r_2}(5 + r_1 r_2)\hat{W}_3(\epsilon\tau_0)}{-9 + r_1 r_2 - 6r_1^2 r_2^2 + r_1^3 r_2^3} + \right. \\
& \quad \left. j \frac{\sqrt{r_1 r_2}(5 + r_1 r_2)\hat{V}_3(\epsilon\tau_0) + (3 + 4r_1 r_2)\hat{W}_2(\epsilon\tau_0)}{-9 + r_1 r_2 - 6r_1^2 r_2^2 + r_1^3 r_2^3} \right] \\
k_{fc_4} &= -\frac{1}{2} \left[\frac{(3 + 4r_1 r_2)\hat{V}_3(\epsilon\tau_0) + \sqrt{r_1 r_2}(5 + r_1 r_2)\hat{W}_2(\epsilon\tau_0)}{-9 + r_1 r_2 - 6r_1^2 r_2^2 + r_1^3 r_2^3} - \right. \\
& \quad \left. j \frac{\sqrt{r_1 r_2}(5 + r_1 r_2)\hat{V}_2(\epsilon\tau_0) + (3 + 4r_1 r_2)\hat{W}_3(\epsilon\tau_0)}{-9 + r_1 r_2 - 6r_1^2 r_2^2 + r_1^3 r_2^3} \right] \\
k_{ss_{4i}} &= \frac{a_i \sqrt{r_1 r_2}(2 - 2r_1 r_2 - 3\alpha_i^2)}{D_4(\alpha_i)} \\
k_{sc_{4i}} &= \frac{a_i \alpha_i(1 - 4r_1 r_2 - \alpha_i^2)}{D_4(\alpha_i)} \\
k_{cs_{4i}} &= -\frac{b_i \beta_i(1 - 4r_1 r_2 - \beta_i^2)}{D_4(\beta_i)} \\
k_{cc_{4i}} &= \frac{b_i(2 - 2r_1 r_2 + 3\beta_i^2)}{D_4(\beta_i)} \\
D_4(\theta) &= 4r_1 r_2 - 8r_1^2 r_2^2 + 4r_1^3 r_2^3 - (1 + 4r_1 r_2 + 4r_1^2 r_2^2)\theta^2 + \\
& \quad (2 + 2r_1 r_2)\theta^4 - \theta^6
\end{aligned} \tag{4.86}$$

with m the number of terms in $W_4(\epsilon\tau_0)$ of the form:

$$a_i \sin \alpha_i \tau_0$$

and n the number of terms in $W_4(\epsilon\tau_0)$ of the form:

$$b_i \cos \beta_i \tau_0$$

Then the second mode can be expressed in real function form as follows.

$$\psi_2(\bar{t}) = B_{2_0} e^{[\epsilon k_{r_4} \bar{t} + \epsilon \Re(\int k_4^*(\bar{t}) d\bar{t})]} \sin(\bar{t} + \epsilon \Im(\int k_4^*(\bar{t}) d\bar{t}) + \theta_{4_0}) \quad (4.87)$$

where B_{2_0} and θ_{4_0} are constants to be determined from the initial conditions. Also, in the above equation, $k_4^*(\bar{t}) = k_4(\bar{t}) - k_{r_4}(\bar{t})$.

The combined yaw motion is then

$$\psi(\bar{t}) = \psi_1(\bar{t}) + \psi_2(\bar{t}) \quad (4.88)$$

with $\psi_1(\bar{t})$ and $\psi_2(\bar{t})$ given by Equations 4.79 and 4.87, respectively.

4.2.3 Summary and Performance Evaluation

The attitude stability criteria for a magnetically controlled asymmetric spinning satellite with the control law given by Equation 3.6 have been derived. The same stability criteria govern both roll and yaw motion of the satellite. The statement of the stability criteria is as follows.

To get an asymptotically stable roll and yaw motion, the following relations must hold :

$$a(1 - r_1)K_1^* + [a(1 - r_1) + b(1 - r_2)] K_2^* > 0 \quad (4.89)$$

$$a(1 - r_1)K_1^* < [ar_1(1 - r_2) + br_2(1 - r_1)] K_2^* \quad (4.90)$$

So, the selection of the control gains for stability depends only on the inertia distribution, the spin rate and the altitude of the satellite, and does not depend on the other orbital parameters.

The time constant of the motion, on the other hand, depends not only on the inertia distribution and the spin rate but also on the orbital parameters of the satellite. From the previous results, the approximate time constants of the roll/yaw motion are as follows :

- First mode :

$$T_{c_1} = \frac{4(1 - r_1 r_2)}{\epsilon 5[a(1 - r_1)K_1^* + [a(1 - r_1) + b(1 - r_2)]K_2^*]\omega_s U} \quad (4.91)$$

- Second mode :

$$T_{c_2} = \frac{4(1 - r_1 r_2)}{\epsilon 5[ar_1(1 - r_2) + br_2(1 - r_1)]K_2^* - a(1 - r_1)K_1^*]\omega_s U} \quad (4.92)$$

These time constants can be useful to predict when the response reaches the steady state condition. The normal steady state criterion is that the response has stayed within 5 % of its initial condition. The time to reach this steady state condition is about three times the time constant of the motion ($t = 3T$).

In Equations 4.91 and 4.92, U is a constant for a particular orbit, the value of which depends on the inclination of the orbit. The value of U as a function of the inclination is plotted in Figure 4-5. The value of U reaches a maximum when the satellite is in polar orbit, and a minimum when the satellite is in equatorial orbit. Thus, the magnetic control system is more effective for satellite in an orbit that makes high angle with respect to the equatorial plane. If the magnetic control is used in a near equatorial orbit, then high gains should be employed.

The altitude of the orbit of the satellite also has influence on the effectiveness of the control system. The higher the altitude of the satellite, the smaller the magnitude of the geomagnetic field it encounters. So, higher gains is needed to achieve a certain time constant requirement.

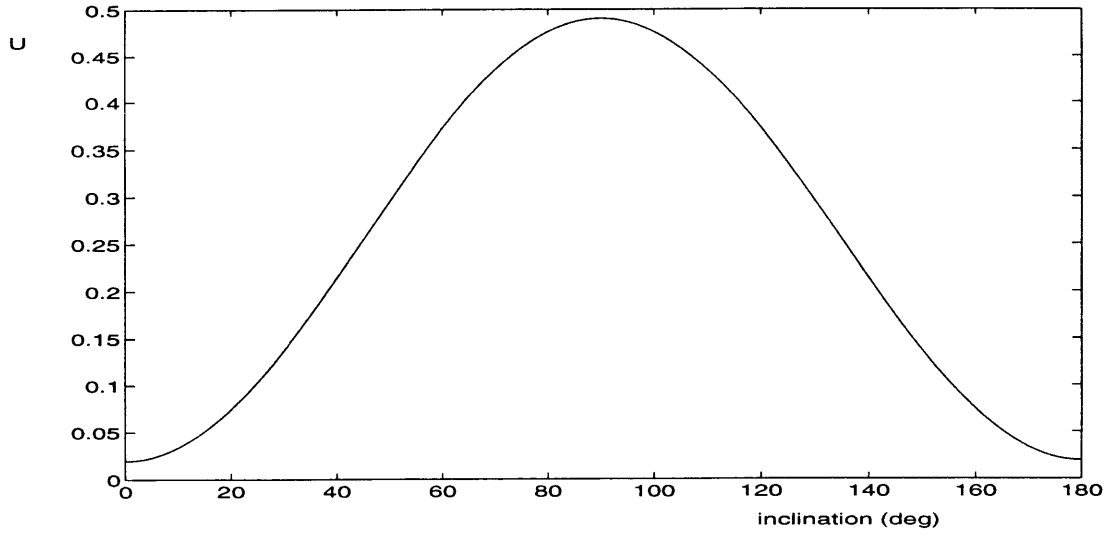


Figure 4-5: Variation of U with inclination

The effectiveness of the magnetic control system also depends on the relative position of the geomagnetic dipole with respect to the orbital plane of the satellite. The effectiveness will be maximum when the geomagnetic dipole lies on the orbital plane, since in this case, for a certain magnitude of the onboard magnetic dipole, the torque produced is the largest. The approximate time constants must be slightly modified if this effect is to be included. However, for preliminary analysis purposes, the approximations 4.91 and 4.92 give fairly accurate prediction for the exact situation.

Spinning axisymmetric satellites, which are very common in practice, are a special case of the satellites treated here. Thus the results obtained are valid for the spinning axisymmetric satellites as well. For this type of satellite,

$$\begin{aligned} r_1 &= r_2 = r \\ a &= b = 1 \end{aligned} \tag{4.93}$$

so that the stability criteria for the roll and yaw motion of the satellite become as follows.

$$K_1^* + K_2^* > 0 \quad (4.94)$$

$$K_1^* < 2rK_2^* \quad (4.95)$$

Also the expressions for the approximate time constants of the roll/yaw motion are simplified to be

- First mode :

$$T_{c_1} = \frac{4(1+r)}{\epsilon 5[K_1^* + K_2^*]\omega_s U} \quad (4.96)$$

- Second mode :

$$T_{c_2} = \frac{4(1+r)}{\epsilon 5[2rK_2^* - K_1^*]\omega_s U} \quad (4.97)$$

Previous discussion on the performance of the system is also valid for this case.

It should be noted that the dependent variables are not expanded into first or higher orders in obtaining the approximations. Therefore, the solutions obtained are only the zeroth order approximations to the exact solutions. The error of the approximations is of the order of the first term neglected, which for this case is of $O(\epsilon)$.

4.2.4 Comparison with Numerical Results

The explicit approximate solutions derived will now be compared with the exact solutions obtained by solving the equations of motion numerically. The numerical simulation was done for a satellite model that has the following parameters.

- Moments of inertia :

$$I_x = 140 \text{ kg m}^2 \quad I_y = 80 \text{ kg m}^2 \quad I_z = 150 \text{ kg m}^2$$

- Spin rate : $\omega_s = 0.2 \text{ rad/s}$

- Altitude of the orbit : $H = 1000 \text{ km}$

- Inclination of the orbit : $i = 60^\circ$

For the numerical values used, the value of ϵ is

$$\epsilon = 0.005$$

The stability criteria for the roll/yaw motion then become

$$\begin{aligned} 0.6614K_1^* + 1.3229K_2^* &> 0 \\ 0.6614K_1^* &< 0.6260K_2^* \end{aligned} \tag{4.98}$$

Several numerical simulations were done near the boundary of the stability to examine the accuracy of the stability criteria. From these simulations we can conclude that the stability criteria obtained give a very accurate stability prediction. Figures 4-6 and 4-7 are the examples of the response of the system when the stability criteria are slightly violated. Figure 4-6 specifically shows the response when the first stability criterion is violated while the second stability criterion is satisfied. We can see from the figure that the second mode is decaying and the amplitude of the first mode (the fast oscillation) is amplified. On the other hand, Figure 4-7 shows the response when only the second stability criterion is violated. From this figure we can observe that the first mode is attenuated while the amplitude of the second mode is slowly increasing (instability), as predicted.

For response comparison purposes, the values of K_1^* and K_2^* selected are

$$\begin{aligned} K_1^* &= 1 \\ K_2^* &= 3 \end{aligned}$$

which still satisfy the stability criteria. Figures 4-8 and 4-9 show the roll and yaw responses of the satellite as obtained using numerical integration and GMS, presented in the long and short scales. We note that the same initial conditions are used in both simulations. The dominant frequencies predicted by using GMS are 0.2 rad/s and 0.0125 rad/s . We can see from the figures that these frequency predictions are very accurate.

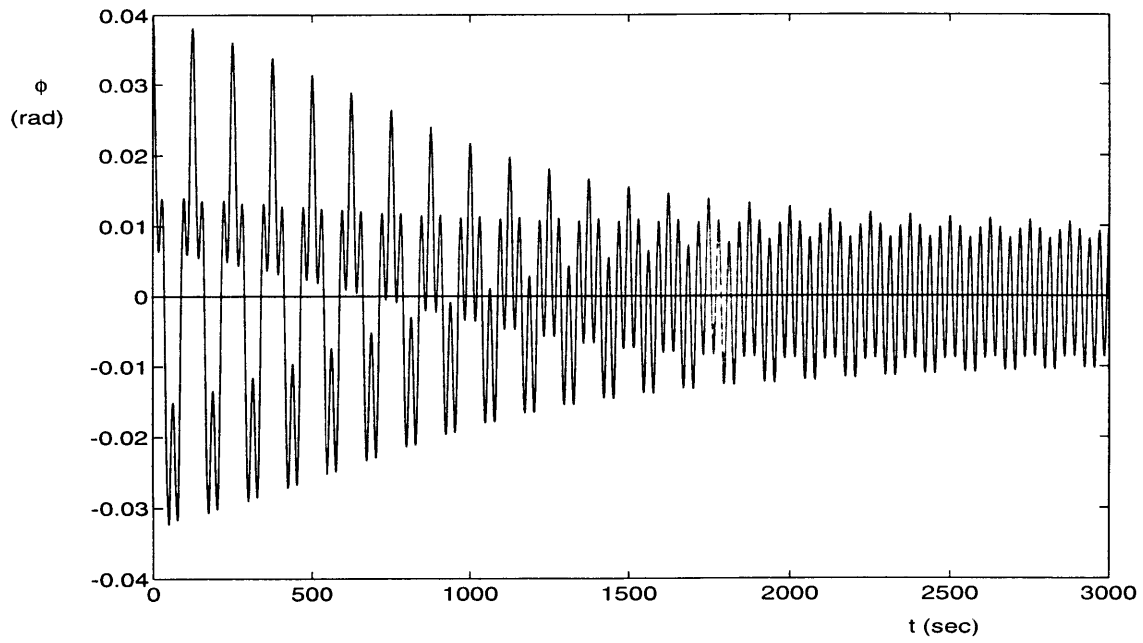


Figure 4-6: Instability due to slight violation of the first mode stability criterion ($K_1^* = -2.1$ and $K_2^* = 1$)

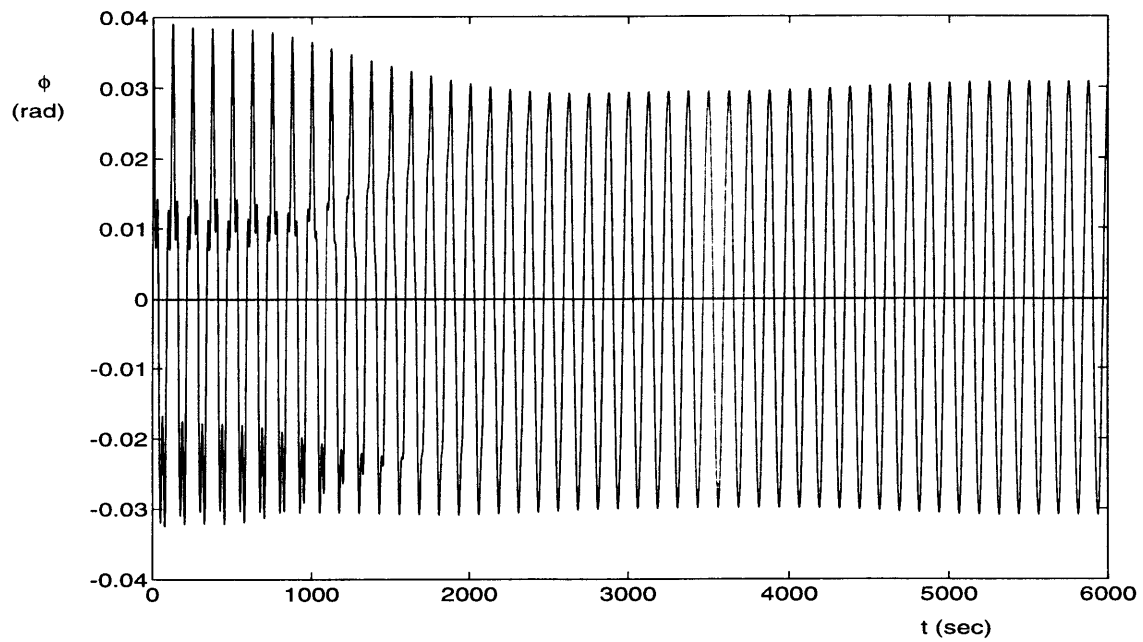


Figure 4-7: Instability due to slight violation of the second mode stability criterion ($K_1^* = 1$ and $K_2^* = 1$)

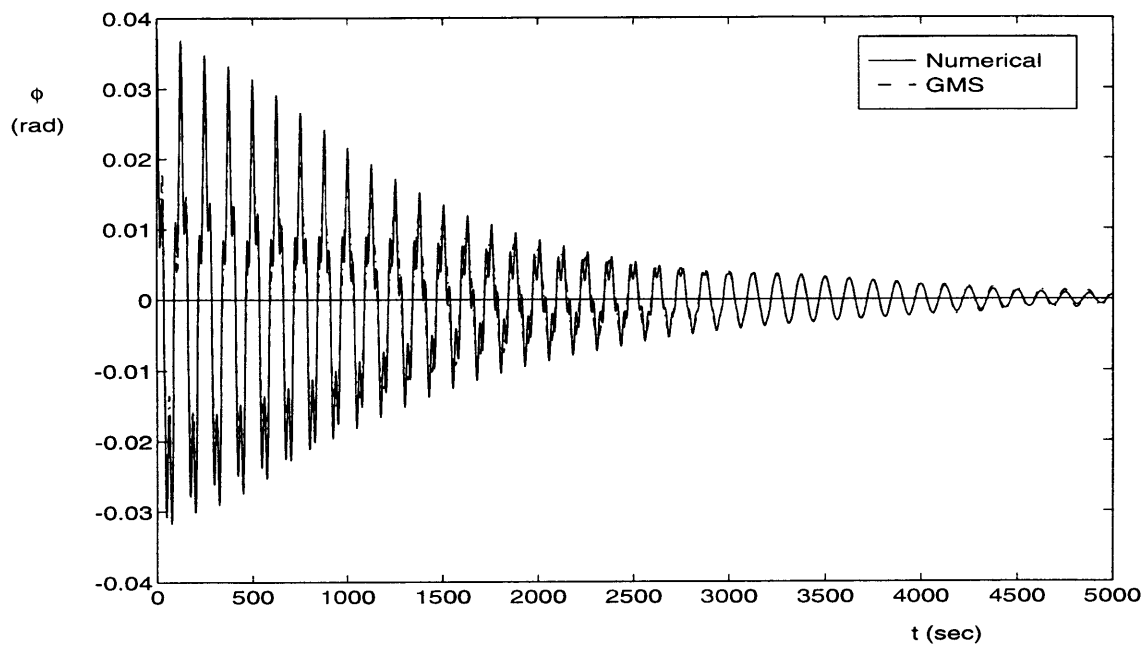
For the numerical values used, the approximate time constants of the motion are

$$T_{c_1} = 610.14 \text{ s} \quad (4.99)$$

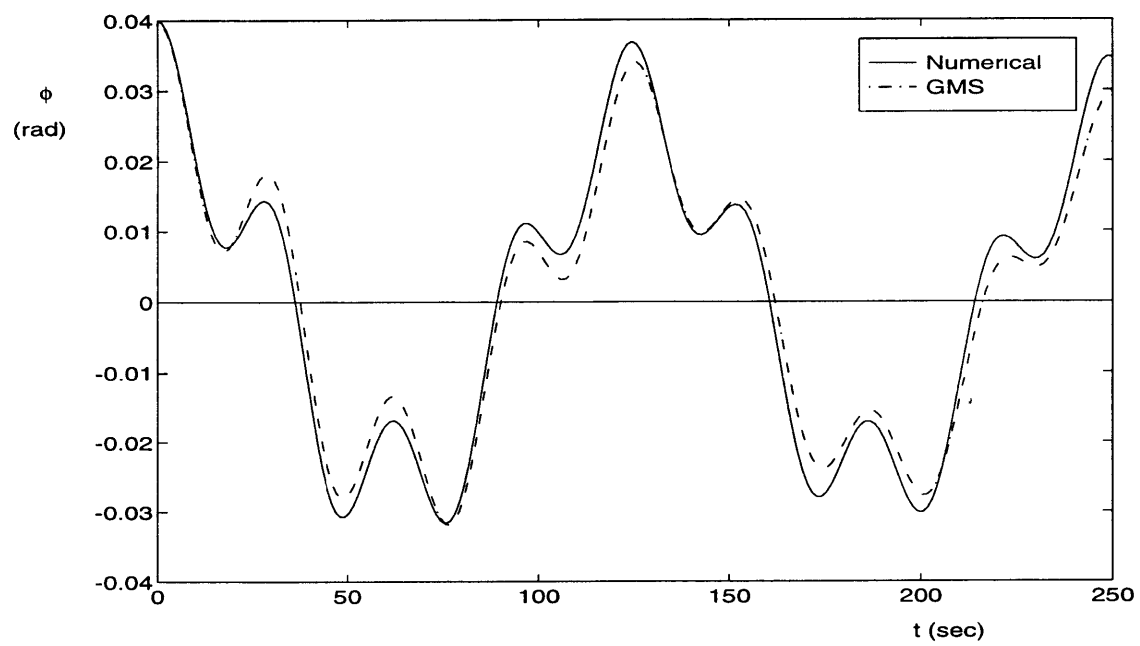
$$T_{c_2} = 1658.6 \text{ s} \quad (4.100)$$

So, the first and second mode are expected to have been attenuated to within 5 % of their initial values after 1830.42 s and 4975.8 s, respectively. Although it is hard to extract the first and second modes from the exact response, however it can be observed from the figures that indeed the fast oscillation (first mode) has been attenuated significantly after 1830 s. Also the slow mode (second mode) has become insignificant close to 5000 s. So, again, approximation using the GMS approach is shown to be fairly good.

Finally we examine the error of the approximations. Figure 4-10 presents the magnitude of the errors of the approximations. As predicted earlier the maximum errors is of $O(\epsilon)$. The errors are mainly due to the neglected terms in the expansion and the simplifying assumption used in deriving the explicit solution. Therefore, they are relatively large in the region where the first mode is significant, because in this region, both modes contribute to the errors. Overall, the approximations using GMS approach obtain a very good agreement with the exact conditions.

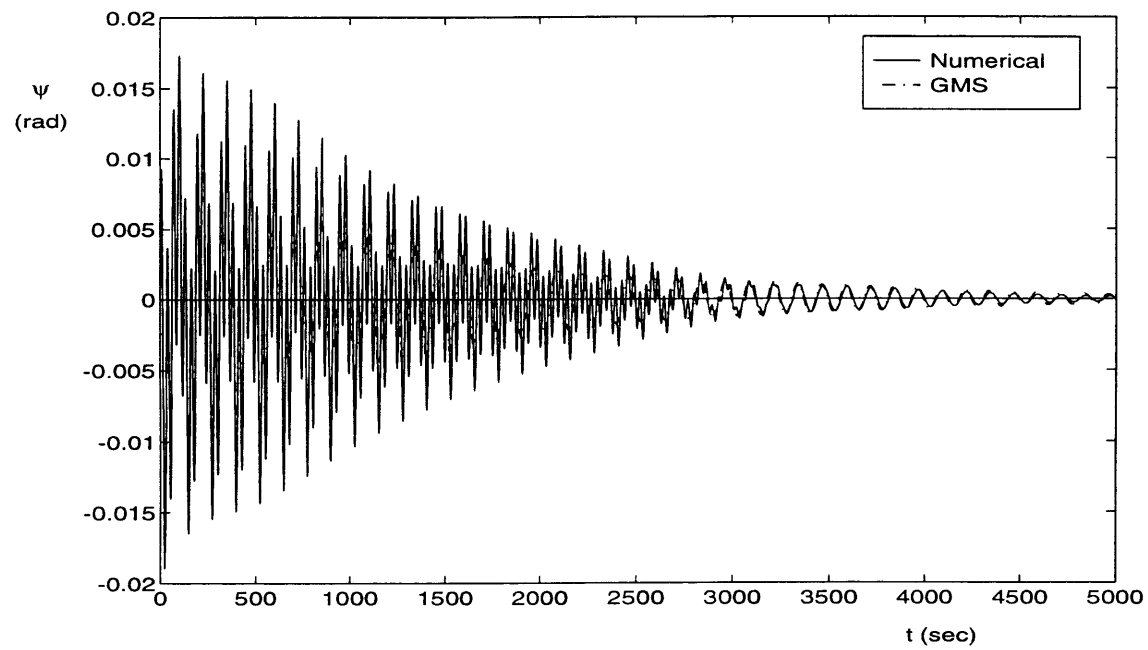


(a) Long term response

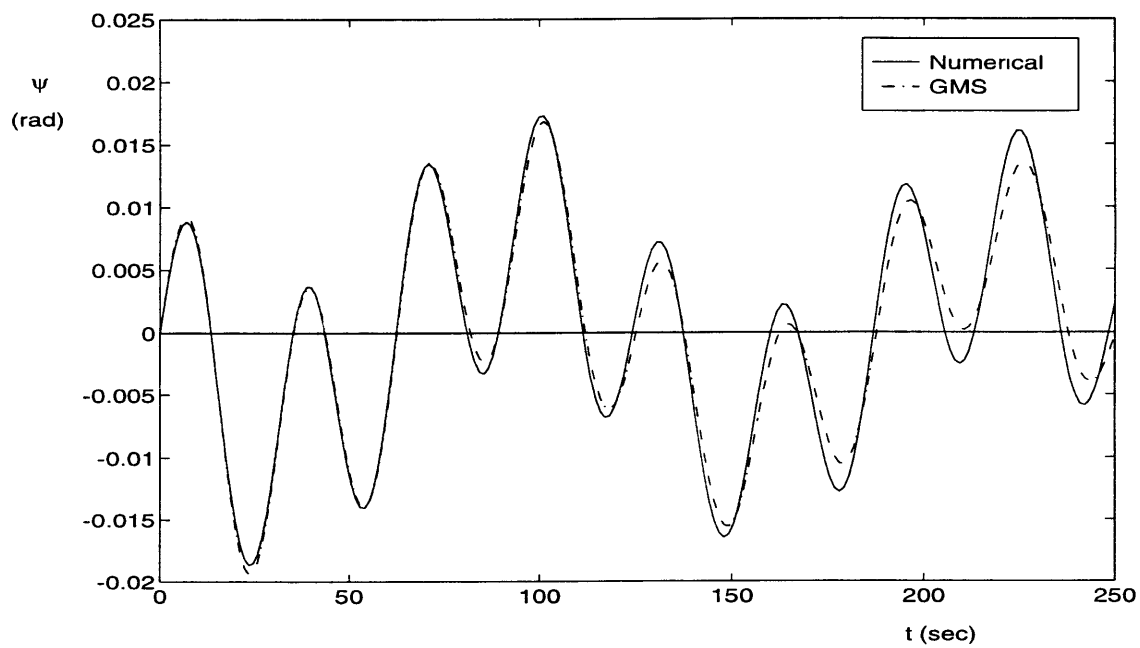


(b) Short term response

Figure 4-8: Comparison of numerical and GMS results for roll motion

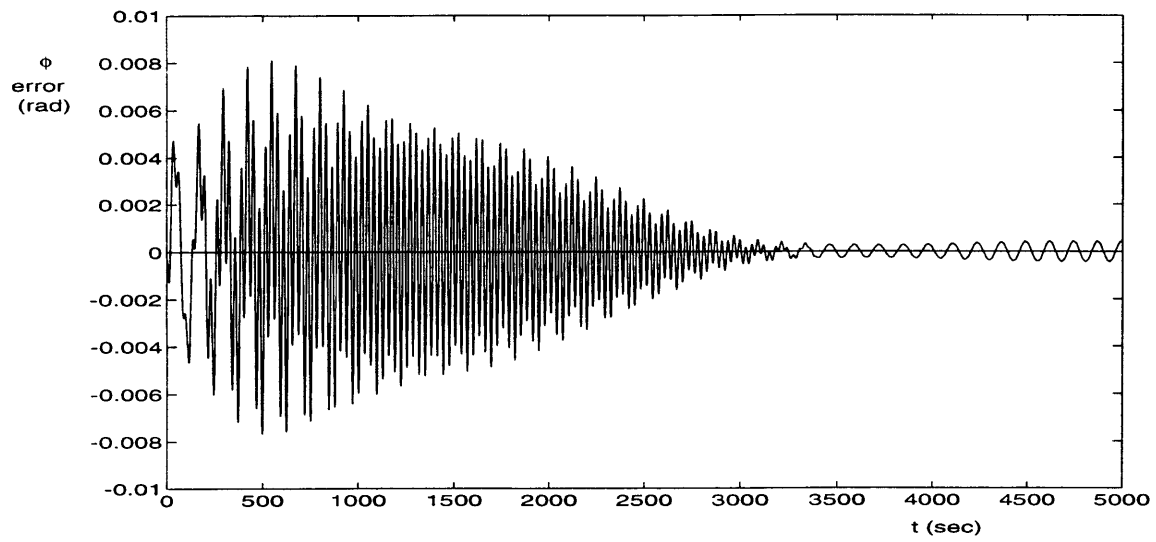


(a) Long term response

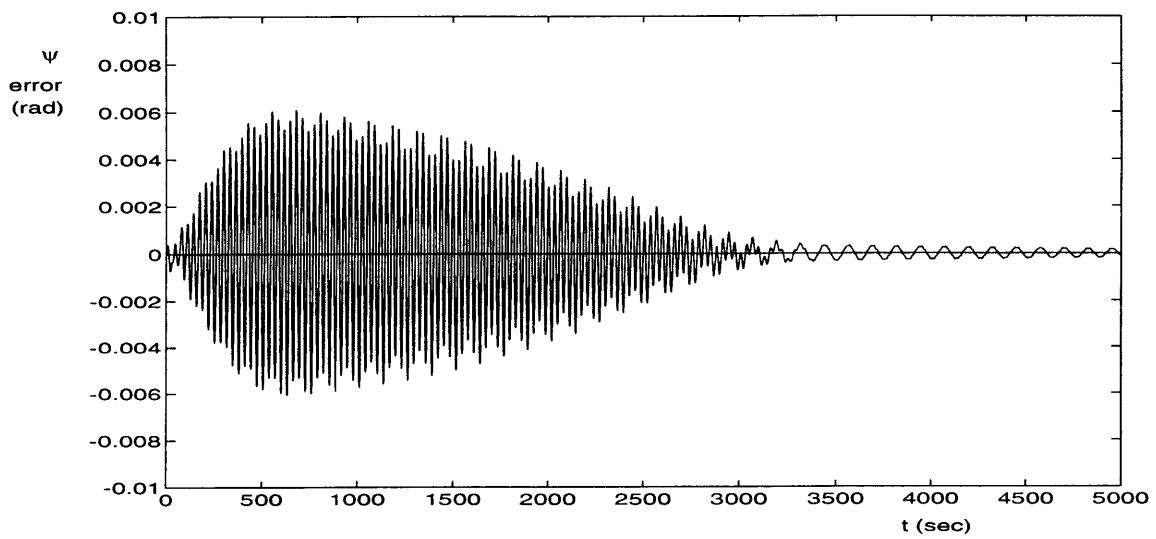


(b) Short term response

Figure 4-9: Comparison of numerical and GMS results for yaw motion



(a)



(b)

Figure 4-10: Error of the approximations

Chapter 5

Magnetic Attitude Control of a Dual Spin Satellite

5.1 The Equations of Motion

5.1.1 The Modified Euler's Equations

Several assumptions that will be used in the analysis are as follows :

- The orbit of the satellite is circular, which implies that the orbital angular speed Ω is constant.
- The satellite is a rigid body and it consists of a despun part, which will be called *platform*, and a spinning part, which will be called *rotor* or *momentum wheel*. The rotor is usually used to provide gyroscopic stability for the satellite. In our discussion here, we will concentrate on the earth-pointing type of satellite, which is most common in practice. For this type of satellite, the platform will rotate at the same angular speed as the orbit.
- The platform may be asymmetric and is oriented such that one of its principal axes is in the direction of the radius vector from the center of the Earth to the satellite's center of mass.

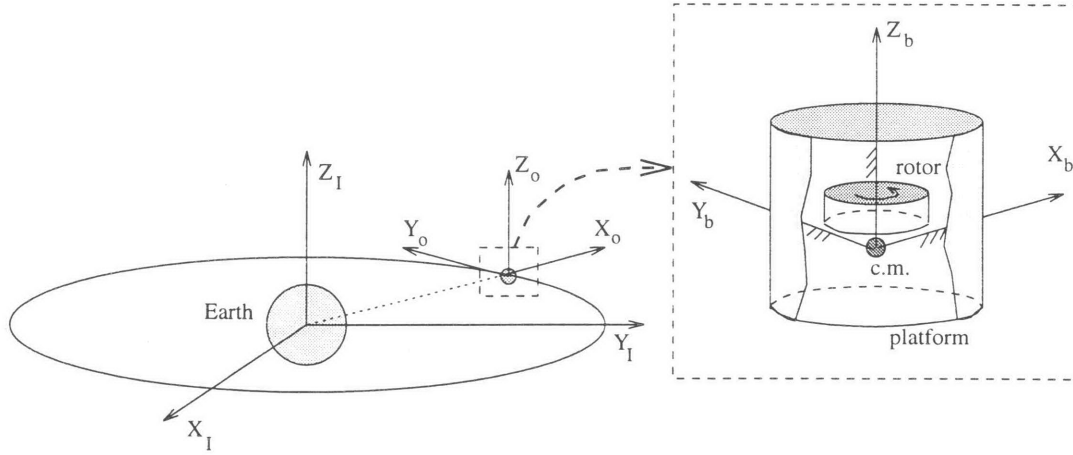


Figure 5-1: The axes system for dual spin satellite

- The rotor of the satellite is axisymmetric. Its spin axis is the axis of symmetry and this axis coincides with the pitch axis of the satellite, which is normal to the orbit plane in nominal condition. Therefore, while spinning, the rotor does not change the inertia distribution of the satellite. We will also assume that the spin rate of the rotor is constant.
- The body-fixed axes ($X_b Y_b Z_b$) of the satellite is fixed to the satellite's platform and coincide with the principal axes of the satellite. The X_b -axis is in the direction of the radius vector from the center of the earth to the center of mass of the satellite. The Z_b -axis is in the direction normal to the satellite's orbital plane. And the Y_b -axis completes the righthanded Cartesian coordinate system. See Figure 5-1. We denote the principal moments of inertial of the satellite about the X_b , Y_b , and Z_b axes as I_x , I_y , and I_z , respectively.

It is clear from the previous assumptions, that in nominal condition, the body-fixed coordinate system of the satellite coincides with the orbiting coordinate system. Because of this, the actual attitude of the satellite will be expressed in terms of deviations from the orbiting coordinate system. The sequence of rotations and the associated Euler angles for the transformation between the orbiting coordinate system and the body-fixed coordinate system as defined in Chapter 4 will be used again here. Expressed in terms of the defined Euler angles, the nominal condition of the satellite

is

$$\phi = \psi = \theta = 0$$

The purpose of the attitude control system is therefore to maintain this nominal condition.

The angular velocity of the satellite is given by

$$\begin{aligned}\omega &= \omega_x \mathbf{i}_{x_b} + \omega_y \mathbf{i}_{y_b} + \omega_z \mathbf{i}_{z_b} \\ &= (\dot{\theta} + \Omega) \mathbf{i}_{z_o} + \dot{\psi} \mathbf{i}_{x_1} + \dot{\phi} \mathbf{i}_{y_b}\end{aligned}\tag{5.1}$$

In our analysis here, we will assume that the pitch motion is controlled separately and that we can always have at any time

$$\theta = \dot{\theta} = 0\tag{5.2}$$

In practice, the pitch motion can be controlled by changing the spin rate of the rotor. Since the spin rate of the rotor is usually high and only small torque needed to compensate the pitch deviation, then only small changes in spin rate for short period of time needed to produce the desired control torque. Hence, even for the satellite that uses rotor spin rate for pitch control, the assumption that the rotor spin rate is constant is justifiable.

We also assume that the angular and angular rate deviations (ϕ , ψ , $\dot{\phi}$, and $\dot{\psi}$) of the satellite with respect to its nominal condition are small. By this assumption, we can express

$$\begin{aligned}\omega_x &= \dot{\psi} - \Omega\phi \\ \omega_y &= \dot{\phi} + \Omega\psi \\ \omega_z &= \Omega\end{aligned}\tag{5.3}$$

and

$$\begin{aligned}
\dot{\omega}_x &= \ddot{\psi} - \Omega \dot{\phi} \\
\dot{\omega}_y &= \ddot{\phi} + \Omega \dot{\psi} \\
\dot{\omega}_z &= 0
\end{aligned} \tag{5.4}$$

Hence, we can write the components of the angular momentum vector as follows :

$$\begin{aligned}
H_x &= I_x(\dot{\psi} - \Omega \phi) \\
H_y &= I_y(\dot{\phi} + \Omega \psi) \\
H_z &= I_z \Omega + h_r
\end{aligned} \tag{5.5}$$

where h_r is magnitude of the angular momentum of the rotor only.

For the dual spin satellite, if we write Equation 4.5 in scalar form, we obtain the followings :

$$\begin{aligned}
I_x \omega_x + (I_z - I_y) \omega_y \omega_z - \omega_y h_r &= L_x \\
I_y \omega_y + (I_x - I_z) \omega_x \omega_z + \omega_x h_r &= L_y \\
I_z \omega_z + (I_y - I_x) \omega_x \omega_y + \dot{h}_r &= L_z
\end{aligned} \tag{5.6}$$

where L_x, L_y , and L_z are the components of the external torques acting on the satellite. These equations are usually called as the modified Euler's equations. The difference with the original Euler's equations is the appearance of terms containing h_r or \dot{h}_r . Then, the substitution of Equations 5.3 and 5.4 into Equations 5.6 yields

$$\begin{aligned}
I_y \ddot{\phi} + \Omega(h - I_x \Omega) \phi - [h - (I_x + I_y) \Omega] \dot{\psi} &= L_y \\
I_x \ddot{\psi} + \Omega(h - I_y \Omega) \psi - [h - (I_x + I_y) \Omega] \dot{\phi} &= L_x
\end{aligned} \tag{5.7}$$

where $h \equiv h_r + I_z \Omega$

We next assume that the only external torque acting on the satellite is the magnetic control torque. All other external torques will be neglected. This is based on the fact that even the gravity gradient torque, which is usually the major contributor of disturbance torque, is only of second order in magnitude for satellites utilizing magnetic attitude control (see Appendix A for detail). It will be clear from our later analysis, that second order magnitude torque does not have significant influence in the approximations developed.

5.1.2 The Magnetic Control Torque

As already discussed in Chapter 3, the magnetic dipole used for attitude control is aligned with the pitch axis of the satellite. For this case, the control torque produced will have components only about the roll and yaw axes of the satellite. This will serve our purpose since we only need to control the roll and yaw attitude of the satellite and do not want to disturb the pitch attitude of the satellite. The control law used in the magnetic attitude control system has already been discussed in Chapter 3. We have also given there the general expression for the components of the magnetic control torques about the roll and yaw axes of the satellite. We need now to develop the expression for the components of the geomagnetic field on these axes to obtain the detail expression for the magnetic control torques.

The components of the geomagnetic field in the orbiting coordinate system are given in Equations 3.5. If C_o^b is the transformation matrix from the orbiting coordinate system to the body-fixed coordinate system, then by the assumptions of small angular deviations and 5.2, we can write

$$C_o^b = \begin{pmatrix} 1 & 0 & -\phi \\ 0 & 1 & \psi \\ \phi & -\psi & 1 \end{pmatrix}$$

By using this transformation, we get

$$B_\phi \approx B_{y_o}$$

$$B_\psi \approx B_{x_o} \quad (5.8)$$

For convenience, we define the followings:

$$\begin{aligned} S_1(t) &= \frac{1}{2} (B_1^2 + B_2^2) \\ S_2(t) &= \frac{1}{2} (B_1^2 - B_2^2) \\ S_3(t) &= B_1 B_2 \end{aligned} \quad (5.9)$$

with B_1 , B_2 , and B_3 given by Equations 3.4. Note that S_i 's here differ from S_i 's in the single spin case by a factor of $\frac{1}{2}$. Then, the components of the magnetic control torque on the roll and yaw axes of the satellite can be expressed as

$$\begin{aligned} L_{c_\phi} &= K_1 B_\phi B_\psi \phi - K_2 (B_\psi^2 \dot{\phi} - B_\phi B_\psi \dot{\psi}) \\ L_{c_\psi} &= -K_1 B_\phi^2 \phi + K_2 (B_\phi B_\psi \dot{\phi} - B_\phi^2 \dot{\psi}) \end{aligned} \quad (5.10)$$

where

$$\begin{aligned} B_\phi^2 &= B_o^2 [S_1(t) - S_2(t) \cos 2\Omega t - S_3(t) \sin 2\Omega t] \\ B_\psi^2 &= 4B_o^2 [S_1(t) + S_2(t) \cos 2\Omega t + S_3(t) \sin 2\Omega t] \\ B_\phi B_\psi &= -2B_o^2 [S_3(t) \cos 2\Omega t - S_2 \sin 2\Omega t] \end{aligned} \quad (5.11)$$

Since S_i 's are periodic functions, then B_ϕ^2 , B_ψ^2 , and $B_\phi B_\psi$ are also periodic functions.

5.1.3 The Controlled Dynamic Equations

Substitution of the control torque given in Equations 5.10 into the equations of motion of the satellite, Equations 5.7, yields

$$\begin{aligned} I_y \ddot{\phi} + K_2 B_\psi^2 \dot{\phi} + \\ [\Omega h - \Omega^2 I_x - K_1 B_\phi B_\psi] \phi - [h - \Omega(I_x + I_y) + K_2 B_\phi B_\psi] \dot{\psi} = 0 \end{aligned}$$

$$\begin{aligned}
I_x \ddot{\psi} + K_2 B_\phi^2 \dot{\psi} + \Omega[h - \Omega I_y] \psi \\
[h - \Omega(I_x + I_y) - K_2 B_\phi B_\psi] \dot{\phi} + K_1 B_\phi^2 \phi = 0
\end{aligned} \tag{5.12}$$

If we consider the torque-free satellite, we find that the motion of the satellite has two natural frequencies (for the detail of this, see Appendix C), namely :

- the orbital frequency Ω , and
- the nutational frequency $\frac{h}{\sqrt{I_x I_y}}$

For satellites in practice, the orbital mode is usually much slower than the nutational mode. This means, that the orbital frequency is much smaller than the nutational frequency, so that we can write

$$\epsilon = \frac{\Omega}{\frac{h}{\sqrt{I_x I_y}}} \quad ; \quad 0 < |\epsilon| \ll 1 \tag{5.13}$$

This ratio will serve as the small parameter that will enable us to utilize the GMS method later.

Without loss of generality, it will be assumed that at $t = 0$, the satellite is at the ascending node and also $u = 0$, so that we can write

$$\begin{aligned}
\Omega t &= \epsilon \bar{t} \\
u &= \omega_e t = n \epsilon \bar{t}
\end{aligned}$$

where

- $\bar{t} \equiv \frac{h}{\sqrt{I_x I_y}} t$ is a nondimensional time
- $n \equiv \frac{\omega_e}{\Omega}$ is the ratio of the earth's spin rate and the orbital angular speed of the satellite.

By using the nondimensional time \bar{t} , the derivative operator becomes

$$\frac{d^i}{dt^i} = \left(\frac{h}{\sqrt{I_x I_y}} \right)^i \frac{d^i}{d\bar{t}^i}$$

Then, if we also define

$$\begin{aligned} a &= \sqrt{\frac{I_x}{I_y}} \\ b &= \sqrt{\frac{I_y}{I_x}} \end{aligned} \quad (5.14)$$

we can write the equations of motion of the satellite as

$$\begin{aligned} \phi'' + 4a \frac{K_2 B_o^2}{h} [S_1(\epsilon \bar{t}) + S_2(\epsilon \bar{t}) \cos 2\epsilon \bar{t} + f_3(\epsilon \bar{t}) \sin 2\epsilon \bar{t}] \phi' + \\ \left[\epsilon a(1 - a) + 2 \frac{K_1 B_o^2}{h^2} I_x (S_3(\epsilon \bar{t}) \cos 2\epsilon \bar{t} - S_2(\epsilon \bar{t}) \sin 2\epsilon \bar{t}) \right] \phi - \\ \left[a - \epsilon(1 + a^2) - 2a \frac{K_2 B_o^2}{h} (S_3(\epsilon \bar{t}) \cos 2\epsilon \bar{t} - S_2(\epsilon \bar{t}) \sin 2\epsilon \bar{t}) \right] \psi' = 0 \end{aligned} \quad (5.15)$$

$$\begin{aligned} \psi'' + b \frac{K_2 B_o^2}{h} [S_1(\epsilon \bar{t}) - S_2(\epsilon \bar{t}) \cos 2\epsilon \bar{t} - S_3(\epsilon \bar{t}) \sin 2\epsilon \bar{t}] \psi' + \\ [\epsilon b(1 - b)] \psi + \\ \left[a - \epsilon(1 + a^2) + 2b \frac{K_2 B_o^2}{h} (S_3(\epsilon \bar{t}) \cos 2\epsilon \bar{t} - S_2(\epsilon \bar{t}) \sin 2\epsilon \bar{t}) \right] \phi' + \\ \frac{K_1 B_o^2}{h^2} I_y (S_1 - S_2(\epsilon \bar{t}) \cos 2\epsilon \bar{t} - S_3(\epsilon \bar{t}) \sin 2\epsilon \bar{t}) \phi = 0 \end{aligned} \quad (5.16)$$

where $(\cdot)'$ denotes the derivative with respect to \bar{t} .

Since the magnitude of the geomagnetic field is relatively small, we can assume

$$\begin{aligned} \frac{K_1 B_o^2}{h^2} \sqrt{I_x I_y} &= \epsilon K_1^* \\ \frac{K_2 B_o^2}{h} &= \epsilon K_2^* \end{aligned} \quad (5.17)$$

Another way to look at this assumption is that the magnetic control torque has small effect on the nutational frequency of the satellite. This can be understood since the control torque is slowly varying and hence it will have small effect on the frequency of the fast mode of the satellite (nutation mode).

Addition of assumption 5.17 will change Equations 5.16 to the following.

$$\begin{aligned}
\phi'' + \epsilon 4aK_2^* [S_1(\epsilon\bar{t}) + S_2(\epsilon\bar{t}) \cos 2\epsilon\bar{t} + S_3(\epsilon\bar{t}) \sin 2\epsilon\bar{t}] \phi' + \\
[\epsilon a(1-a) + \epsilon 2aK_1^* (S_3(\epsilon\bar{t}) \cos 2\epsilon\bar{t} - S_2(\epsilon\bar{t}) \sin 2\epsilon\bar{t})] \phi - \\
[a - \epsilon(1+a^2) - \epsilon 2aK_2^* (S_3(\epsilon\bar{t}) \cos 2\epsilon\bar{t} - S_2(\epsilon\bar{t}) \sin 2\epsilon\bar{t})] \phi' = 0 \quad (5.18) \\
\psi'' + \epsilon bK_2^* [S_1(\epsilon\bar{t}) - S_2(\epsilon\bar{t}) \cos 2\epsilon\bar{t} - S_3(\epsilon\bar{t}) \sin 2\epsilon\bar{t}] \psi' + \\
[\epsilon b(1-b)] \psi + \\
[a - \epsilon(1+a^2) + \epsilon 2bK_2^* (S_3(\epsilon\bar{t}) \cos 2\epsilon\bar{t} - S_2(\epsilon\bar{t}) \sin 2\epsilon\bar{t})] \psi' + \\
\epsilon bK_1^* (S_1 - S_2(\epsilon\bar{t}) \cos 2\epsilon\bar{t} - S_3(\epsilon\bar{t}) \sin 2\epsilon\bar{t}) \psi = 0 \quad (5.19)
\end{aligned}$$

The above equations form a system of coupled linear nonautonomous second order ordinary differential equations. To be more precise, the coefficients of the differential equations are slowly periodic functions with the frequency of the order of the orbital frequency of the satellite. We can also observe that some of the coefficients are large ($O(1)$) and some are small ($O(\epsilon)$). Obviously, exact solutions of Equation /refeq:finalds are not possible to obtain. Hence, we will try to find the approximate solutions of the above equations analytically using the GMS approach.

5.2 Stability Analysis and Performance Prediction Using the GMS Method

5.2.1 Roll Motion

As in the previous chapter, we will study the motion about each axis separately. So, we will decouple Equations 5.19. We first look at the roll motion of the satellite in this subsection. The yaw motion will be discussed in the next subsection. Decoupling Equations 5.19 is a lengthy process, however it is straightforward, so we will not present the detail here. The final result for roll motion is as follows.

$$\phi^{IV} + \epsilon P_1(\epsilon\bar{t}) \phi''' + P_2(\epsilon\bar{t}) \phi'' + \epsilon P_3(\epsilon\bar{t}) \phi' + \epsilon^2 P_4(\epsilon\bar{t}) \phi = 0 \quad (5.20)$$

where

$$\begin{aligned}
P_1(\epsilon \bar{t}) &= K_2^* [(4a + b)S_1(\epsilon \bar{t}) + (4a - b)(S_2(\epsilon \bar{t}) \cos 2\epsilon \bar{t} + S_3(\epsilon \bar{t}) \sin 2\epsilon \bar{t})] + O(\epsilon) \\
&\equiv p_{11}(\epsilon \bar{t}) + O(\epsilon) \\
P_2(\epsilon \bar{t}) &= 1 - \epsilon [a + b + 2aK_1^*(S_2(\epsilon \bar{t}) \sin 2\epsilon \bar{t} - S_3(\epsilon \bar{t}) \cos 2\epsilon \bar{t})] + O(\epsilon^2) \\
&\equiv p_{21}(\epsilon \bar{t}) + \epsilon p_{22}(\epsilon \bar{t}) + O(\epsilon^2) \\
P_3(\epsilon \bar{t}) &= K_1^* [S_1(\epsilon \bar{t}) - S_2(\epsilon \bar{t}) \cos 2\epsilon \bar{t} - S_3(\epsilon \bar{t}) \sin 2\epsilon \bar{t}] + O(\epsilon) \\
&\equiv p_{31}(\epsilon \bar{t}) + O(\epsilon) \\
P_4(\epsilon \bar{t}) &= 1 + nK_1^* [S_4(\epsilon \bar{t}) - S_5(\epsilon \bar{t}) \cos 2\epsilon \bar{t} - S_6(\epsilon \bar{t}) \sin 2\epsilon \bar{t}] + O(\epsilon) \\
&\equiv p_{41}(\epsilon \bar{t}) + O(\epsilon)
\end{aligned} \tag{5.21}$$

In the above, S_4 , S_5 , and S_6 are defined by the following relations.

$$\begin{aligned}
S'_1 &= n\epsilon S_4 \\
S'_2 &= n\epsilon S_5 \\
S'_3 &= n\epsilon S_6
\end{aligned} \tag{5.22}$$

We next define the new nondimensional independent variable

$$\tau = \epsilon \bar{t} \tag{5.23}$$

so that

$$(\cdot)^{\cdot} = \frac{d^{\cdot}}{d\bar{t}^{\cdot}} = \epsilon^{\cdot} \frac{d^{\cdot}}{d\tau^{\cdot}}$$

Written in terms of this new independent variable τ , Equation 5.20 becomes

$$\epsilon^2 \phi^{\cdot\cdot\cdot} + \epsilon^2 P_1(\tau) \phi^{\cdot\cdot\cdot} + P_2(\tau) \phi^{\cdot\cdot} + P_3(\tau) \phi^{\cdot} + P_4(\tau) \phi = 0 \tag{5.24}$$

We then invoke the GMS method to solve Equation 5.24. As before, two time scales are used. First the independent and dependent variables are extended as fol-

lows.

$$\begin{aligned}\tau &\longrightarrow \{\tau_0, \tau_1\} \\ \phi(\tau, \epsilon) &\longrightarrow \phi(\tau_0, \tau_1)\end{aligned}\tag{5.25}$$

where

$$\begin{aligned}\tau_0 &= \tau \\ \tau_1 &= \epsilon^\nu \int k(\tau) d\tau\end{aligned}\tag{5.26}$$

$k(\tau)$ is a clock function that will be determined in the course of the analysis. Also ν in Equation 5.26 is still arbitrary and its proper value will be found using the principle of minimal simplification.

◆

In terms of the extensions, Equation 5.24 becomes as follows (see Appendix B for the extended derivative operators).

$$\begin{aligned}&P_2(\tau_0)\frac{\partial^2\phi}{\partial\tau_0^2} + P_3(\tau_0)\frac{\partial\phi}{\partial\tau_0} + P_4(\tau_0)\phi + \epsilon^2\left[\frac{\partial^4\phi}{\partial\tau_0^4} + P_1(\tau_0)\frac{\partial^3\phi}{\partial\tau_0^3}\right] + \\&\epsilon^\nu\left[k^1P_2(\tau_0)\frac{\partial\phi}{\partial\tau_1} + 2kP_2(\tau_0)\frac{\partial^2\phi}{\partial\tau_0\partial\tau_1} + kP_3(\tau_0)\frac{\partial\phi}{\partial\tau_1}\right] + \\&\epsilon^{2\nu}\left[k^2P_2(\tau_0)\frac{\partial^2\phi}{\partial\tau_1^2}\right] + \\&\epsilon^{2+\nu}\left[k^{111}\frac{\partial\phi}{\partial\tau_1} + k^{11}P_1(\tau_0)\frac{\partial\phi}{\partial\tau_1} + 3k^{11}\frac{\partial^2\phi}{\partial\tau_0\partial\tau_1} + 5k^1\frac{\partial^3\phi}{\partial\tau_0^2}\partial\tau_1 + \right. \\&\left.2k^1P_1(\tau_0)\frac{\partial^2\phi}{\partial\tau_0\partial\tau_1} + 4k\frac{\partial^4\phi}{\partial\tau_0^3\partial\tau_1} + 3kP_1(\tau_0)\frac{\partial^3\phi}{\partial\tau_0^2\partial\tau_1}\right] + \\&\epsilon^{2+2\nu}\left[4kk^{11}\frac{\partial^2\phi}{\partial\tau_1^2} + 3k^{12}\frac{\partial^2\phi}{\partial\tau_1^2} + 11kk^1\frac{\partial^3\phi}{\partial\tau_0\partial\tau_1^2} + 3kk^1P_1(\tau_0)\frac{\partial^2\phi}{\partial\tau_1^2} + \right. \\&\left.6k^2\frac{\partial^4\phi}{\partial\tau_0^2\partial\tau_1^2} + 3k^2P_1(\tau_0)\frac{\partial^3\phi}{\partial\tau_0\partial\tau_1^2}\right] + \\&\epsilon^{2+3\nu}\left[6k^2k^1\frac{\partial^3\phi}{\partial\tau_1^3} + 4k^3\frac{\partial^4\phi}{\partial\tau_0\partial\tau_1^3} + P_1(\tau_0)\frac{\partial^3\phi}{\partial\tau_1^3}\right] + \\&\epsilon^{2+4\nu}\left[k^4\frac{\partial^4\phi}{\partial\tau_1^4}\right] = 0\end{aligned}\tag{5.27}$$

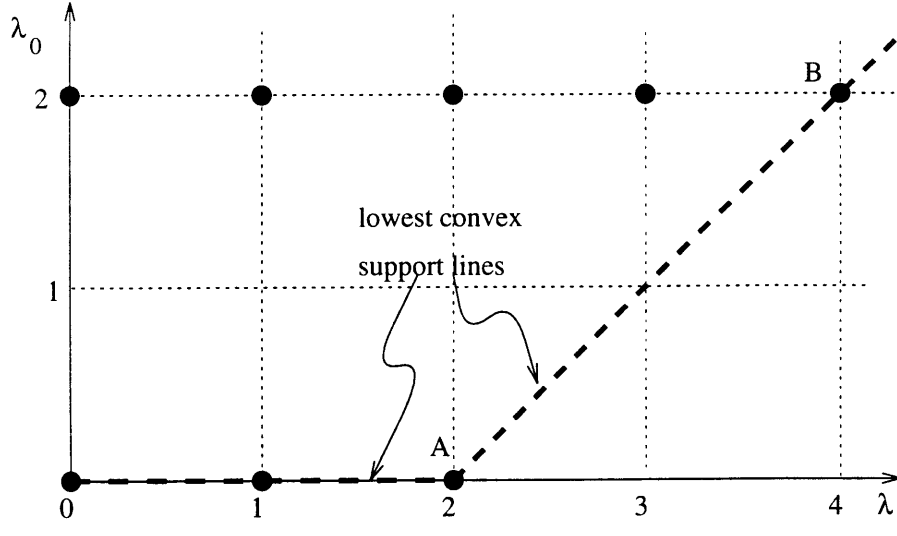


Figure 5-2: PMS diagram to determine the value of ν

We see that the terms in Equation 5.27 are of the form $\epsilon^{\lambda_0 + \lambda_1 \nu}(\cdot)$, where the quantities in the parenthesis can be assumed to be of $O(1)$. We will then draw PMS diagram similar to Figures 2-2 and 2-3 to determine the value of ν . The order of each term will be represented by a point on the diagram. This diagram is shown in Figure 5-2.

From the diagram, we see that the lowest convex support line that is not horizontal connects the two points indicated by A and B. These two points represent the dominant terms in Equation 5.27. By balancing these dominant points, we get

$$\begin{aligned} 2\nu &= 2 + 4\nu \\ \Leftrightarrow \nu &= -1 \end{aligned} \tag{5.28}$$

By substituting the value of ν found using the principle of minimal simplification above into Equation 5.27 and equating each group of terms with the same order to zero, we get the following for the dominant order.

$$O(\epsilon^{-2}) : k^4 \frac{\partial^4 \phi}{\partial \tau_1^4} + k^2 \frac{\partial^2 \phi}{\partial \tau_1^2} = 0 \tag{5.29}$$

k has to be selected such that we are able to solve for ϕ from Equation 5.29. The

simplest choice is

$$k^4 = k^2 \quad (5.30)$$

This is an algebraic equation, which can be easily solved. The possible values of k that satisfies Equation 5.30 are

$$k = 0, 1, -1$$

$k = 0$ is trivial, and hence, it will not be used. We are left with two possible values of k that are meaningful. However, observation shows that $k = 1$ or $k = -1$ will only influence the phase of the solution. So, we need use only one of them in our next analysis. For simplicity, we choose $k = 1$. By this choice of k , the time scale τ_1 becomes

$$\tau_1 = \frac{\tau}{\epsilon} \quad (5.31)$$

So, the time scale is linear in this case. Note also that from this result, that τ_1 is the fast time scale and τ_0 is the slow time scale.

Since we have already selected k to satisfy Equation 5.30, then Equation 5.29 becomes

$$\frac{\partial^4 \phi}{\partial \tau_1^4} + \frac{\partial^2 \phi}{\partial \tau_1^2} = 0 \quad (5.32)$$

Equation 5.32 is a fourth order linear partial differential equation, and has the solution of the form

$$\phi = A(\tau_0) \sin(\tau_1 + B(\tau_0)) + C(\tau_0) + D(\tau_0) \tau_1 \quad (5.33)$$

The last term in the above equation is a secular term. This term does not have physical meaning and appears because Equation 5.32 is in fact a degenerate fourth order partial differential equation. This secular term will also destroy the ordering of terms in Equation 5.27. The existence of such a term is not uncommon in an asymptotic expansion. However, appropriate counterterm can be constructed to cancel this *bad* term. The construction of this counterterm is based on the compatibility conditions that must be satisfied by the expansion. Detailed discussion on this subject is presented in Reference [14]. For this specific problem, mathematical elaboration on this point will not be done, however it is clear from the physical reason that this secular

term must be dropped and in our next discussion we will deal only with the solution of the form

$$\phi = A(\tau_0) \sin(\tau_1 + B(\tau_0)) + C(\tau_0) \quad (5.34)$$

The first term in the equation describes the nutational (fast) mode of the satellite, while the second term, which is only a function of τ_0 , describes the orbital (slow) mode of the satellite. The two terms in Equation 5.34 are two independent solutions of Equation 5.32, thus in the following we will treat them separately. To find the detail form of the dependency of A , B , and C with respect to τ_0 we will go to the next dominant order of the group of terms in Equation 5.27, which is :

$$O(\epsilon^{-1}) : 4 \frac{\partial^4 \phi}{\partial \tau_0 \partial \tau_1^3} + p_{11}(\tau_0) \frac{\partial^3 \phi}{\partial \tau_1^3} + 2p_{21}(\tau_0) \frac{\partial^2 \phi}{\partial \tau_0 \partial \tau_1} + p_{31}(\tau_0) \frac{\partial \phi}{\partial \tau_1} + p_{22}(\tau_0) \frac{\partial^2 \phi}{\partial \tau_1^2} = 0 \quad (5.35)$$

Nutational Mode

We concentrate now on the nutational mode of the satellite :

$$\phi_1 = A(\tau_0) \sin(\tau_1 + B(\tau_0)) \quad (5.36)$$

By substituting Equation 5.36 into Equation 5.35, we get the following.

$$\begin{aligned} & \left[(2p_{21}(\tau_0) - 4) \frac{dA}{d\tau_0} + (p_{31}(\tau_0) - p_{11}(\tau_0)A) \right] \cos(\tau_1 + B) \\ & + \left[-(2p_{21}(\tau_0) - 4) \frac{dB}{d\tau_0} - p_{22}(\tau_0) \right] A \sin(\tau_1 + B) = 0 \end{aligned} \quad (5.37)$$

In order that Equation 5.37 be satisfied for all values of τ_1 , the quantities in the parentheses must be identically zero for all τ_0 . By using the detail expressions for p_{ij} 's given in Equation 5.21, this requirement becomes :

$$\begin{aligned} & \frac{dA}{d\tau_0} - \frac{1}{2} [K_1^*(S_1(\tau_0) - S_2(\tau_0) \cos 2\tau_0 - S_3(\tau_0) \sin 2\tau_0) \\ & - K_2^*((4a - b)S_1(\tau_0) + (4a - b)(S_2(\tau_0) \cos 2\tau_0 + S_3(\tau_0) \sin 2\tau_0))] A = 0 \end{aligned} \quad (5.38)$$

and

$$\frac{dB}{d\tau_0} + \frac{a+b}{2} + aK_1^* [S_2(\tau_0) \cos 2\tau_0 - S_3(\tau_0) \sin 2\tau_0] = 0 \quad (5.39)$$

Equation 5.38 governs the amplitude of the nutational mode, while Equation 5.39 governs the phase of the nutational mode. The stability of the nutational mode is determined by whether its amplitude is decaying or growing. So, the stability of the amplitude equation, Equation 5.38, determines the stability of the fast mode. We can also see the presence of K_1^* and K_2^* in the amplitude equation. This implies the dependency of the amplitude variation of the nutational mode on the control gains. We should select K_1^* and K_2^* such that this nutational mode becomes stable and has desired characteristics.

Equation 5.38 is a linear first order ordinary differential equation, and thus, its exact solution can be obtained. The solution is as follows.

$$A(\tau_0) = A_0 e^{\frac{1}{2}[K_1^* - (4a+b)K_2^*]U\tau_0} e^{\frac{1}{2}[K_1^* - (4a+b)K_2^*]R_1(\tau_0) - \frac{1}{2}[K_1^* + (4a-b)K_2^*]R_2(\tau_0)} \quad (5.40)$$

where

- $U = \frac{1}{4} \sin^2 \gamma (1 + \cos^2 i) + \frac{1}{2} \cos^2 \gamma \sin^2 i$, is a positive constant.
- $R_1(\tau_0)$ and $R_2(\tau_0)$ are periodic functions in τ_0 , as follows :

$$\begin{aligned} R_1(\tau_0) &= -\frac{1}{4n} \sin 2\gamma \sin 2i \cos n\tau_0 + \frac{1}{8n} \sin^2 \gamma \sin^2 i \sin 2n\tau_0 + R_{10} \\ R_2(\tau_0) &= \sin 2\gamma \left[\frac{1}{8(2+n)} \sin 2i - \frac{1}{4(2+n)} \sin i \right] \cos(2+n)\tau_0 - \\ &\quad \sin 2\gamma \left[\frac{1}{8(2-n)} \sin 2i + \frac{1}{4(2-n)} \sin i \right] \cos(2-n)\tau_0 - \\ &\quad \sin^2 \gamma \left[\frac{1}{16(1+n)} (1 + \cos^2 i) - \frac{1}{8(1+n)} \cos i \right] \sin(2+2n)\tau_0 + \\ &\quad \sin^2 \gamma \left[\frac{1}{16(1-n)} (1 + \cos^2 i) + \frac{1}{8(1-n)} \cos i \right] \sin(2-2n)\tau_0 + \\ &\quad \left(\frac{1}{4} \cos^2 \gamma \sin^2 i - \frac{1}{8} \sin^2 \gamma \sin^2 i \right) \sin 2\tau_0 + R_{20} \end{aligned} \quad (5.41)$$

where R_{10} and R_{20} are arbitrary constants

We observe that only the first exponential factor in Equation 5.40 determines the decaying or growing of $A(\tau_0)$. The second exponential factor only contributes to a periodic variation. In other words, the first exponential factor determines the stability of the nutational mode. In order to make this factor decay, which corresponds to asymptotically stable motion, we must have

$$K_1^* - (4a + b)K_2^* < 0 \quad (5.42)$$

This is the stability criterion of the nutational mode. By tracing back to the definitions of K_1^* and K_2^* , we can write this stability criterion in terms of K_1 and K_2 as follows.

$$K_1 < \frac{4I_x + I_y}{I_x I_y} h K_2 \quad (5.43)$$

We see that the stability criterion of the nutational mode depends on the inertia distribution of the satellite, and does not depend on the orbit characteristics, except the orbital angular speed that contains in h . However, it should be noted that the performance of the control system does depend on the orbit characteristics. This point will be discussed later in this section.

The nutational phase shift is determined by Equation 5.39. The solution of this equation is as follows.

$$\begin{aligned} B(\tau_0) = & B_0 - \frac{1}{2}(a + b)\tau_0 - aK_1^* \left[\left(\frac{1}{4} \cos^2 \gamma \sin^2 i - \frac{1}{8} \sin^2 \gamma \sin^2 i \right) \sin 2\tau_0 - \right. \\ & \sin 2\gamma \left[\frac{1}{8(2+n)} \sin 2i - \frac{1}{4(2+n)} \sin i \right] \cos(2+n)\tau_0 - \\ & \sin 2\gamma \left[\frac{1}{8(2-n)} \sin 2i - \frac{1}{4(2-n)} \sin i \right] \cos(2-n)\tau_0 + \\ & \sin^2 \gamma \left[\frac{1}{16(1+n)} (1 + \cos^2 i) + \frac{1}{8(1+n)} \cos i \right] \sin(2+2n)\tau_0 + \\ & \left. \sin^2 \gamma \left[\frac{1}{16(1-n)} (1 + \cos^2 i) - \frac{1}{8(1-n)} \cos i \right] \sin(2-2n)\tau_0 \right] \quad (5.44) \end{aligned}$$

with B_0 an arbitrary constant.

Note that the phase shift consists of secular and oscillatory (periodic) terms. The

oscillatory terms depend on the parameters ϵ and n . This means that the earth rotation has influence on the phase of the nutational mode.

Orbital Mode

In Equation 5.34, the orbital mode is represented by

$$\phi_2 = C(\tau_0) \quad (5.45)$$

Substitution of Equation 5.45 into Equation 5.35 will yield identically zero terms, since the orbital mode does not depend on τ_1 . So, the governing equation for the orbital mode will be found using the next rank of order in Equation 5.27, namely : (the parts that contain partial derivative with respect to τ_1 are not written, since they will become zero)

$$O(\epsilon^0) : p_{21}(\tau_0) \frac{d^2 \phi}{d\tau_0^2} + p_{31}(\tau_0) \frac{d\phi}{d\tau_0} + p_{41}(\tau_0) \phi = 0 \quad (5.46)$$

By substituting Equation 5.45 into the above equation and using the expanded expression of p_{ij} 's given by Equations 5.21, we get

$$\begin{aligned} \frac{d^2 C}{d\tau_0^2} + K_1^*(S_1(\tau_0) - S_2(\tau_0) \cos 2\tau_0 - S_3(\tau_0) \sin 2\tau_0) \frac{dC}{d\tau_0} \\ + [1 + nK_1^*(S_4(\tau_0) - S_5(\tau_0) \cos 2\tau_0 - S_6(\tau_0) \sin 2\tau_0)] C = 0 \end{aligned} \quad (5.47)$$

The above equation shows that the orbital mode is affected by K_1 but not by K_2 . Equation 5.47 is still of the form linear second order ordinary differential equation with periodic coefficients, thus, it is not readily solvable. Approximation of the solution of Equation 5.47, however, is still possible to obtain for the limiting values of K_1^* . Again, the GMS method is utilized to obtain the approximate solution. Note that in this case, the multiple scaling is not applied to the original independent variable τ , but to τ_0 , which is a time scale of the original problem. So, in essence, we do multiple scaling inside multiple scaling. We will call this *nested multiple scaling*.

The first limiting case considered is the case where the value of K_1^* is small, that

is

$$K_1^* = \delta \bar{K}_1 \quad ; \quad 0 < \delta \ll 1 \quad (5.48)$$

where \bar{K}_1 is assumed to be of $O(1)$. Written in terms of δ and \bar{K}_1 , Equation 5.47 becomes

$$\begin{aligned} & \frac{d^2 C}{d\tau_0^2} + \delta \bar{K}_1 (S_1(\tau_0) - S_2(\tau_0) \cos 2\tau_0 - S_3(\tau_0) \sin 2\tau_0) \frac{dC}{d\tau_0} \\ & + [1 + n\delta \bar{K}_1 (S_4(\tau_0) - S_5(\tau_0) \cos 2\tau_0 - S_6(\tau_0) \sin 2\tau_0)] C = 0 \end{aligned} \quad (5.49)$$

The variables in Equation 5.49 are then extended as follows.

$$\begin{aligned} \tau_0 & \longrightarrow \{\xi_0, \xi_1\} \\ C(\tau_0, \delta) & \longrightarrow C(\xi_0, \xi_1) \end{aligned}$$

where

$$\begin{aligned} \xi_0 &= \tau_0 \\ \xi_1 &= \delta^\mu \int \kappa(\tau_0) d\tau_0 \end{aligned} \quad (5.50)$$

As before $\kappa(\tau_0)$ is the clock function. In terms of the extended variables, Equation 5.49 becomes

$$\begin{aligned} & \frac{\partial^2 C}{\partial \xi_0^2} + C + \delta \left[g_1(\xi_0) \frac{\partial C}{\partial \xi_0} + g_2(\xi_0) C \right] + \delta^\mu \left[2\kappa \frac{\partial^2 C}{\partial \xi_0 \partial \xi_1} + \kappa' \frac{\partial C}{\partial \xi_1} \right] \\ & + \delta^{1+\mu} \kappa g_1(\xi_0) \frac{\partial C}{\partial \xi_1} + \delta^{2\mu} \kappa^2 \frac{\partial^2 C}{\partial \xi_1^2} = 0 \end{aligned} \quad (5.51)$$

where in the above equation we have defined the followings to shorten the notation :

$$\begin{aligned} g_1(\xi_0) &= \bar{K}_1 (S_1(\xi_0) - S_2(\xi_0) \cos 2\xi_0 - S_3(\xi_0) \sin 2\xi_0) \\ g_2(\xi_0) &= n\bar{K}_1 (S_4(\xi_0) - S_5(\xi_0) \cos 2\xi_0 - S_6(\xi_0) \sin 2\xi_0) \end{aligned} \quad (5.52)$$

The principle of minimal simplification is then applied to determine the right value

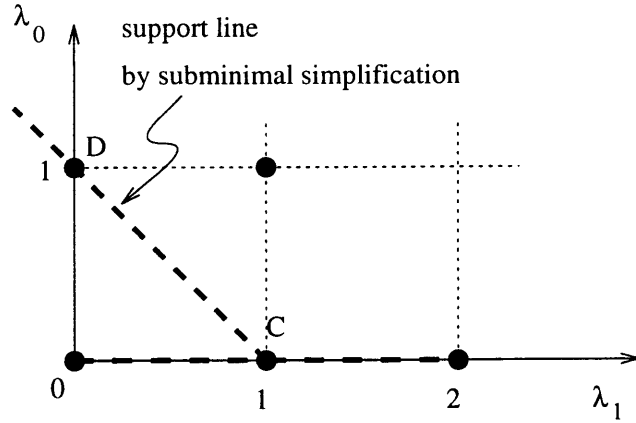


Figure 5-3: PMS diagram for determining μ

of μ . The PMS diagram for this problem is shown in Figure 5-3 (we note that the terms in Equation 5.51 are of the form $\delta^{\lambda_0 + \lambda_1 \mu}(\cdot)$, with the quantity in the parenthesis is assumed to be of $O(1)$). We see from the diagram that the only lowest convex support line is the horizontal axis (λ_1 -axis). So, in this case the principle of minimal simplification fails to obtain a meaningful result. Because of this, the next rank of minimal simplification is applied, namely the principle of subminimal simplification, as already explained in Chapter 2. By this principle, the line connecting points C and D in the diagram will serve as our lowest convex support line, in addition to the horizontal axis. This suggest the balance between points C and D as the dominating order. By balancing these two points, we obtain

$$\mu = 1 \quad (5.53)$$

Order by order analysis of Equation 5.51 then will give us the followings. First we look at the dominant one :

$$O(\delta^0) : \frac{\partial^2 C}{\partial \xi_0^2} + C = 0 \quad (5.54)$$

which obtains

$$C = \bar{C}_0(\xi_1) e^{j\xi_0} + c.c. \quad (5.55)$$

where $j = \sqrt{-1}$ and *c.c.* denotes the complex conjugate of the preceding terms.

The second dominant order of Equation 5.51 is given by

$$O(\delta) : \kappa^i \frac{\partial C}{\partial \xi_1} + 2\kappa \frac{\partial C}{\partial \xi_0 \partial \xi_1} + g_1(\xi_0) \frac{\partial C}{\partial \xi_0} + g_2(\xi_0) C = 0 \quad (5.56)$$

Substitution of Equation 5.55 into Equation 5.56 yields

$$\left[(\kappa^i + j2\kappa) \frac{d\bar{C}_0}{d\xi_1} + (jg_1(\xi_0) + g_2(\xi_0)) \bar{C}_0 \right] e^{j\xi_0} + c.c. = 0 \quad (5.57)$$

Since this equation must be satisfied at all ξ_0 , then the quantity in the parenthesis must be identically zero.

$$(\kappa^i + j2\kappa) \frac{d\bar{C}_0}{d\xi_1} + (jg_1(\xi_0) + g_2(\xi_0)) \bar{C}_0 = 0 \quad (5.58)$$

Now, if we assume \bar{C}_0 to be of the form

$$\bar{C}_0 = C_0 e^{-\xi_1} \quad (5.59)$$

with C_0 a constant determined by the initial conditions, then the clock function κ must satisfy the following relation.

$$\kappa^i + j2\kappa = jg_1(\xi_0) + g_2(\xi_0) \quad (5.60)$$

From this relation, we can conclude that the clock function κ in this case is complex and nonlinear. By using the integrating factor $e^{2j\xi_0}$, Equation 5.60 can be written as follows.

$$\frac{d}{d\xi_0} [\kappa e^{2j\xi_0}] = (jg_1(\xi_0) + g_2(\xi_0)) e^{2j\xi_0} \quad (5.61)$$

Integration of this equation will result in

$$\begin{aligned} \kappa e^{2j\xi_0} &= \int^{\xi_0} (jg_1(\sigma_0) + g_2(\sigma_0)) e^{2j\sigma_0} d\sigma_0 \\ \iff \kappa &= \frac{1}{2} \bar{K}_1 U + e^{-2j\xi_0} G_1(\xi_0) + \kappa_0 e^{-2j\xi_0} \end{aligned} \quad (5.62)$$

where

- σ_0 is a dummy variable.
- U is the positive constant defined earlier in this subsection.
- κ_0 is an arbitrary constant, which will be taken to be zero for simplicity.
- $G_1(\xi_0)$ is defined as follows:

$$G_1(\xi_0) = \int^{\xi_0} (jg_1^*(\sigma_0) + g_2(\sigma_0))e^{2j\sigma_0} d\sigma_0 \quad (5.63)$$

with

$$g_1^*(\sigma_0) = g_1(\sigma_0) - \bar{K}_1 U$$

Evaluating Equation 5.62 further, we arrive at the following expression of κ .

$$\kappa = \frac{1}{2}\bar{K}_1 U + \frac{1}{2}V(\tau_0 \sin 2\tau_0 + j\tau_0 \cos 2\tau_0) + e^{-2j\tau_0}\hat{G}_1(\tau_0) \quad (5.64)$$

where

$$\begin{aligned} V &= \frac{1}{4}\sin^2 \gamma \sin^2 i - \frac{1}{2}\cos^2 \gamma \sin^2 i \\ \hat{G}_1 &= \int^{\tau_0} (jg_1^{**}(\sigma_0) + g_2(\sigma_0))e^{2j\sigma_0} d\sigma_0 \end{aligned} \quad (5.65)$$

with

$$g_1^{**}(\sigma_0) = g_1^*(\sigma_0) + V \cos 2\sigma_0$$

The second group of terms in Equation 5.64 is secular. The existence of these terms will destroy the uniformity of the approximate solution. This can be understood by examining Equation 5.56. The secular terms will ruin the ordering of terms in this equation for large values of τ_0 . Hence, once again we are faced with the uniformization problem. Using the terms used in Reference [14], κ consists of the good part and the bad part. It is clear from the above discussion that the secular terms constitute the bad part of κ . Reference [14] also shows that counterterms can be constructed

to eliminate the bad part of an asymptotic expansion, and so, only the good part remains. The degree of freedom for constructing the counterterms in this case will come from the higher order expansions of the dependent variable (note that here only the zeroth order expansion is used). We will not elaborate the detail of the process here. However, based on the above reason, we will drop the bad part of the κ solution in the next analysis, so that we are left with

$$\kappa = \frac{1}{2}\bar{K}_1 U + e^{-2j\tau_0}\hat{G}_1(\tau_0) \quad (5.66)$$

Using this expression for κ the time scale ξ_1 becomes

$$\begin{aligned} \xi_1 &= \frac{1}{2}\delta\bar{K}_1 U\tau_0 + \delta G_2(\tau_0) \\ &= \frac{1}{2}K_1^* U\tau_0 + \delta G_2(\tau_0) \end{aligned} \quad (5.67)$$

where

$$G_2(\tau_0) = \int e^{-2j\tau_0}\hat{G}_1(\tau_0)d\tau_0 \quad (5.68)$$

The real and imaginary parts of $G_2(\tau_0)$ are in the form of long trigonometric functions and will not be written here. Interested reader may see Appendix D for the detail. Since $G_2(\tau_0)$ is an oscillatory function, then the time scale ξ_1 is also oscillatory in nature.

Finally, we can write the expression for the orbital mode of the dual spin satellite for small K_1^* as follows.

$$\begin{aligned} C(\tau_0) &= C_0 e^{-\frac{1}{2}K_1^* U\tau_0} e^{G_2(\tau_0)} e^{j\tau_0} + c.c. \\ &= C_0 e^{-\frac{1}{2}K_1^* U\tau_0 - \Re(G_2(\tau_0))} \sin(\tau_0 + \Im(G_2(\tau_0)) + C_1) \end{aligned} \quad (5.69)$$

where C_1 is a constant to be determined from the initial conditions, and the symbols $\Re(\cdot)$ and $\Im(\cdot)$ indicate the real and imaginary parts of the quantity in the parenthesis, respectively.

Examination of Equation 5.69 shows that the stability of the orbital mode for small K_1^*

is determined by the exponential factor. From Appendix D, we see that $\Re(G_2(\tau_0))$ is only a periodic function around zero equilibrium with small amplitude. So, the stability is determined by $\frac{1}{2}K_1^*U\tau_0$. U is always positive. Hence, for small K_1^* , the orbital mode will be asymptotically stable if

$$K_1^* > 0 \quad (5.70)$$

or equivalently,

$$K_1 > 0 \quad (5.71)$$

This is the stability criterion for the orbital mode in case K_1^* small. To get the stability of the overall roll motion, both stability criteria, 5.43 and 5.71, must be satisfied.

Now we consider the stability of the orbital mode for large K_1^* , that is

$$K_1^* = \frac{1}{\varrho} \bar{K}_1 \quad ; \quad 0 < \varrho \ll 1 \quad (5.72)$$

We note here, that in the above equation $O(\varrho) > O(\epsilon)$, so that our earlier assumption, given by Equation 5.17, is not violated. Equation 5.47 then can be written as

$$\frac{d^2 C}{d\tau_0^2} + \varrho^{-1} g_1(\tau_0) \frac{dC}{d\tau_0} + [1 + \varrho^{-1} g_2(\tau_0)] C = 0 \quad (5.73)$$

Although the appearance of Equation 5.73 looks simple, it is a quite complex equation. We cannot assume that the coefficients containing ϱ^{-1} are always large. This is because $g_1(\tau_0)$ and $g_2(\tau_0)$ are periodic functions that become small and even zero at some τ_0 . The nature of $g_1(\tau_0)$ and $g_2(\tau_0)$ is given in Figure 5-4. As we proceed to examine the characteristic roots of the differential equation 5.73, we found that the characteristic roots change back and forth from real to complex as τ_0 increases. This does not happen for the case where K_1^* is small. The comparison of the characteristic roots pattern of the orbital mode equation between small and large K_1^* case is presented in Figure 5-5. Point where the two characteristic roots coalesce (in the real axis) is called *turning point*. The existence of such point indicates the changes

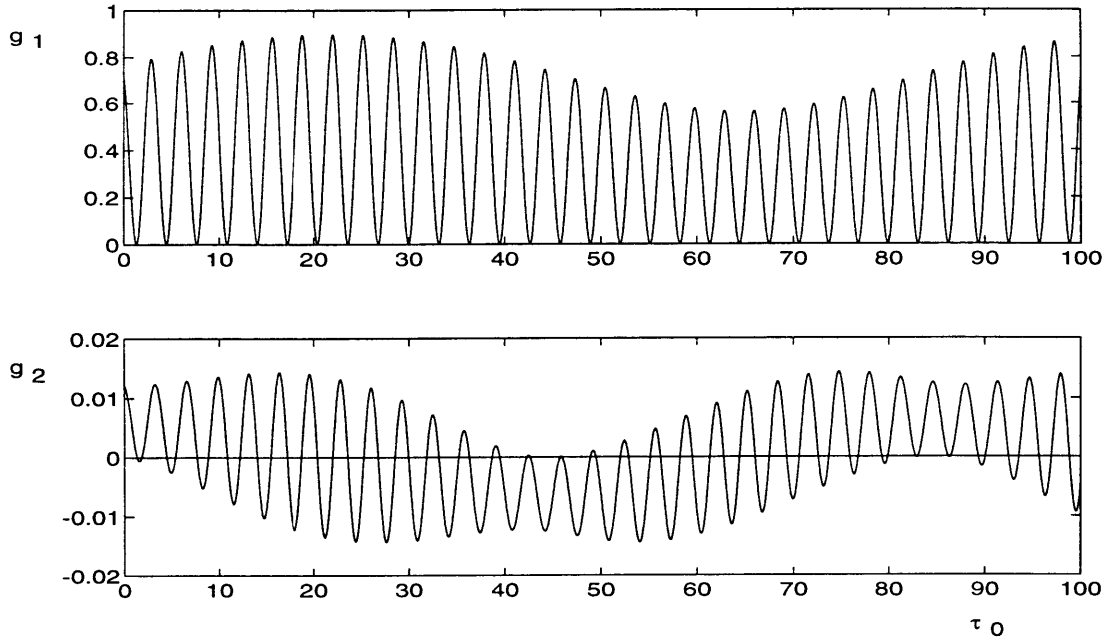
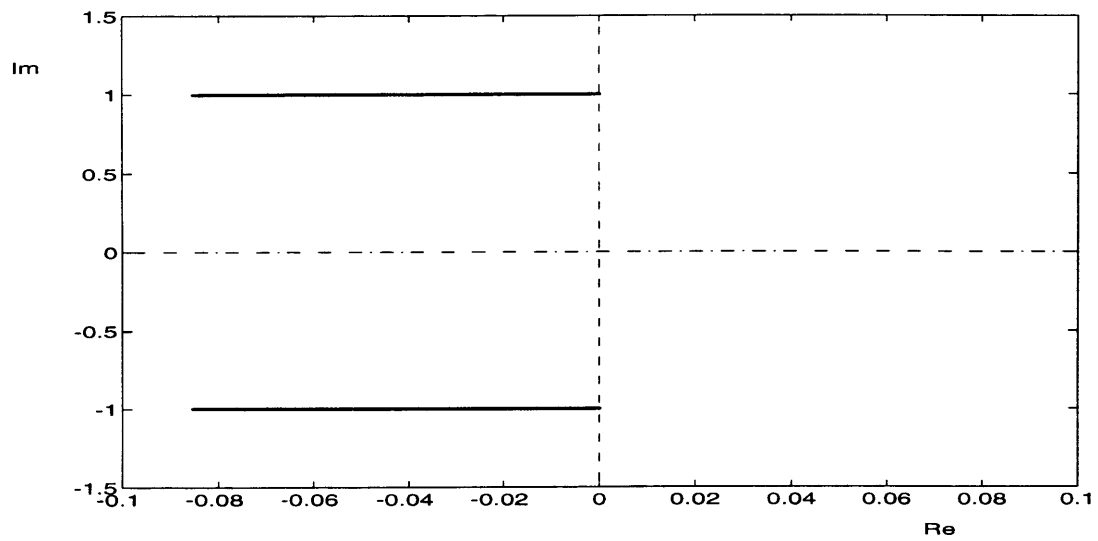


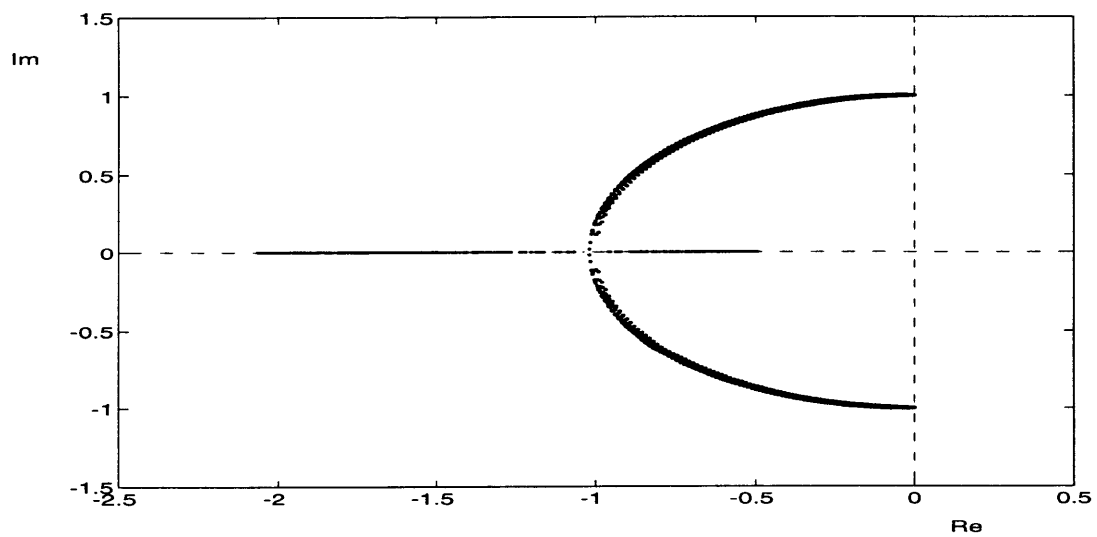
Figure 5-4: $g_1(\tau_0)$ and $g_2(\tau_0)$

in the topologic nature of the solution, for example from oscillatory to aperiodic. We point out that in our case here, there are infinitely many turning points, although all the turning points lie at the about the same place on the real axis . Approximations of the solution will only be valid on one side of the turning point, and cannot be both. To obtain a uniformly valid approximation of the solution across even a single turning point we need the so-called *connection formulae*, which is beyond our present scope. Moreover, from the power consideration, K_1^* small is desired. And we have already seen that satisfactory result can be achieved by using small K_1^* .

Because of the difficulties mentioned for K_1^* large, to evaluate the stability, numerical simulation is used. The result shows that as long as K_1^* is positive, the stability is guaranteed.



(a) $K_1^* = 0.2$



(b) $K_1^* = 3$

Figure 5-5: Characteristic roots pattern for K_1^* small and large

5.2.2 Yaw Motion

The decoupled yaw equation is as follows.

$$\psi^{iv} + \epsilon Q_1(\epsilon \bar{t}) \psi''' + Q_2(\epsilon \bar{t}) \psi'' + \epsilon Q_3(\epsilon \bar{t}) \psi' + \epsilon^2 Q_4(\epsilon \bar{t}) \psi = 0 \quad (5.74)$$

where

$$\begin{aligned} Q_1(\epsilon \bar{t}) &= \frac{K_2^* [(4a+b)S_1(\epsilon \bar{t}) + (4a-b)(S_2(\epsilon \bar{t}) \cos 2\epsilon \bar{t} + S_3(\epsilon \bar{t}) \sin 2\epsilon \bar{t})] + 2K_1^* [(2S_2(\epsilon \bar{t}) - nS_6(\epsilon \bar{t})) \cos 2\epsilon \bar{t} + (2S_3(\epsilon \bar{t}) + nS_5(\epsilon \bar{t}) \sin 2\epsilon \bar{t})] \sin 2\epsilon \bar{t}}{1 + 2K_1^* [S_3(\epsilon \bar{t}) \cos 2\epsilon \bar{t} - S_2(\epsilon \bar{t}) \sin 2\epsilon \bar{t}]} \\ &\quad + O(\epsilon) \\ &\equiv q_{11}(\epsilon \bar{t}) + O(\epsilon) \\ Q_2(\epsilon \bar{t}) &= 1 - \epsilon [a + b + 2aK_1^* (S_2(\epsilon \bar{t}) \sin 2\epsilon \bar{t} - S_3(\epsilon \bar{t}) \cos 2\epsilon \bar{t})] + O(\epsilon^2) \\ &\equiv q_{21}(\epsilon \bar{t}) + \epsilon q_{22}(\epsilon \bar{t}) + O(\epsilon^2) \\ Q_3(\epsilon \bar{t}) &= \frac{K_1^* [S_1(\epsilon \bar{t}) - S_2(\epsilon \bar{t}) \cos 2\epsilon \bar{t} - S_3(\epsilon \bar{t}) \sin 2\epsilon \bar{t}] + 2K_1^* [(2S_2(\epsilon \bar{t}) - nS_6(\epsilon \bar{t})) \cos 2\epsilon \bar{t} + (2S_3(\epsilon \bar{t}) + nS_5(\epsilon \bar{t}) \sin 2\epsilon \bar{t})] \sin 2\epsilon \bar{t}}{1 + 2K_1^* [S_3(\epsilon \bar{t}) \cos 2\epsilon \bar{t} - S_2(\epsilon \bar{t}) \sin 2\epsilon \bar{t}]} \\ &\quad + O(\epsilon) \\ &\equiv q_{31}(\epsilon \bar{t}) + O(\epsilon) \\ Q_4(\epsilon \bar{t}) &= 1 + 2K_1^* [S_3(\epsilon \bar{t}) \cos 2\epsilon \bar{t} - S_2(\epsilon \bar{t}) \sin 2\epsilon \bar{t}] + O(\epsilon) \\ &\equiv q_{41}(\epsilon \bar{t}) + O(\epsilon) \end{aligned} \quad (5.75)$$

with $S_5(\epsilon \bar{t})$ and $S_6(\epsilon \bar{t})$ as defined by Equation 5.22

As before, we change the independent variable from \bar{t} to τ according to

$$\tau = \epsilon \bar{t} \quad (5.76)$$

The yaw equation 5.74 becomes

$$\epsilon^2 \psi^{iv} + \epsilon^2 Q_1(\tau) \psi''' + Q_2(\tau) \psi'' + Q_3(\tau) \psi' + Q_4(\tau) \psi = 0 \quad (5.77)$$

Note that the ordering of terms in Equation 5.77 is the same with the corresponding roll equation (Equation 5.24).

We then extend the variables as follows.

$$\begin{aligned}\tau &\longrightarrow \{\tau_0, \tau_1\} \\ \psi(\tau, \epsilon) &\longrightarrow \psi(\tau_0, \tau_1)\end{aligned}\tag{5.78}$$

where

$$\begin{aligned}\tau_0 &= \tau \\ \tau_1 &= \epsilon^\nu \int k(\tau) d\tau\end{aligned}\tag{5.79}$$

where $k(\tau)$ is a clock function which will be determined later on. ν is determined by the application of the principle of minimal simplification. As have been pointed out earlier, the terms in Equation 5.77 have the same ordering as the ones in Equation 5.24. Therefore, it is clear without repeating the detail that the proper value of ν is

$$\nu = -1\tag{5.80}$$

Then, the dominant order of the extended yaw equation will be

$$O(\epsilon^{-2}) : k^4 \frac{\partial^4 \psi}{\partial \tau_1^4} + k^2 \frac{\partial^2 \psi}{\partial \tau_1^2} = 0\tag{5.81}$$

Again we see that the simplest choice of k is

$$k^4 = k^2\tag{5.82}$$

The possible values of k that satisfies this equation are

$$k = 0, -1, 1\tag{5.83}$$

As before, $k = 0$ is trivial, and also there will be no difference in the result by selecting

$k = -1$ or $k = 1$. So, for convenience, we select $k = 1$. The time scale τ_1 will then be linear, that is

$$\tau_1 = \frac{1}{\epsilon} \tau \quad (5.84)$$

With the value of k selected, we get

$$\psi(\tau_0, \tau_1) = X(\tau_0) \sin(\tau_1 + Y(\tau_0)) + Z(\tau_0) \quad (5.85)$$

The first term, which is fast, describes the nutational mode, while the second term, which is only a function of the slow time scale τ_0 , describes the orbital mode. As in the roll case, these modes will be studied separately.

Nutational mode

The subdominant order analysis of the nutational mode will yield the amplitude and phase equations as follows.

$$\begin{aligned} \frac{dX}{d\tau_0} - \frac{1}{2} [K_1^*(S_1(\tau_0) - S_2(\tau_0) \cos 2\tau_0 - S_3(\tau_0) \sin 2\tau_0) \\ - K_2^*((4a - b)S_1(\tau_0) + (4a - b)(S_2(\tau_0) \cos 2\tau_0 + S_3(\tau_0) \sin 2\tau_0))] X = 0 \end{aligned} \quad (5.86)$$

and

$$\frac{dY}{d\tau_0} + \frac{a + b}{2} + aK_1^*[S_2(\tau_0) \cos 2\tau_0 - S_3(\tau_0) \sin 2\tau_0] = 0 \quad (5.87)$$

These amplitude and phase equations are the same as the amplitude and phase equations for the nutational mode of the roll motion (Equations 5.38 and 5.39), hence the solutions will also have the same form, namely

$$X(\tau_0) = X_0 e^{\frac{1}{2}[K_1^* - (4a+b)K_2^*]U\tau_0} e^{\frac{1}{2}[K_1^* - (4a+b)K_2^*]R_1(\tau_0) - \frac{1}{2}[K_1^* + (4a-b)K_2^*]R_2(\tau_0)} \quad (5.88)$$

and

$$\begin{aligned}
Y(\tau_0) = & Y_0 - \frac{1}{2}(a+b)\tau_0 - aK_1^* \left[\left(\frac{1}{4} \cos^2 \gamma \sin^2 i - \frac{1}{8} \sin^2 \gamma \sin^2 i \right) \sin 2\tau_0 - \right. \\
& \sin 2\gamma \left[\frac{1}{8(2+n)} \sin 2i - \frac{1}{4(2+n)} \sin i \right] \cos(2+n)\tau_0 - \\
& \sin 2\gamma \left[\frac{1}{8(2-n)} \sin 2i - \frac{1}{4(2-n)} \sin i \right] \cos(2-n)\tau_0 + \\
& \sin^2 \gamma \left[\frac{1}{16(1+n)} (1 + \cos^2 i) + \frac{1}{8(1+n)} \cos i \right] \sin(2+2n)\tau_0 + \\
& \left. \sin^2 \gamma \left[\frac{1}{16(1-n)} (1 + \cos^2 i) - \frac{1}{8(1-n)} \cos i \right] \sin(2-2n)\tau_0 \right] \quad (5.89)
\end{aligned}$$

with U , $R_1(\tau_0)$, and $R_2(\tau_0)$ as defined by Equation 5.41. X_0 and Y_0 are constants determined by the initial conditions.

We see from Equation 5.88 that for this mode to be asymptotically stable, the following must be satisfied.

$$K_1^* < (4a + b)K_2^* \quad (5.90)$$

Note that this is the same criterion with the one for the roll motion.

Orbital Mode

For the orbital mode, the subdominant order analysis will obtain

$$\begin{aligned}
& \frac{d^2 Z}{d\tau_0^2} + [K_1^*[S_1(\tau_0) - S_2(\tau_0) \cos 2\tau_0 - S_3(\tau_0) \sin 2\tau_0] + \\
& \frac{2K_1^*[(2S_2(\tau_0) - nS_6(\tau_0)) \cos 2\tau_0 + (2S_3(\tau_0) + nS_5(\tau_0)) \sin 2\tau_0]}{1 + 2K_1^*[S_3(\tau_0) \cos 2\tau_0 - S_2(\tau_0) \sin 2\tau_0]}] \frac{dZ}{d\tau_0} + \\
& [1 + 2K_1^*[S_3(\tau_0) \cos 2\tau_0 - S_2(\tau_0) \sin 2\tau_0]]Z = 0 \quad (5.91)
\end{aligned}$$

This equation is a linear second order nonautonomous differential equation, therefore its exact solution cannot be obtained. Before deriving the approximate solution of Equation 5.91, we will first examine the pattern of its characteristic roots. Figure 5-6 presents the representative patterns of the characteristic roots locus that we will get for small and large K_1^* . Once again we see that for large K_1^* , we encounter the turning

point problem. Since the system is periodic, there will be many turning points. We will not elaborate this case further and will now concentrate on the case where K_1^* is small, since this is of interest from power consideration. However, we mention here, that numerical simulation shows that for large values of K_1^* the motion is stable as long as K_1^* is positive.

For small K_1^* , that is

$$K_1^* = \delta \bar{K}_1 ; \quad 0 < \delta \ll 1 \quad (5.92)$$

Equation 5.91 becomes

$$\begin{aligned} \frac{d^2 Z}{d\tau_0^2} + \left[\delta g_1(\tau_0) + \frac{\delta g_3(\tau_0)}{1 + g_4(\tau_0)} \right] \frac{dZ}{d\tau_0} \\ + [1 + \delta g_4(\tau_0)] Z = 0 \end{aligned} \quad (5.93)$$

where

$$\begin{aligned} g_3(\tau_0) &= 2\bar{K}_1[(2S_2(\tau_0) - nS_6(\tau_0)) \cos 2\tau_0 + (2S_3(\tau_0) + nS_5(\tau_0)) \sin 2\tau_0] \\ g_4(\tau_0) &= 2\bar{K}_1[S_3(\tau_0) \cos 2\tau_0 - S_2(\tau_0) \sin 2\tau_0] \end{aligned} \quad (5.94)$$

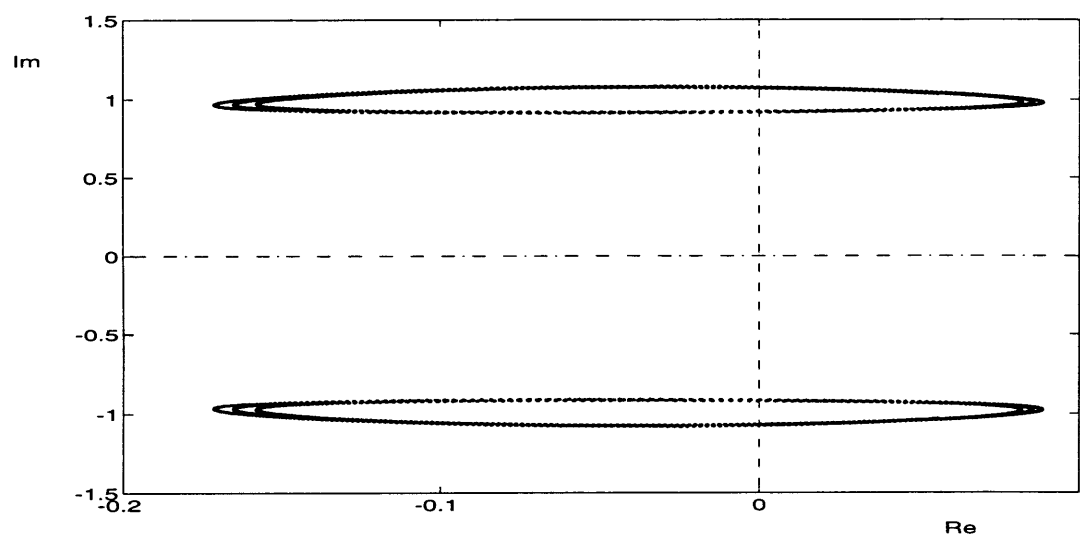
and $g_1(\tau_0)$ is given in Equation 5.52.

By extending the independent and independent variables in Equation 5.93 as follows

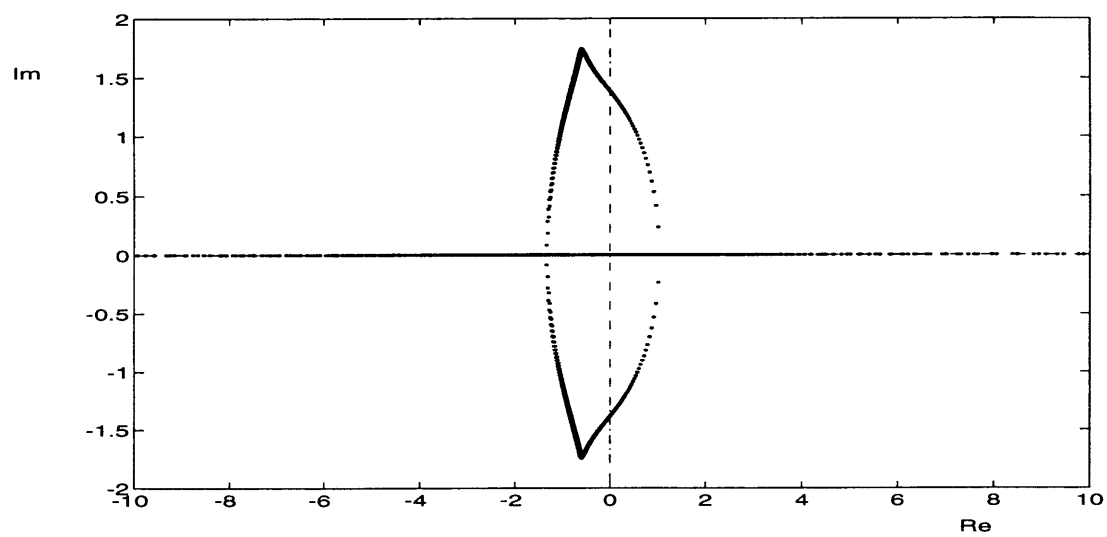
$$\begin{aligned} \tau_0 &\longrightarrow \{\xi_0, \xi_1\} \\ Z(\tau_0, \delta) &\longrightarrow Z(\xi_0, \xi_1) \end{aligned}$$

where

$$\begin{aligned} \xi_0 &= \tau_0 \\ \xi_1 &= \delta^\mu \int \kappa(\tau_0) d\tau_0 \end{aligned} \quad (5.95)$$



(a) $K_1^* = 0.2$



(b) $K_1^* = 3$

Figure 5-6: Characteristic roots locus of the yaw orbital mode

and as before $\kappa(\tau_0)$ is the clock function, Equation 5.93 becomes

$$\begin{aligned} \frac{\partial^2 Z}{\partial \xi_0^2} + Z + \delta \left[\left(g_1(\xi_0) + \frac{g_3(\xi_0)}{1 + \delta g_4(\xi_0)} \right) \frac{\partial Z}{\partial \xi_0} + g_4(\xi_0) Z \right] + \delta^\mu \left[2\kappa \frac{\partial^2 Z}{\partial \xi_0 \partial \xi_1} + \kappa' \frac{\partial Z}{\partial \xi_1} \right] \\ + \delta^{1+\mu} \kappa \left(g_1(\xi_0) + \frac{g_3(\xi_0)}{1 + \delta g_4(\xi_0)} \right) \frac{\partial Z}{\partial \xi_1} + \delta^{2\mu} \kappa^2 \frac{\partial^2 Z}{\partial \xi_1^2} = 0 \end{aligned} \quad (5.96)$$

If δ is small enough, then

$$1 + \delta g_4(\xi_0) \approx 1 \quad (5.97)$$

so that Equation 5.96 can be simplified into

$$\begin{aligned} \frac{\partial^2 Z}{\partial \xi_0^2} + Z + \delta \left[(g_1(\xi_0) + g_3(\xi_0)) \frac{\partial Z}{\partial \xi_0} + g_4(\xi_0) Z \right] + \delta^\mu \left[2\kappa \frac{\partial^2 Z}{\partial \xi_0 \partial \xi_1} + \kappa' \frac{\partial Z}{\partial \xi_1} \right] \\ + \delta^{1+\mu} \kappa (g_1(\xi_0) + g_3(\xi_0)) \frac{\partial Z}{\partial \xi_1} + \delta^{2\mu} \kappa^2 \frac{\partial^2 Z}{\partial \xi_1^2} = 0 \end{aligned} \quad (5.98)$$

This equation has the same ordering of terms as Equation 5.51, therefore without repeating the details, the proper value of μ will also be the same, that is

$$\mu = 1 \quad (5.99)$$

Order by order analysis will then obtain the following.

$$O(\delta^0) : \frac{\partial^2 Z}{\partial \xi_0^2} + Z = 0 \quad (5.100)$$

This equation yields

$$Z = \bar{Z}_0(\xi_1) e^{j\xi_0} + c.c. \quad (5.101)$$

Then, the subdominant order of Equation 5.98 gives

$$O(\delta) : \kappa' \frac{\partial Z}{\partial \xi_1} + 2\kappa \frac{\partial Z}{\partial \xi_0 \partial \xi_1} + (g_1(\xi_0) + g_3(\xi_0)) \frac{\partial Z}{\partial \xi_0} + g_4(\xi_0) Z = 0 \quad (5.102)$$

Substitution of Equation 5.101 into Equation 5.102 results in

$$\left[(\kappa' + j2\kappa) \frac{d\bar{Z}_0}{d\xi_1} + [j(g_1(\xi_0) + g_3(\xi_0)) + g_4(\xi_0)] \bar{Z}_0 \right] e^{j\xi_0} + c.c. = 0 \quad (5.103)$$

For this equation to be satisfied, we must have

$$(\kappa' + j2\kappa) \frac{d\bar{Z}_0}{d\xi_1} + [j(g_1(\xi_0) + g_3(\xi_0)) + g_4(\xi_0)] \bar{Z}_0 = 0 \quad (5.104)$$

We then assume \bar{Z}_0 to be of the form

$$\bar{Z}_0 = Z_0 e^{-\xi_1} \quad (5.105)$$

with Z_0 a constant to be determined from the initial conditions.

Using this assumed form of \bar{Z}_0 , the clock function κ must satisfy the following relation.

$$\kappa' + j2\kappa = j[g_1(\xi_0) + g_3(\xi_0)] + g_4(\xi_0) \quad (5.106)$$

By using the integrating factor $e^{2j\xi_0}$, Equation 5.106 can be written as follows.

$$\frac{d}{d\xi_0} [\kappa e^{2j\xi_0}] = [j(g_1(\xi_0) + g_3(\xi_0)) + g_4(\xi_0)] e^{2j\xi_0} \quad (5.107)$$

Integration of this equation will give us

$$\begin{aligned} \kappa e^{2j\xi_0} &= \int^{\xi_0} [j(g_1(\sigma_0) + g_3(\sigma_0)) + g_4(\sigma_0)] e^{2j\sigma_0} d\sigma_0 \\ \iff \kappa &= \frac{1}{2} \bar{K}_1 U + e^{-2j\xi_0} G_3(\xi_0) + \kappa_0 e^{-2j\xi_0} \end{aligned} \quad (5.108)$$

where κ_0 is an arbitrary constant which will be taken to be zero for simplicity. $G_3(\xi_0)$ is defined by the following expression.

$$G_3(\xi_0) = \int^{\xi_0} [j(g_1^*(\sigma_0) + g_3(\sigma_0)) + g_4(\sigma_0)] e^{2j\sigma_0} d\sigma_0 \quad (5.109)$$

with

$$g_1^*(\sigma_0) = g_1(\sigma_0) - \bar{K}_1 U$$

as before.

Equation 5.108 can also be written as follows.

$$\kappa = \frac{1}{2} \bar{K}_1 U + \frac{1}{2} V (\tau_0 \sin 2\tau_0 + j \cos 2\tau_0) + \hat{G}_3(\tau_0) \quad (5.110)$$

where V is as defined previously and

$$\hat{G}_3(\tau_0) = \int^{\tau_0} [j(g_1^{**}(\sigma_0) + g_3^*(\sigma_0)) + g_4^{ast}(\sigma_0)] e^{2j\sigma_0} d\sigma_0 \quad (5.111)$$

with

$$\begin{aligned} g_1^{**}(\sigma_0) &= g_1^*(\sigma_0) + V \cos \sigma_0 \\ g_3^*(\sigma_0) &= g_3(\sigma_0) - 4\bar{K}_1 V \cos \sigma_0 \\ g_4^*(\sigma_0) &= g_4(\sigma_0) + 2\bar{K}_1 V \sin \sigma_0 \end{aligned} \quad (5.112)$$

$\hat{G}_3(\tau_0)$ contains only periodic terms.

By using the previous argument on uniformity, the secular terms in the κ solution are dropped since they are the bad part of the solution and can be eliminated by constructing proper counterterms. Hence, the uniform solution will be

$$\kappa = \frac{1}{2} \bar{K}_1 U + e^{-2j\tau_0} \hat{G}_3(\tau_0) \quad (5.113)$$

Using Equation 5.113, the time scale ξ_1 becomes

$$\begin{aligned} \xi_1 &= \frac{1}{2} \delta \bar{K}_1 U \tau_0 + \delta G_4(\tau_0) \\ &= \frac{1}{2} K_1^* U \tau_0 + G_4(\tau_0) \end{aligned} \quad (5.114)$$

where

$$G_4(\tau_0) = \int e^{-2j\tau_0} G_3(\tau_0) d\tau_0 \quad (5.115)$$

The real and imaginary parts of $G_4(\tau_0)$ are in the form of long trigonometric functions, which are given in detail in Appendix D.

Finally, the expression for the yaw orbital mode of the dual spin satellite for small K_1^* can be written as follows.

$$\begin{aligned} Z(\tau_0) &= Z_0 e^{-\frac{1}{2}K_1^* U \tau_0} e^{G_4(\tau_0)} e^{j\tau_0} + c.c. \\ &= Z_0 e^{-\frac{1}{2}K_1^* U \tau_0 - \Re(G_4(\tau_0))} \sin(\tau_0 + \Im(G_4(\tau_0)) + Z_1) \end{aligned} \quad (5.116)$$

where Z_1 is a constant to be determined from the initial conditions.

From Appendix D, we see that $\Re(G_4(\tau_0))$ is only a periodic function with small amplitude. So, the stability of the yaw orbital mode for small K_1^* is only determined by $\frac{1}{2}K_1^* U \tau_0$. Since U is always positive, then for small K_1^* , the orbital mode will be asymptotically stable if

$$K_1^* > 0 \quad (5.117)$$

or equivalently,

$$K_1 > 0 \quad (5.118)$$

Note that this is the same the stability criterion with that of the roll orbital mode. Hence, to get the stability of the overall roll/yaw motion, both stability criteria, 5.43 and 5.71, must be satisfied.

5.2.3 Summary and Performance Evaluation

In this chapter, the attitude stability criteria for a dual spin satellite with the magnetic control law given by Equation 3.6 have been obtained. These stability criteria govern the stability of the roll and yaw motion of the satellite, and can be stated as follows. Asymptotic stability of the roll and yaw motion can be achieved if the following

relations hold :

$$K_1^* < (4a + b)K_2^* \quad (5.119)$$

$$K_1^* > 0 \quad (5.120)$$

From the previous results, it is also possible to estimate the time constants of the roll/yaw motion for the case where K_1^* is small. The approximate time constants for this case are as follows.

- Nutational mode :

$$T_{c_n} = \frac{2}{\epsilon[(4a + b)K_2^* - K_1^*] \frac{h}{\sqrt{I_x I_y}} U} \quad (5.121)$$

- Orbital mode :

$$T_{c_o} = \frac{2}{\epsilon K_1^* \frac{h}{\sqrt{I_x I_y}} U} \quad (5.122)$$

Note that U here is the same with U in the previous chapter. So, this magnetic control scheme is more effective for satellites at orbit that makes high angle with respect to the equatorial plane.

The effect of altitude on the control system is also clear. The higher the altitude of the satellite the larger control gains needed to achieve a certain time constant requirement.

The earth rotation mainly causes a slight phase shift in the nutational and orbital modes of the satellite. Thus, for accurate frequency prediction, this effect should be included.

The true effectiveness of the control system is also determined by the relative position of the geomagnetic dipole with respect to the orbital plane of the satellite. The most effective situation is attained if the geomagnetic dipole lies in the satellite's orbital plane. Some modifications need to be made on the approximate time constant expressions to account for this effect. For preliminary analysis purposes, however, a fairly accurate prediction can be achieved using the approximate time constants above.

The approximate solutions obtained in this chapter are the zeroth order expansions

only. The first and higher order expansions are not included in the analysis. The maximum error of the approximations, which is of the order of the first term neglected, is therefore of $O(\epsilon)$.

5.2.4 Comparison with Numerical Results

The values of the parameters chosen for this purpose are those of the ITOS satellite in a circular orbit of altitude 1000 km and an inclination of 60° . The values of the satellite parameters are as follows.

$$I_x = 155.3 \text{ kg m}^2$$

$$I_y = 135.5 \text{ kg m}^2$$

$$I_z = 138.9 \text{ kg m}^2$$

$$h = 26.6 \text{ kg m}^2$$

Using these parameter values,

$$\epsilon = 0.0054$$

The stability criteria of the roll/yaw motion of the satellite become

$$K_1^* < 5.2164 K_2^*$$

$$K_1^* > 0$$

Numerical simulations show that these stability criteria have good accuracy. Examples of simulation results when the control gains are chosen to slightly violate the stability criteria are presented in Figures 5-7 and 5-8. Figure 5-7 shows the response of the system when only the nutational mode stability criterion is violated. The amplitude of the nutational mode (fast oscillation) in this case grows slowly in time (instability). Figure 5-8 shows the other case, namely when only the orbital mode stability criterion is violated. We see that the amplitude of the orbital mode (slow oscillation) slowly increases with time.

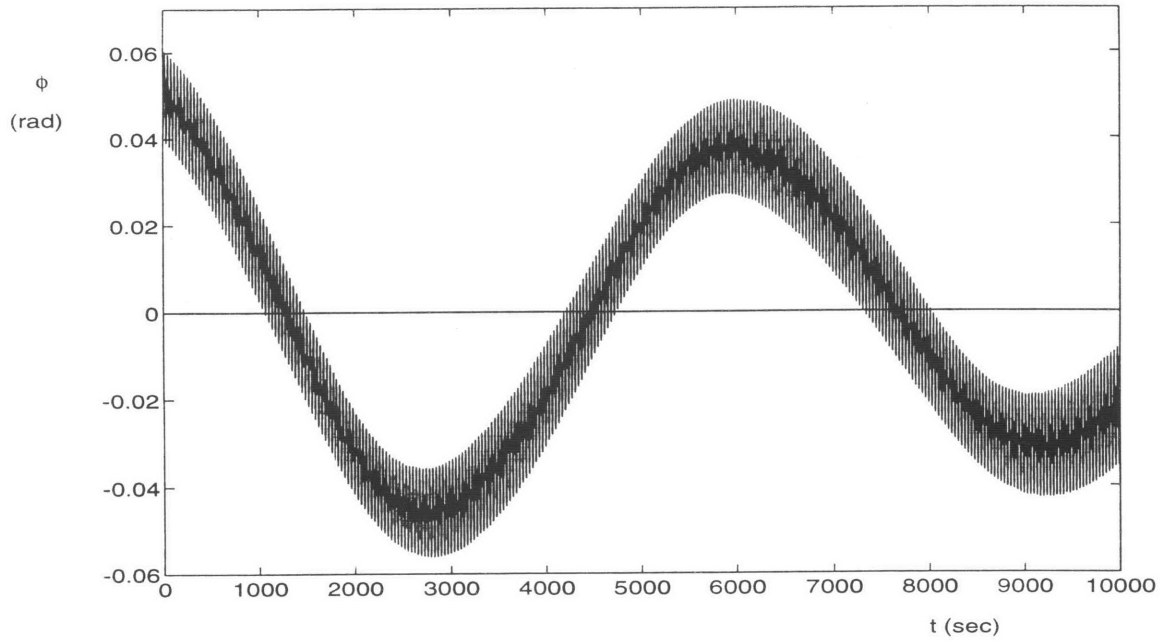


Figure 5-7: Instability due to slight violation of nutational mode stability criterion ($K_1^* = 0.6$ and $K_2^* = 0.1$)

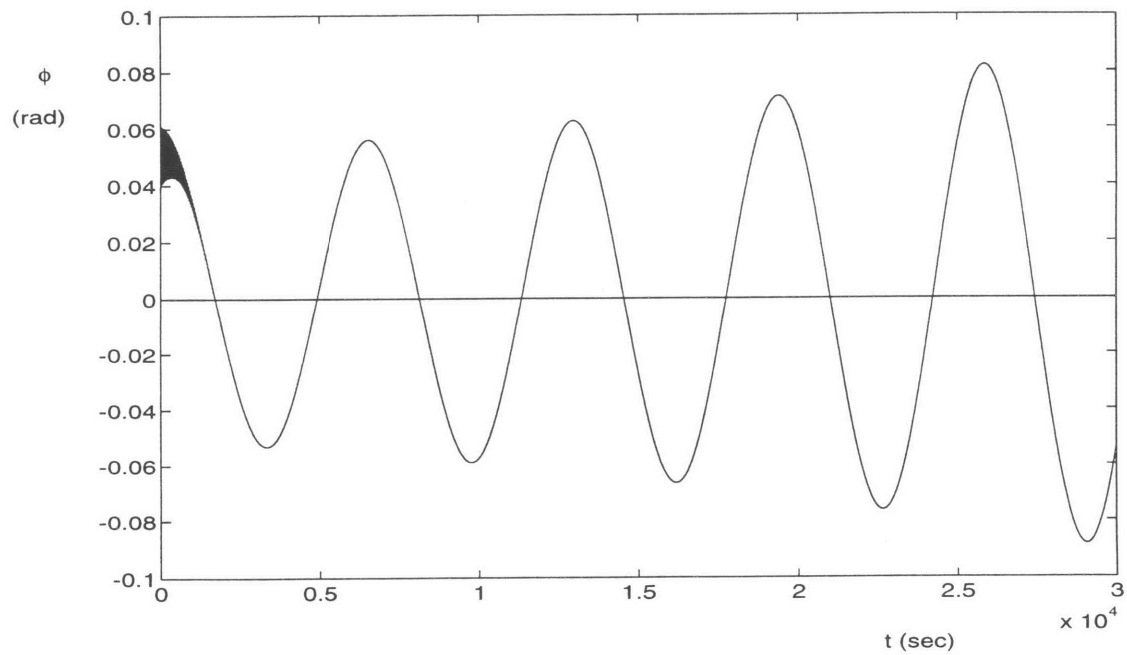


Figure 5-8: Instability due to slight violation of orbital mode stability criterion ($K_1^* = -0.2$ and $K_2^* = 2$)

Next we select specific values of K_1^* and K_2^* and compare the numerical and GMS results. The specific values selected are

$$K_1^* = 0.2$$

$$K_2^* = 2$$

or equivalently,

$$K_1 = 1.349 \times 10^6 A m^2/T$$

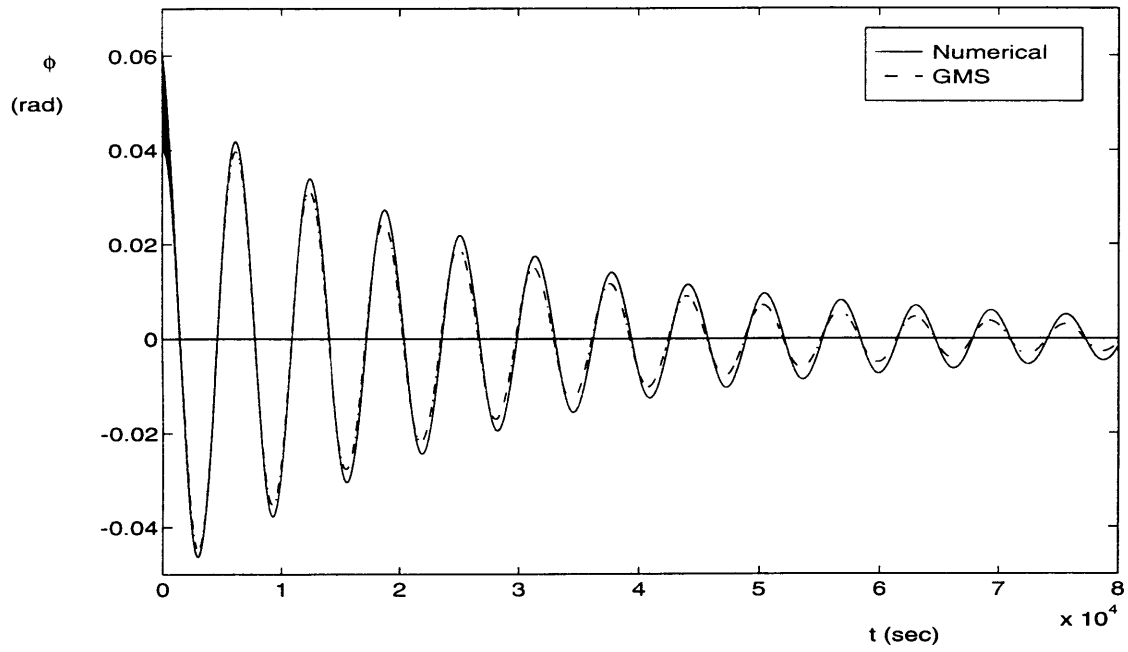
$$K_2 = 7.358 \times 10^8 A m^2 s/T$$

For the selected numerical values, the approximate frequencies and time constants from the GMS result are as follows.

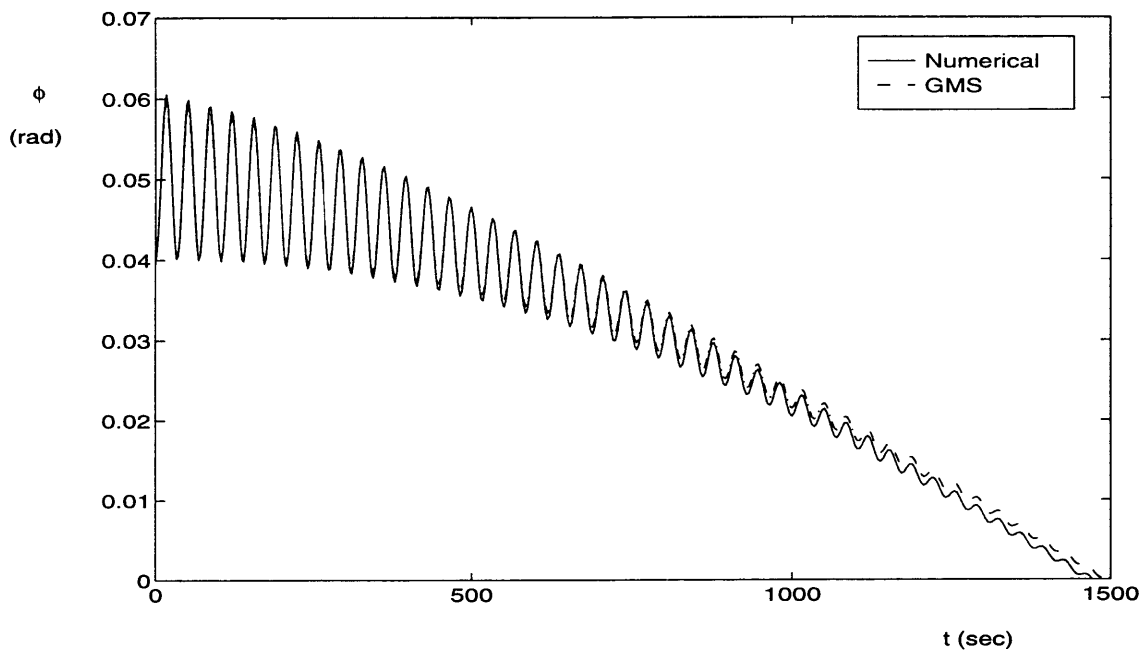
- Nutational mode : $\omega_n = 0.1834 \text{ rad/s}$, $T_{c_n} = 526 \text{ s}$
- Orbital mode : $\omega_o = 0.000998 \text{ rad/s}$, $T_{c_o} = 26905 \text{ s}$

The comparisons of the results are presented in Figures 5-9 and 5-10. The nutational and orbital frequencies are shown to be predicted accurately by the GMS method. The time constants of the motion as predicted by GMS method are also fairly accurate. The errors are due to the neglected first and higher order terms in the expansion. Figure 5-11 shows the magnitude of the error of the approximations. Clearly this agrees with our previous statement that the maximum magnitude of the error is of $O(\epsilon)$. Based on this discussion, we see that the approximations obtained by using the GMS approach] attain a good agreement with the exact solution.

As K_1^* is increased further, the approximations become worse, as can be seen in Figure 5-12. This can be understood since our approximation on the orbital mode is based upon the assumption of small K_1^* . Therefore the smaller K_1^* , the better the approximation is.

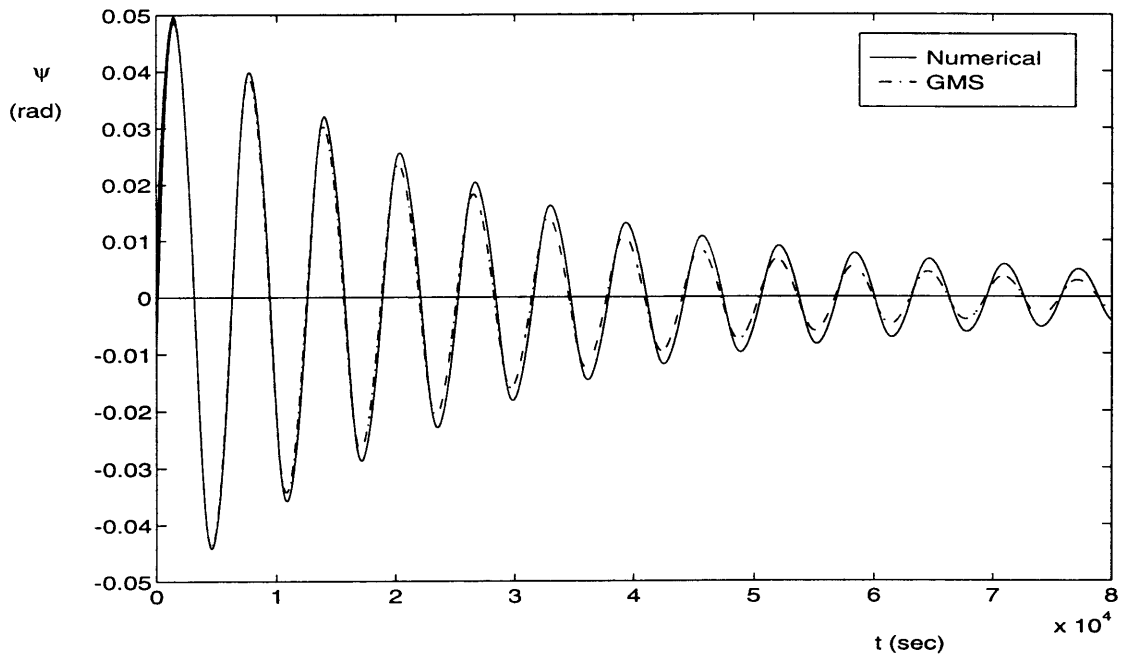


(a) Long term response

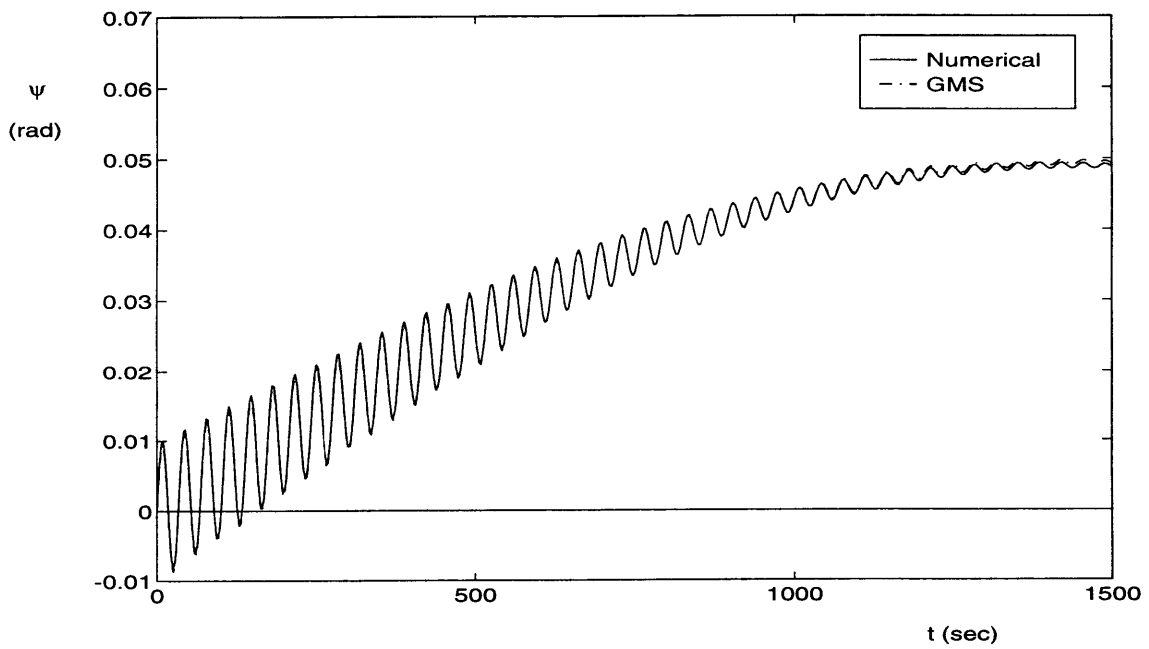


(b) Short term response

Figure 5-9: Comparison of numerical and GMS results for roll motion

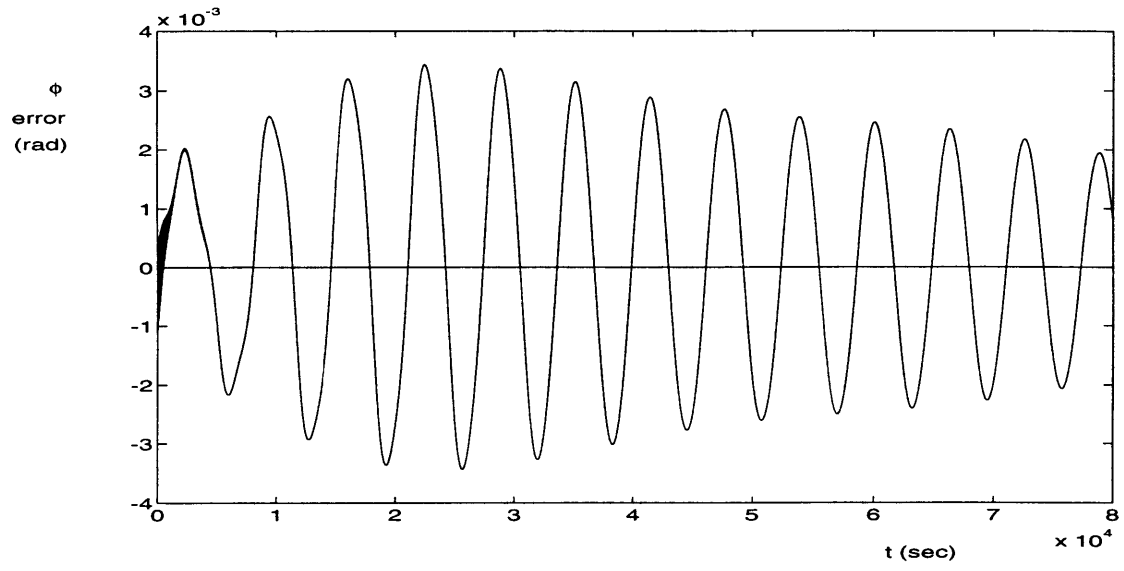


(a) Long term response

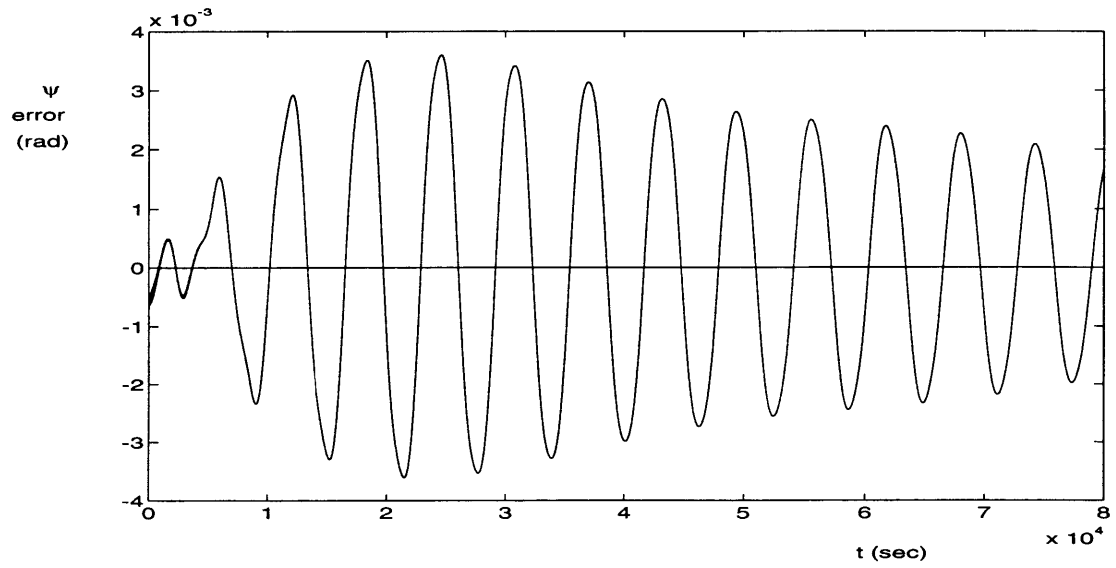


(b) Short term response

Figure 5-10: Comparison of numerical and GMS results for yaw motion

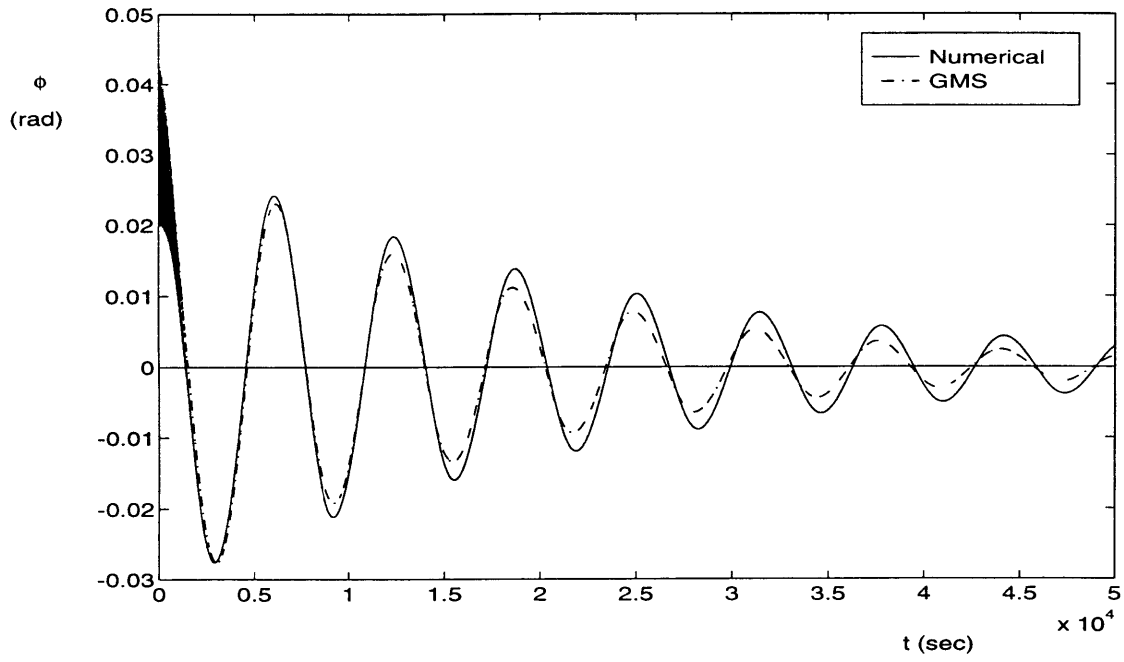


(a)

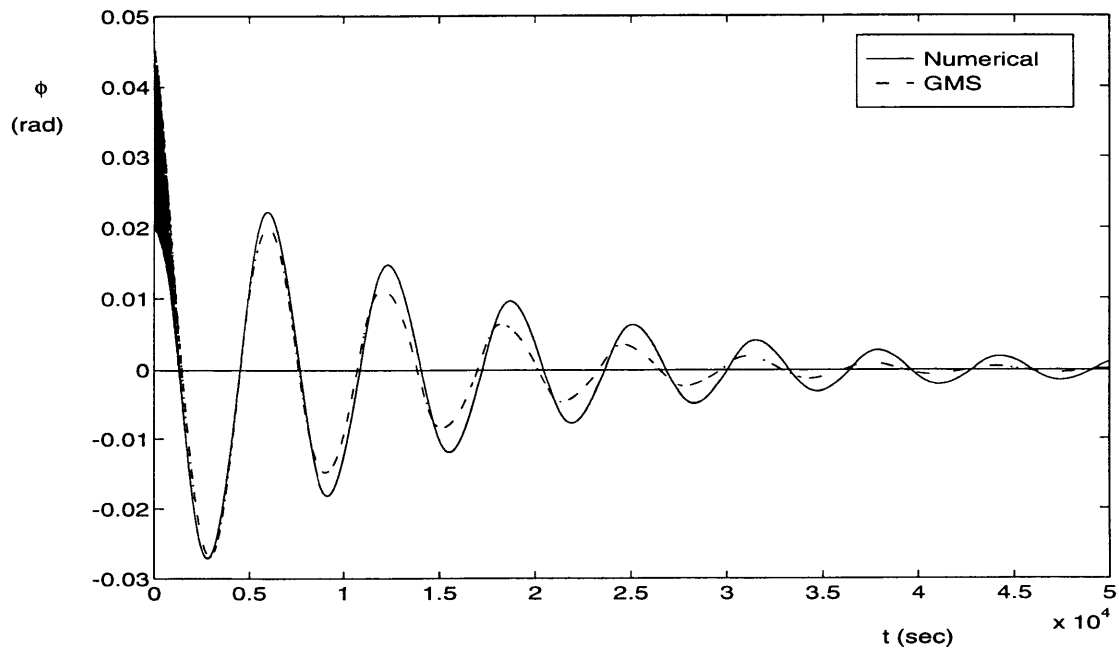


(b)

Figure 5-11: Errors of the approximations for $K_1^* = 0.2$ and $K_2^* = 2$



(a) $K_1^* = 0.3, K_2^* = 2$



(b) $K_1^* = 0.5, K_2^* = 2$

Figure 5-12: Comparison of numerical and GMS results for larger values of K_1^*

Chapter 6

Conclusion

In this dissertation, the attitude control of satellites using geomagnetic field has been investigated. A specific but fairly general control law has been selected to be analyzed. Two types of satellites are considered in the analysis, one is the spin-stabilized asymmetric satellites and the other is the dual spin asymmetric satellites. Only satellites in circular earth orbit are considered. The analysis performed shows that the control law considered (with the proper choice of gains) can provide the necessary damping to obtain an asymptotically stable system.

Results in parametric form were obtained using the Generalized Multiple Scales (GMS) method. Each dominant mode of the satellite motion is systematically separated by using proper time scales, leading to insight of the nature of the system dynamics. Both linear and nonlinear time scales are used in deriving the results.

The stability criteria for both types of satellite have been obtained. These stability criteria provide the boundaries for the choice of the control gains to assure stability. In general, the parameters that influence the stability criteria for both cases are as follows :

- the inertia distribution of a satellite
- the spin rate of the spinning part of a satellite
- the altitude of the orbit of the satellite.

It is worth mentioning here that none of the above parameters influences the stability of the orbital mode of a dual spin satellite. The stability of this particular mode is only determined by the sign of the control gain K_1 . It should also be noted that for the single spin satellite case, one can still obtain stability by dropping one of the control gains ($K_1 = 0$). For the dual spin case, however, the use of the two control gains is required to achieve stability.

The approximate dynamic responses of the system are also obtained in explicit analytical form using the GMS approach. Conclusion that can be drawn from these results is that the performance of the system is affected not only by the parameters mentioned in the previous paragraph but also by the relative orientation of the satellite's orbit with respect to the earth. It has been pointed out previously that the magnetic control system is effective for a satellite in an orbit making high angle with respect to the equator.

Good agreement between the approximate analytical results, as obtained using the GMS method, with the exact results, as obtained using direct numerical integration, are also demonstrated. Note that only zeroth order expansions are used in the approximations. The maximum order of errors of the approximations is also shown to be consistent with the prediction, which is the order of the first term neglected in the expansions. Overall, we may say, that for preliminary analysis purposes, the approximations obtained are fairly accurate.

Appendix A

Gravity Gradient Torque on a Satellite Orbiting the Earth

We assume that the Earth is a perfect sphere and has a radially symmetric mass distribution, so that the Newtonian force field theory can be applied. The satellite considered is rigid and its orbit is circular. See Figure A-1. In the figure :

\mathbf{R} is vector from the center of the earth to the center of mass of the satellite.

\mathbf{r} is vector from the center of the earth to a mass element dm of the satellite.

ρ is position vector of the mass element dm with respect to the center of mass of the satellite.

Obviously,

$$\mathbf{r} = \mathbf{R} + \rho \quad (\text{A.1})$$

Then, if \mathbf{i}_{x_b} , \mathbf{i}_{y_b} , \mathbf{i}_{z_b} are the unit vectors along the body-fixed axes $X_b Y_b Z_b$, then ρ can be expressed as follows.

$$\rho = x \mathbf{i}_{x_b} + y \mathbf{i}_{y_b} + z \mathbf{i}_{z_b} \quad (\text{A.2})$$

The attractive force on dm is

$$\mathbf{dF} = -\mu \frac{dm}{r^3} \mathbf{r} \quad (\text{A.3})$$

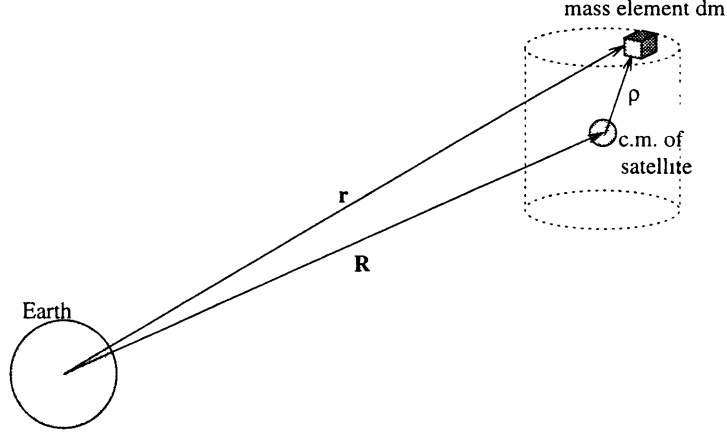


Figure A-1: Vector Definitions

where μ is the earth's gravitational parameter. This force will produce the torque about the center of mass of the satellite, which can be expressed as follows :

$$\begin{aligned} d\mathbf{L}_g &= -\rho \times \frac{\mu dm}{r^3} \mathbf{r} \\ &= -\frac{\mu dm}{r^3} \rho \times \mathbf{R} \end{aligned} \quad (\text{A.4})$$

Next, since

$$\begin{aligned} r^2 &= (\mathbf{R} + \rho) \cdot (\mathbf{R} + \rho) \\ &= R^2 \left[1 + \left(\frac{\rho}{R} \right)^2 + \frac{2\mathbf{R} \cdot \rho}{R^2} \right] \end{aligned} \quad (\text{A.5})$$

then r^{-3} can be written as

$$r^{-3} = \frac{1}{R^3} \left[1 + \left(\frac{\rho}{R} \right)^2 + \frac{2\mathbf{R} \cdot \rho}{R^2} \right]^{-\frac{3}{2}} \quad (\text{A.6})$$

By using the fact that the satellite's dimension is normally much smaller than the dimension of the orbit ($\rho \ll R$), the second and higher order terms in the binomial expansion of Equation A.6 can be neglected, so that

$$r^{-3} \approx \frac{1}{R^3} \left[1 - 3 \frac{\mathbf{R} \cdot \rho}{R^2} \right] \quad (\text{A.7})$$

Using the result so far, the total torque exerted on the satellite is

$$\begin{aligned}\mathbf{L}_g &= -\frac{\mu}{R^3} \int_m \left[1 - 3 \frac{\mathbf{R} \cdot \boldsymbol{\rho}}{R^2} \right] (\boldsymbol{\rho} \times \mathbf{R}) dm \\ &= -\frac{\mu}{R^3} \int_m \boldsymbol{\rho} dm \times \mathbf{R} + \frac{3\mu}{R^3} \int_m \frac{(\mathbf{R} \cdot \boldsymbol{\rho})(\boldsymbol{\rho} \times \mathbf{R})}{R^2} dm\end{aligned}\quad (\text{A.8})$$

Since the origin of the body-fixed axes coincides with the center of mass of the satellite, then

$$\int_m \boldsymbol{\rho} dm = 0 \quad (\text{A.9})$$

so that Equation A.8 becomes

$$\mathbf{L}_g = \frac{3\mu}{R^3} \int_m \frac{(\mathbf{R} \cdot \boldsymbol{\rho})(\boldsymbol{\rho} \times \mathbf{R})}{R^2} dm \quad (\text{A.10})$$

The attitude of the satellite can be identified by three successive rotations from the orbiting coordinate system (this coordinate system is defined in Chapter 3). The sequence of rotations used here is the same as the one used in Chapter 4 and 5, namely ψ about Z_o -axis, θ about the newly displaced Y_o -axis, and ϕ about the final orientation of X_o -axis ($\equiv X_b$). Using this defined sequence of rotation, \mathbf{R} can be expressed as

$$\mathbf{R} = R(c_1 \mathbf{i}_{x_b} + c_2 \mathbf{i}_{y_b} + c_3 \mathbf{i}_{z_b}) \quad (\text{A.11})$$

where

$$\begin{aligned}c_1 &= \sin \theta \\ c_2 &= -\cos \theta \sin \phi \\ c_3 &= -\cos \theta \cos \phi\end{aligned}\quad (\text{A.12})$$

Substitution of Equations A.2 and A.11 into Equation A.10 will obtain the components of the gravity gradient torque along the body-fixed axes of the satellite as

follows.

$$\begin{aligned}
L_{g_x} &= \frac{3}{2}\Omega^2(I_z - I_y)\sin 2\phi \cos^2 \theta \\
L_{g_y} &= \frac{3}{2}\Omega^2(I_z - I_x)\cos \phi \sin 2\theta \\
L_{g_z} &= \frac{3}{2}\Omega^2(I_x - I_y)\sin \phi \sin 2\theta
\end{aligned} \tag{A.13}$$

where I_x , I_y , and I_z are the moments of inertia of the satellite about X_b , Y_b , and Z_b , respectively, and defined by

$$\begin{aligned}
I_x &= \int_m (y^2 + z^2) dm \\
I_y &= \int_m (x^2 + z^2) dm \\
I_z &= \int_m (x^2 + y^2) dm
\end{aligned} \tag{A.14}$$

Ω in Equation A.13 is the orbital angular speed of the satellite, which is

$$\Omega = \frac{\mu}{R^3} \tag{A.15}$$

The order of magnitude of this torque will now be examined for the single spin and dual spin satellites discussed in Chapter 4 and 5, respectively.

We will look first on the single spin satellite case. By using the definition of ϵ in Chapter 4 ($\epsilon = \frac{\Omega}{\omega_s}$), then the components of the gravity gradient torque along the body-fixed axes for small ϕ and ψ become

$$\begin{aligned}
\frac{L_{g_x}}{I_x} &= \epsilon^2 \omega_s^2 \frac{(I_y - I_z)}{I_x} (\phi \sin 2\theta + 2\psi \sin^2 \theta) \\
\frac{L_{g_y}}{I_y} &= \epsilon^2 \omega_s^2 \frac{(I_x - I_z)}{I_x} (\psi \sin 2\theta + 2\phi \cos^2 \theta) \\
\frac{L_{g_z}}{I_z} &= \epsilon^2 \omega_s^2 \frac{(I_x - I_y)}{I_x} \sin 2\theta
\end{aligned} \tag{A.16}$$

So, it is clear that the gravity gradient torque in this case only contributes to second order terms in Equations 4.20 and 4.21.

For the dual spin case, θ is assumed zero. Then, using ϵ as defined in Chapter 5 and the assumption that ϕ and ψ are small, we can write

$$\begin{aligned} L_{g_x} &= 0 \\ L_{g_y} &= 3\epsilon^2 h^2 \frac{I_y - I_z}{I_x I_y} \phi \\ L_{g_z} &= 0 \end{aligned} \tag{A.17}$$

It is also obvious here, that the contribution of the gravity gradient torque in the controlled equations of motion 5.19 is only of second order in magnitude.

Appendix B

Extended First to Fourth Order Derivative Operators

Ramnath [6] has developed the GMS extension of the n-th order derivative operator by means of mathematical induction. The result for the first to the fourth order is given below. Here, τ denotes the independent variable of an ordinary differential equation. The extension is defined as follows

$$\tau \longrightarrow \{\tau_0, \tau_1\} \quad (\text{B.1})$$

where

$$\begin{aligned} \tau_0 &= \tau \\ \tau_1 &= \epsilon^\nu \int k(\tau) d\tau \end{aligned} \quad (\text{B.2})$$

The derivative operators : (prime denotes differentiation with respect to τ)

$$\frac{d}{d\tau} \longrightarrow \frac{\partial}{\partial \tau_0} + \epsilon^\nu k \frac{\partial}{\partial \tau_1} \quad (\text{B.3})$$

$$\frac{d^2}{d\tau^2} \longrightarrow \frac{\partial^2}{\partial \tau_0^2} + \epsilon^\nu 2k \frac{\partial^2}{\partial \tau_0 \partial \tau_1} + \epsilon^{2\nu} k^2 \frac{\partial^2}{\partial \tau_1^2} + \epsilon^\nu k' \frac{\partial}{\partial \tau_1} \quad (\text{B.4})$$

$$(\text{B.5})$$

$$\begin{aligned}
\frac{d^3}{d\tau^3} \longrightarrow & \frac{\partial^3}{\partial\tau_0^3} + \epsilon^\nu 3k \frac{\partial^3}{\partial\tau_0^2 \partial\tau_1} + \epsilon^{2\nu} 3k^2 \frac{\partial^3}{\partial\tau_0 \partial\tau_1^2} + \epsilon^{3\nu} k^3 \frac{\partial^3}{\partial\tau_1^3} + \\
& \epsilon^\nu k'' \frac{\partial}{\partial\tau_1} + \epsilon^\nu 2k' \frac{\partial^2}{\partial\tau_0 \partial\tau_1} + \epsilon^2 3kk' \frac{\partial^2}{\partial\tau_1^2}
\end{aligned} \tag{B.6}$$

$$\begin{aligned}
\frac{d^4}{d\tau^4} \longrightarrow & \frac{\partial^4}{\partial\tau_0^4} + \epsilon^\nu 4k \frac{\partial^4}{\partial\tau_0^3 \partial\tau_1} + \epsilon^{2\nu} 6k^2 \frac{\partial^4}{\partial\tau_0^2 \partial\tau_1^2} + \epsilon^{3\nu} 4k^3 \frac{\partial^4}{\partial\tau_0 \partial\tau_1^3} + \\
& \epsilon^{4\nu} k^4 \frac{\partial^4}{\partial\tau_1^4} + \epsilon^\nu k''' \frac{\partial}{\partial\tau_1} + \epsilon^\nu 3k'' \frac{\partial^2}{\partial\tau_0 \partial\tau_1} + \epsilon^{2\nu} 4kk'' \frac{\partial^2}{\partial\tau_1^2} + \epsilon^{2\nu} 3k'^2 \frac{\partial^2}{\partial\tau_1^2} + \\
& \epsilon^{3\nu} 6k^2 k' \frac{\partial^3}{\partial\tau_1^3} + \epsilon^{2\nu} 11kk' \frac{\partial^3}{\partial\tau_0 \partial\tau_1^2} + \epsilon^\nu 5k' \frac{\partial^3}{\partial\tau_0^2 \partial\tau_1}
\end{aligned} \tag{B.7}$$

Appendix C

Natural Frequencies of Torque-Free Dual Spin Satellite

The equations of motion for a dual spin satellite have been derived in Chapter 5. In torque-free case, the equations of motion become

$$\begin{aligned} I_y \ddot{\phi} + \Omega(h - I_x \Omega)\phi - [h - (I_x + I_y)\Omega]\dot{\psi} &= 0 \\ I_x \ddot{\psi} + \Omega(h - I_y \Omega)\psi - [h - (I_x + I_y)\Omega]\dot{\phi} &= 0 \end{aligned} \quad (\text{C.1})$$

Note that these equations have constant coefficients. The Laplace transform of these equations by assuming zero initial conditions is as follows

$$\begin{aligned} [I_y s + \Omega(h - I_x \Omega)]\phi(s) - [h - (I_x + I_y)\Omega]s\psi(s) &= 0 \\ [I_x s + \Omega(h - I_y \Omega)]\psi(s) - [h - (I_x + I_y)\Omega]s\phi(s) &= 0 \end{aligned} \quad (\text{C.2})$$

The characteristic equation of this system of equations can be obtained by equating the determinant of the coefficient matrix to zero, that is

$$I_x I_y s^4 + [(h - I_x \Omega)(h - I_y \Omega) + I_x I_y \Omega^2]s^2 + \Omega^2(h - I_x \Omega)(h - I_y \Omega) = 0 \quad (\text{C.3})$$

This equation can be factorized as follows.

$$[I_x I_y s^2 + (h - I_x \Omega)(h - I_y \Omega)][s^2 + \Omega^2] = 0 \quad (\text{C.4})$$

The roots of the characteristic equation are the eigenvalues of the system, which also represent the natural frequencies of the system. The eigenvalues are as follows.

$$\begin{aligned} s &= \pm j\Omega \\ s &= \pm j\sqrt{\frac{(h - I_x \Omega)(h - I_y \Omega)}{I_x I_y}} \end{aligned} \quad (\text{C.5})$$

So, the system has two natural modes with natural frequencies Ω and $\sqrt{\frac{(h - I_x \Omega)(h - I_y \Omega)}{I_x I_y}}$. These modes are normally called the orbital mode and the nutational mode, respectively. If Ω is very small, then the natural frequencies can be approximated as follows:

- orbital frequency : Ω
- nutational frequency : $\frac{h}{\sqrt{I_x I_y}}$

Appendix D

Detail of the Functions $G_2(\tau_0)$ and $G_4(\tau_0)$ in Chapter 5

First we define the following:

$$\begin{aligned}\Delta_1 &= -4 + 4n^2 \\ \Delta_2 &= -4 + n^2 \\ \Delta_3 &= -4 + (2 - 2n)^2 \\ \Delta_4 &= -4 + (2 + 2n)^2 \\ \Delta_5 &= -4 + (2 - n)^2 \\ \Delta_6 &= -4 + (2 + n)^2\end{aligned}\tag{D.1}$$

$$\begin{aligned}s_{12} &= \frac{1}{4} \sin^2 \gamma \sin^2 i \\ s_{13} &= \frac{1}{4} \sin 2\gamma \sin 2i \\ s_{21} &= \frac{1}{4} \sin^2 \gamma \sin^2 i - \frac{1}{2} \cos^2 \gamma \sin^2 i \\ s_{22} &= \frac{1}{4} \sin^2 \gamma (1 + \cos^2 i) \\ s_{23} &= -s_{13} \\ s_{31} &= \frac{1}{2} \sin 2\gamma \sin i\end{aligned}$$

$$\begin{aligned}
s_{32} &= \frac{1}{2} \sin^2 \gamma \cos i \\
s_{41} &= -\frac{1}{2} n \sin^2 \gamma \sin^2 i \\
s_{42} &= \frac{1}{4} n \sin 2\gamma \sin 2i \\
s_{51} &= -\frac{1}{2} n \sin^2 \gamma (1 + \cos^2 i) \\
s_{52} &= -s_{42} \\
s_{61} &= -\frac{1}{2} n \sin 2\gamma \sin i \\
s_{62} &= n \sin^2 \gamma \cos i
\end{aligned} \tag{D.2}$$

Using these definitions, we can write

$$\begin{aligned}
\Re(G_2(\tau_0)) &= -s_{12} \frac{\sin 2n\tau_0}{n\Delta_1} + 2s_{13} \frac{\cos n\tau_0}{n\Delta_2} - \frac{1}{4} s_{21} \sin 2\tau_0 + \\
& s_{22} \left[\frac{\sin(2-2n)\tau_0}{(2-2n)\Delta_3} + \frac{\sin(2+2n)\tau_0}{(2+2n)\Delta_4} \right] - s_{23} \left[\frac{\cos(2+n)\tau_0}{(2+n)\Delta_6} - \frac{\cos(2-n)\tau_0}{(2-n)\Delta_5} \right] - \\
& s_{31} \left[\frac{\cos(2+n)\tau_0}{(2+n)\Delta_6} + \frac{\cos(2-n)\tau_0}{(2-n)\Delta_5} \right] - s_{32} \left[\frac{\sin(2+2n)\tau_0}{(2+2n)\Delta_4} - \frac{\sin(2-2n)\tau_0}{(2-2n)\Delta_3} \right] - \\
& s_{41} \frac{\sin 2n\tau_0}{\Delta_1} - s_{42} \frac{\cos n\tau_0}{\Delta_2} + \\
& s_{51} \left[\frac{\sin(2+2n)\tau_0}{2\Delta_4} - \frac{\sin(2-2n)\tau_0}{2\Delta_3} \right] + s_{52} \left[\frac{\cos(2-n)\tau_0}{2\Delta_5} - \frac{\cos(2+n)\tau_0}{2\Delta_6} \right] - \\
& s_{61} \left[\frac{\cos(2+n)\tau_0}{2\Delta_6} - \frac{\cos(2-n)\tau_0}{2\Delta_5} \right] + s_{62} \left[\frac{\sin(2+2n)\tau_0}{2\Delta_4} + \frac{\sin(2-2n)\tau_0}{2\Delta_3} \right]
\end{aligned} \tag{D.3}$$

$$\begin{aligned}
\Im(G_2(\tau_0)) &= -s_{12} \frac{\cos 2n\tau_0}{\Delta_1} - s_{13} \frac{\sin n\tau_0}{\Delta_2} - \frac{1}{8} s_{21} \cos 2\tau_0 + \\
& s_{22} \left[\frac{\cos(2-2n)\tau_0}{2\Delta_3} + \frac{\cos(2+2n)\tau_0}{2\Delta_4} \right] + s_{23} \left[\frac{\sin(2+n)\tau_0}{2\Delta_6} - \frac{\sin(2-n)\tau_0}{2\Delta_5} \right] + \\
& s_{31} \left[\frac{\sin(2+n)\tau_0}{2\Delta_6} + \frac{\sin(2-n)\tau_0}{2\Delta_5} \right] - s_{32} \left[\frac{\cos(2+2n)\tau_0}{2\Delta_4} - \frac{\cos(2-2n)\tau_0}{2\Delta_3} \right] - \\
& s_{41} \frac{\cos 2n\tau_0}{n\Delta_1} + 2s_{42} \frac{\sin n\tau_0}{n\Delta_2} - \\
& s_{51} \left[\frac{\cos(2-2n)\tau_0}{(2-2n)\Delta_3} - \frac{\cos(2+2n)\tau_0}{(2+2n)\Delta_4} \right] - s_{52} \left[\frac{\sin(2-n)\tau_0}{(2-n)\Delta_5} + \frac{\sin(2+n)\tau_0}{(2+n)\Delta_6} \right] -
\end{aligned}$$

$$s_{61} \left[\frac{\sin(2-n)\tau_0}{(2-n)\Delta_5} - \frac{\sin(2+n)\tau_0}{(2+n)\Delta_6} \right] + s_{62} \left[\frac{\cos(2-2n)\tau_0}{(2-2n)\Delta_3} + \frac{\cos(2+2n)\tau_0}{(2+2n)\Delta_4} \right] \quad (\text{D.4})$$

$$\begin{aligned} \Re(G_4(\tau_0)) = & -s_{12} \frac{\sin 2n\tau_0}{n\Delta_1} + 2s_{13} \frac{\cos n\tau_0}{n\Delta_2} + \frac{1}{2}s_{21} \frac{1}{2} \sin 2\tau_0 - \\ & 3s_{22} \left[\frac{\sin(2-2n)\tau_0}{(2-2n)\Delta_3} + \frac{\sin(2+2n)\tau_0}{(2+2n)\Delta_4} \right] + 3s_{23} \left[\frac{\cos(2+n)\tau_0}{(2+n)\Delta_6} - \frac{\cos(2-n)\tau_0}{(2-n)\Delta_5} \right] + \\ & 3s_{31} \left[\frac{\cos(2+n)\tau_0}{(2+n)\Delta_6} + \frac{\cos(2-n)\tau_0}{(2-n)\Delta_5} \right] + 3s_{32} \left[\frac{\sin(2+2n)\tau_0}{(2+2n)\Delta_4} - \frac{\sin(2-2n)\tau_0}{(2-2n)\Delta_3} \right] + \\ & s_{22} \left[\frac{\sin(2-2n)\tau_0}{\Delta_3} + \frac{\sin(2+2n)\tau_0}{\Delta_4} \right] + s_{23} \left[\frac{\cos(2-n)\tau_0}{\Delta_5} - \frac{\cos(2+n)\tau_0}{\Delta_6} \right] - \\ & s_{31} \left[\frac{\cos(2-n)\tau_0}{2\Delta_4} + \frac{\sin(2-2n)\tau_0}{\Delta_3} \right] + s_{32} \left[\frac{\sin(2-2n)\tau_0}{\Delta_3} - \frac{\sin(2+2n)\tau_0}{\Delta_4} \right] - \\ & 2s_{51} \left[\frac{\sin(2+2n)\tau_0}{(2+2n)\Delta_4} - \frac{\sin(2-2n)\tau_0}{(2-2n)\Delta_3} \right] + 2s_{52} \left[\frac{\cos(2-n)\tau_0}{(2-n)\Delta_5} + \frac{\cos(2+n)\tau_0}{(2+n)\Delta_6} \right] + \\ & 2s_{61} \left[\frac{\cos(2-n)\tau_0}{(2-n)\Delta_5} - \frac{\cos(2+n)\tau_0}{(2+n)\Delta_6} \right] + 2s_{62} \left[\frac{\sin(2-2n)\tau_0}{(2-2n)\Delta_3} + \frac{\sin(2+2n)\tau_0}{(2+2n)\Delta_4} \right] \quad (\text{D.5}) \end{aligned}$$

$$\begin{aligned} \Im(G_4(\tau_0)) = & -s_{12} \frac{\cos 2n\tau_0}{\Delta_1} - s_{13} \frac{\sin n\tau_0}{\Delta_2} + \frac{1}{8}s_{21} \cos 2\tau_0 - \\ & 3s_{22} \left[\frac{\cos(2-2n)\tau_0}{2\Delta_3} + \frac{\cos(2+2n)\tau_0}{2\Delta_4} \right] - 3s_{23} \left[\frac{\sin(2+n)\tau_0}{2\Delta_6} - \frac{\sin(2-n)\tau_0}{2\Delta_5} \right] - \\ & 3s_{31} \left[\frac{\sin(2+n)\tau_0}{2\Delta_6} + \frac{\sin(2-n)\tau_0}{2\Delta_5} \right] + 3s_{32} \left[\frac{\cos(2+2n)\tau_0}{2\Delta_4} - \frac{\cos(2-2n)\tau_0}{2\Delta_3} \right] + \\ & 2s_{22} \left[\frac{\cos(2-2n)\tau_0}{(2-2n)\Delta_3} + \frac{\cos(2+2n)\tau_0}{(2+2n)\Delta_4} \right] - 2s_{23} \left[\frac{\sin(2-n)\tau_0}{(2-n)\Delta_5} - \frac{\sin(2+n)\tau_0}{(2+n)\Delta_6} \right] + \\ & 2s_{31} \left[\frac{\sin(2-n)\tau_0}{(2-n)\Delta_5} + \frac{\sin(2+n)\tau_0}{(2+n)\Delta_6} \right] + 2s_{32} \left[\frac{\cos(2-2n)\tau_0}{(2-2n)\Delta_3} - \frac{\cos(2+2n)\tau_0}{(2+2n)\Delta_4} \right] + \\ & s_{51} \left[\frac{\cos(2+2n)\tau_0}{\Delta_4} - \frac{\cos(2-2n)\tau_0}{\Delta_3} \right] - s_{52} \left[\frac{\sin(2-n)\tau_0}{\Delta_5} + \frac{\sin(2+n)\tau_0}{\Delta_6} \right] - \\ & s_{61} \left[\frac{\sin(2-n)\tau_0}{\Delta_5} - \frac{\sin(2+n)\tau_0}{\Delta_6} \right] + s_{62} \left[\frac{\cos(2-2n)\tau_0}{\Delta_3} + \frac{\cos(2+2n)\tau_0}{\Delta_4} \right] \quad (\text{D.6}) \end{aligned}$$

References

- [1] Wheeler, P. C., *Spinning Spacecraft Attitude Control via the Environmental Magnetic Field*, Journal of Spacecraft and Rockets, vol. 4, no. 12, 1967.
- [2] Shigehara, M., *Geomagnetic Attitude Control of an Axisymmetric Spinning Satellite*, Journal of Spacecraft and Rockets, vol. 9, no. 6, 1972.
- [3] Goel, P. S. and Rajaram, S., *Magnetic Attitude Control of a Momentum-Biased Satellite in Near-Equatorial Orbit*, Journal of Guidance and Control, vol. 2, no. 4, 1979.
- [4] Alfried, K. T., *Magnetic Attitude Control System for Dual-Spin Satellites*, AIAA Journal, vol. 13, no. 6, 1975.
- [5] Stickler, A. C. and Alfried, K. T., *Elementary Magnetic Attitude Control System*, Journal of Spacecraft and Rockets, vol. 13, no. 5, 1976.
- [6] Ramnath, R. V., *A Multiple Scales Approach to the Analysis of Linear Systems*, USAFFDL-TR-68-60, Wright-Patterson AFB, OH, 1960,
also Ramnath, R. V. and Sandri, G., *A Generalized Multiple Scales Approach to a Class of Linear Differential Equations*, Journal of Mathematical Analysis and Applications, vol. 28, 1969.
- [7] Ramnath, R. V., et. al. (ed.), *Nonlinear System Analysis and Synthesis : vol. 2 - Techniques and Applications*, chapter 3, The American Society of Mechanical Engineers, New York, 1980.

- [8] Tao, Y. C. and Ramnath, R. V., *On the Attitude Motion of an Orbiting Rigid Body Under the Influence of Gravity Gradient Torque*, AIAA Paper 78-1397.
- [9] Ramnath, R. V., *Minimal and Subminimal Simplification*, Journal of Guidance and Control, vol. 3, no. 1, 1980.
- [10] Ramnath, R. V., *Gravitational Perturbations of Equatorial Orbits*, Celestial Mechanics, vol. 8, 1973.
- [11] Ramnath, R. V. and Sinha P., *Dynamics of the Space Shuttle During Entry into Earth's Atmosphere*, AIAA Journal, vol. 13, no. 3, 1975.
- [12] Nayfeh, A. H., *Perturbation Methods*, John Wiley and Sons, Inc., 1973.
- [13] Wertz, J. R. (ed.), *Spacecraft Attitude Determination and Control : Appendix H*, D. Reidel Publishing Co., 1978.
- [14] Klimas, A., Ramnath, R. V., and Sandri, G., *On the Compatibility Problem for the Uniformization of Asymptotic Expansions*, Journal of Mathematical Analysis and Applications, vol. 32, 1970.